EFFECT OF CHRONIC PARACETAMOL TREATMENT ON THE CORTICAL

SPREADING DEPRESSION INDUCED THE ALTERATION OF

BLOOD BRAIN BARRIER INTEGRITY

Miss Waranurin Yisarakun

A Dissertation Submitted in Partial Fulfillment of the Requirements

for the Degree of Doctor of Philosophy Program in Medical Science

Faculty of Medicine

Chulalongkorn University

Academic Year 2014

ผลกระทบของการได้รับยาพาราเซตามอลอย่างเรื้อรังต่อการเปลี่ยนแปลง
ของ blood brain barrier integrity เมื่อถูกกระตุ้นด้วย
ปรากฏการณ์ cortical spreading depression

นางสาววรานุรินทร์ ยิสารคุณ

วิทยานิพนธ์นี้เป็นส่วนหนึ่งของการศึกษาตามหลักสูตรปริญญาวิทยาศาสตรดุษฎีบัณฑิต
สาขาวิชาวิทยาศาสตร์การแพทย์
คณะแพทยศาสตร์ จุฬาลงกรณ์มหาวิทยาลัย
ปีการศึกษา 2557

Thesis Title	EFFECT OF CHRONIC PARACETAMOL TREATMENT ON THE CORTICAL SPREADING DEPRESSION INDUCED THE ALTERATION OF BLOOD BRAIN BARRIER INTEGRITY
By	Miss Waranurin Yisarakun
Field of Study	Medical Science
Thesis Advisor	Assistant Professor Supang Maneesri le grand, Ph.D.
Thesis Co-Advisor	Professor Anan Srikiatkhachorn, M.D.
	Assistant Professor Thananya Thongtan, Ph.D.

Accepted by the Faculty of Medicine, Chulalongkorn University in Partial Fulfillment of the Requirements for the Doctoral Degree

⋯⋯⋯⋯⋯⋯⋯⋯⋯⋯⋯⋯⋯⋯⋯Dean of the Faculty of Medicine

(Associate Professor Sophon Napathorn, M.D.)

THESIS COMMITTEE

⋯⋯⋯⋯⋯⋯⋯⋯⋯⋯⋯⋯⋯⋯⋯Chairman

(Professor Vilai Chentanez, M.D.)

⋯⋯⋯⋯⋯⋯⋯⋯⋯⋯⋯⋯⋯⋯⋯Thesis Advisor

(Assistant Professor Supang Maneesri le grand, Ph.D.)

⋯⋯⋯⋯⋯⋯⋯⋯⋯⋯⋯⋯⋯⋯⋯Thesis Co-Advisor

(Professor Anan Srikiatkhachorn, M.D.)

⋯⋯⋯⋯⋯⋯⋯⋯⋯⋯⋯⋯⋯⋯⋯Thesis Co-Advisor

(Assistant Professor Thananya Thongtan, Ph.D.)

⋯⋯⋯⋯⋯⋯⋯⋯⋯⋯⋯⋯⋯⋯⋯Examiner

(Associate Professor Supathra Amatyakul, Ph.D.)

⋯⋯⋯⋯⋯⋯⋯⋯⋯⋯⋯⋯⋯⋯⋯Examiner

(Professor Shanop Shuangshoti, M.D.)

⋯⋯⋯⋯⋯⋯⋯⋯⋯⋯⋯⋯⋯⋯⋯External Examiner

(Associate Professor Banthit Chetsawang, Ph.D.)

วรานุรินทร์ ยิสารคุณ : ผลกระทบของการได้รับยาพาราเซตามอลอย่างเรื้อรังต่อการเปลี่ยนแปลงของ blood brain barrier integrity เมื่อถูกกระตุ้นด้วยปรากฏการณ์ cortical spreading depression (EFFECT OF CHRONIC PARACETAMOL TREATMENT ON THE CORTICAL SPREADING DEPRESSION INDUCED THE ALTERATION OF BLOOD BRAIN BARRIER INTEGRITY) อ.ที่ปรึกษาวิทยานิพนธ์หลัก: ผศ. ดร. ศุภางค์ มณีศรี เลอกรองด์, อ.ที่ปรึกษาวิทยานิพนธ์ร่วม: ศ. ดร. นพ. อนันต์ ศรีเกียรติขจร, ผศ. ดร. ธัญญา ทองตัน, หน้า.

ยาพาราเซตามอลเป็นยาที่นิยมใช้ในการรักษาอาการปวดต่างๆ รวมถึงโรคปวดศีรษะไมเกรนมาเป็นระยะเวลานาน ในปัจจุบัน มีงานวิจัยจำนวนหนึ่งได้รายงานถึงผลด้านลบของการใช้ยาพาราเซตามอลอย่างเรื้อรังต่อระบบต่างๆของร่างกายรวมถึงระบบหลอดเลือด เนื่องจากยานี้สามารถผ่านเข้าระบบ blood brain barrier (BBB) ของสมองได้โดยตรง ดังนั้นจึงอาจจะมีผลกระทบต่อ BBB integrity ได้เช่นกัน ดังนั้นงานวิจัยนี้จึงต้องการศึกษาผลกระทบของการได้รับยาพาราเซตามอลอย่างเฉียบพลัน (1 ชั่วโมง) และอย่างเรื้อรัง (15 วัน และ30 วัน) ที่มีต่อการเปลี่ยนแปลงของหลอดเลือดสมองและการแสดงออกของสาร calcitonin gene related peptide (CGRP) ร่วมกับการกระตุ้นด้วยปรากฏการณ์คอร์ติคัล สเปรดดิ้ง ดีเพรสชั่น (CSD) โดยทำการแบ่งหนูทดลองสายพันธุ์วิสต้าออกเป็น 4 กลุ่ม คือ กลุ่มควบคุม กลุ่มที่ได้รับการกระตุ้นด้วยปรากฏการณ์ CSD กลุ่มที่ได้รับยาพาราเซตามอล และกลุ่มที่ได้รับยาพาราเซตามอลร่วมกับการกระตุ้นด้วยปรากฏการณ์ CSD โดยกลุ่มที่ได้รับยาพาราเซตามอล จะได้รับยา (200 มิลลิกรัมต่อน้ำหนักตัวหนึ่งกิโลกรัม) ฉีดเข้าช่องท้องเพียงครั้งเดียวสำหรับกลุ่มที่ได้รับแบบเฉียบพลัน และได้รับหนึ่งครั้งต่อวันต่อเนื่องเป็นเวลา 15 และ30 วัน สำหรับหนูกลุ่มที่ได้รับยาอย่างเรื้อรังเป็นเวลา 15 และ30 วัน ตามลำดับ ส่วนกลุ่มที่มีการชักนำให้เกิดปรากฏการณ์ CSD จะได้รับการวางโพแทสเซียมคลอไรด์บนผิวสมอง

ผลจากการทดลองแสดงให้เห็นว่าปรากฏการณ์ CSD ส่งผลให้เกิดการเปลี่ยนแปลงต่อ BBB integrity โดยพบการเปลี่ยนแปลงโครงสร้างระดับจุลภาคของเซลล์เอนโดธีเลียม มีการแสดงออกของ cell adhesion molecules (ICAM-1,VCAM-1) เพิ่มมากขึ้น ร่วมกับการลดลงของโปรตีน tight junction (ZO-1, occludin และ claudin-5) ร่วมกับพบการรั่วไหลของโปรตีนออกนอกเส้นเลือดที่เพิ่มมากขึ้น โดยการได้รับยาพาราเซตามอลอย่างเฉียบพลันสามารถลดการเปลี่ยนแปลงที่กล่าวมาข้างต้นได้ แต่ผลการวิจัยนี้กลับพบว่า การได้รับยานี้อย่างเรื้อรังส่งผลให้ความผิดปกติของ BBB integrity ที่เกิดจากการกระตุ้นด้วยปรากฏการณ์ CSD เพิ่มมากขึ้น นอกจากนี้ยังพบว่าการได้รับยาพาราเซตามอลอย่างต่อเนื่องตั้งแต่ 2 สัปดาห์ขึ้นไป ก็ส่งผลให้เกิดการเปลี่ยนแปลงของBBB ดังกล่าวมากกว่ากลุ่มควบคุม นอกจากนี้การกระตุ้นด้วยปรากฏการณ์ CSD สามารถทำให้มีการแสดงออกของ CGRP ที่ปมประสาทไตรเจอมินัลมากกว่ากลุ่มควบคุม ผลงานวิจัยนี้แสดงให้เห็นว่าการแสดงออกของ CGRP ลดลงเมื่อได้รับยาพาราเซตามอลแบบเฉียบพลันก่อนการได้รับการกระตุ้นดังกล่าว แต่กลับพบว่าหนูที่ได้รับยาอย่างเรื้อรังเพียงอย่างเดียวส่งผลให้มีการเพิ่มขึ้นของ CGRP อย่างมีนัยสำคัญทางสถิติ โดยเฉพาะอย่างยิ่งกลุ่มที่ได้รับกระตุ้นด้วยปรากฏการณ์ CSD ร่วมด้วย

เพื่อยืนยันถึงผลของการได้รับยาพาราเซตามอลอย่างเรื้อรังและความเกี่ยวข้องกับการเพิ่มขึ้นของ CGRP ต่อการเปลี่ยนแปลงของหลอดเลือดสมอง งานวิจัยนี้จึงได้ทำการศึกษาวิจัยผลกระทบดังกล่าวในเซลล์เพาะเลี้ยงเอนเธลเลียมจากสมองหนูเมาส์ (bEnd.3) ด้วย ผลการศึกษาพบว่า การได้รับยาพาราเซตามอลอย่างเฉียบพลันสามารถลดการเปลี่ยนแปลงของโปรตีน tight junction ที่เกิดจากการกระตุ้นด้วย CGRPลงได้ ในขณะที่เซลล์ที่ได้รับยาพาราเซตามอลอย่างเรื้อรัง พบการแสดงออกของโปรตีน tight junction ลดต่ำลงกว่ากลุ่มควบคุม นอกจากนี้ผลงานวิจัยยังพบว่าเซลล์เพาะเลี้ยงที่ได้รับยาพาราเซตามอลอย่างเรื้อรัง (มากกว่า 2 สัปดาห์ขึ้นไป) ทั้งในภาวะที่กระตุ้นและไม่ได้รับการกระตุ้นด้วย CGRP มีการเพิ่มขึ้นของเอนไซม์ CYP2E1, cell adhesion molecules (ICAM-1 และ VCAM-1) และปริมาณของ phosphor-NF-kB เพิ่มสูงขึ้นอย่างมีนัยสำคัญทางสถิติเมื่อเปรียบเทียบกับกลุ่มทดลอง และยังพบว่าการแสดงออกของ phospoho-PKA ซึ่งก็พบว่ามีปริมาณเพิ่มสูงขึ้นในเซลล์ที่ได้รับการกระตุ้นด้วย CGRP ทั้งในสภาวะที่ได้รับหรือไม่ได้รับยาพาราเซตามอลก็ตาม ผลการศึกษาแสดงให้เห็นว่า การได้รับยาพาราเซตามอลอย่างเรื้อรังเพียงอย่างเดียวสามารถชักนำให้เกิดการเปลี่ยนแปลงของ BBB integrity ได้ นอกจากนี้ภาวะที่มีการกระตุ้นด้วย CSD หรือ CGRP ร่วมด้วย ก็ทำให้มีการเปลี่ยนแปลงเพิ่มสูงยิ่งขึ้น

จากผลการศึกษาทั้งในสัตว์ทดลองและเซลล์เพาะเลี้ยง สรุปได้ว่า การได้รับยาพาราเซตามอลอย่างเฉียบพลันสามารถปกป้องหลอดเลือดสมองจากการได้รับการกระตุ้นด้วยปรากฏการณ์ CSD แต่อย่างไรก็ตาม การได้รับยาพาราเซตามอลอย่างเรื้อรังสามารถทำให้เกิดความเสียหายต่อหลอดเลือดได้ นอกจากนี้เมื่อมีการกระตุ้นด้วยปรากฏการณ์ CSD ร่วมด้วย จะส่งผลให้หลอดเลือดเกิดความเสียหายเพิ่มมากขึ้น ผลงานวิจัยนี้ยังบ่งชี้ว่าการเพิ่มขึ้นของการแสดงออก CGRP ในปมประสาทไตรเจอมินัล เป็นกลไกหนึ่งที่มีความเกี่ยวข้องกับการเปลี่ยนแปลงของหลอดเลือดสมองที่เกิดจากการได้รับยาพาราเซตามอลอย่างเรื้อรัง ดังนั้นการใช้ยาพาราเซตามอลในการรักษาโรคปวดศีรษะเรื้อรังโดยเฉพาะอย่างยิ่งโรคปวดศีรษะไมเกรน จึงควรมีความระมัดระวังต่อการใช้ยานี้อย่างต่อเนื่อง

สาขาวิชา   วิทยาศาสตร์การแพทย์   ลายมือชื่อนิสิต ....

ปีการศึกษา 2557   ลายมือชื่อ อ.ที่ปรึกษาหลัก ....

                                              ลายมือชื่อ อ.ที่ปรึกษาร่วม ....

                                              ลายมือชื่อ อ.ที่ปรึกษาร่วม ....

5375360030 : MAJOR MEDICAL SCIENCE

KEYWORDS: PARACETAMOL, BLOOD BRAIN BARRIER, CORTICAL SPREADING DEPRESSION, CALCITONIN GENE RELATED PEPTIDE, CHRONIC TREATMENT, NF-KB SIGNALING PATHWAY, PKA SIGNALING PATHWAY

WARANURIN YISARAKUN: EFFECT OF CHRONIC PARACETAMOL TREATMENT ON THE CORTICAL SPREADING DEPRESSION INDUCED THE ALTERATION OF BLOOD BRAIN BARRIER INTEGRITY. ADVISOR: ASST. PROF. SUPANG MANEESRI LE GRAND, Ph.D., CO-ADVISOR: PROF. ANAN SRIKIATKHACHORN, M.D., ASST. PROF. THANANYA THONGTAN, Ph.D., pp.

Paracetamol (APAP) has long been used as a drug for treatment of pain and headache including migraine. Recently, a number of non-beneficial effects of chronic treatment with APAP have been reported in several systems, including the circulatory system. Since APAP can easily cross the blood brain barrier (BBB), the effect of chronic treatment of this drug on the BBB integrity can be expected. In order to prove this hypothesis, the effect of acute (1 hour) and chronic (15 and 30 days) APAP treatments on the alteration of cerebral microvessels and CGRP expression were studied in a cortical spreading depression (CSD) migraine animal model. Wistar rats were divided into the control, CSD, and APAP treatment and APAP treatment with CSD group. APAP (200 mg/kg body weight) was i.p. injected as a single or once-daily dose for the acute and chronic APAP treated groups, respectively. CSD was induced by KCl application on the cortical surface. The results demonstrated that the induction of CSD caused alterations of the BBB integrity, as indicated by increases in ultrastructural alteration of the endothelial cell and expression of cell adhesion molecules (ICAM-1, VCAM-1). Tight junction proteins (ZO-1occludin, claudin-5) were decreased while the IgG extravasation was increased in the CSD group. Acute APAP treatment attenuated those alterations induced by CSD. However, chronic APAP treatment resulted in an enhancement of the abnormalities of BBB integrity induced by CSD. Interestingly, the rats that received chronic (2 weeks) APAP treatment alone also induced alterations in the BBB integrity as compared with the control group. Moreover, the CGRP immunohistochemistry demonstrated that CSD activation could increase the CGRP expression in TG as compared with the control group. Acute APAP treatment significantly reduced the CGRP expression in TG. In contrast, chronic APAP treatment alone (15 and 30 days) significantly enhanced CGRP expression, especially in the combination with CSD activation.

In order to confirm the effect of chronic APAP treatment and the involvement of CGRP on the alteration of the brain endothelial cell, in vitro study using cultured mouse brain endothelial (bEnd.3) cells was performed as well. The results revealed that acute APAP treatment could attenuate the CGRP-induced alteration of the tight junction protein in bEnd.3 cells, whereas the chronic treatment demonstrated the opposite effect showing the significantly lower the level of tight junction proteins (ZO-1, occludin, and claudin-5) than those observed in control. Furthermore, chronic treatment with APAP (more than 2 weeks) either alone or in combination with CGRP could significantly enhance the CYP2E1 activity, cell adhesion molecules (ICAM-1 and VCAM-1), and phospho-NF-KB in cultured bEnd.3 cells. The expression of phosphorylated-PKA was also increased in the CGRP treated bEnd.3 cells with or without APAP treatment groups. These data suggested that chronic APAP treatment alone induces the alterations of BBB integrity. Additionally, the severity of those alterations is more prominent when combined with either CSD or CGRP activation.

In summary, the results obtained from both *in vivo* and *in vitro* studies demonstrate that the short-term treatment of APAP has a protective effect on cerebral microvessels against CSD activation. However, long-term treatment with this drug can induce the damage to these vessels. With CSD activation, the damage to cerebral microvessels induced by long-term APAP treatment is more severe. The increment of the CGRP expression in TG due to the chronic APAP treatment is at least one mechanism involved in those alterations. Thus, long-term treatment with APAP for patients with CSD-related disorders, particularly migraine headaches, might need to be carefully monitored.

Field of Study: Medical Science   Student's Signature ....

Academic Year: 2014   Advisor's Signature ....

                                           Co-Advisor's Signature ....

                                           Co-Advisor's Signature ....

ACKNOWLEDGEMENTS

CONTENTS

LIST OF TABLES

LIST OF FIGURES

CHAPTER I

INTRODUCTION

1.1 Background and rationale

Paracetamol (acetaminophen, *N*-acetyl-*p*-aminophenol, APAP) is one of the most popular drugs for the treatment of pain associated symptoms. Several lines of evidence have demonstrated that this drug efficiently controls a variety of chronic pain, including migraine headaches. Due to its several properties including low price, minimal side effects, and easy availability without a prescription, the possibility exists that this drug is used for chronic treatment. Even though APAP has been distributed since 1893 [1], the exact mechanism of action of this drug is still obscure. Several mechanisms underlying its analgesic effect have been accepted such as the inhibition of prostaglandin synthesis, promotion of serotonergic descending inhibitory pathways, association with endocannabinoid signaling, and interaction with opioid system [2-4]. Additionally, it is generally accepted that mechanisms of action of APAP which involved analgesic effects are predominant in the central nervous system (CNS) [4-6].

APAP has been recognized as a relatively safe drug; hepatotoxicity is one of the only reported toxic effects of a high-dose APAP. Several evidences revealed that usage of APAP at therapeutic doses has protective effects to several pathological conditions [7, 8]. A study in the cortical neurons that were pretreated with APAP before menadione activation demonstrated an increase in the cell survival and a decrease in the cytokine and chemokine productions compared with those observed in the neurons without APAP pretreatment [9]. The experiment in the brain endothelial cell culture also indicated a protective effect of this drug on the

oxidative stress [10]. Moreover, the recent study in rats that were received a single APAP treatment demonstrated the enhancement of P-glycoprotein (P-gp), the efflux transporter, both of expression and activity which resulted in the decrease of morphine accumulation in the brain [11].

On the other hand, in the last decade, adverse effects of APAP treatment, even used at the therapeutic range, in several systems have gradually been reported including in the CNS and the circulatory system [12-18]. The studies in the cortical spreading depression (CSD) migraine animal model have demonstrated that chronic APAP treatment (200 mg/kg bw) induced the hyperexcitability of cortical neurons as well as the up-regulation of the $5-HT_{2A}$ receptors in the brain and trigeminal ganglion (TG) [16, 17]. Moreover, in the circulatory system, several studies have also revealed that chronic APAP treatment induced the increases in blood pressure and the risk of hypertension in patients [12-15]. In the brain, the study by Posadas and colleague (2010) has revealed that APAP at the doses below those required to produce hepatotoxicity could produce the neurotoxic effect both *in vitro* and *in vivo* experiments [19]. The increase in the toxic metabolite of APAP, *n*-acetyl-*p*-benzoquinoneimine (NAPQI), has been proposed as the mechanisms underlying those non-beneficent effects of this drug [19, 20].

Accumulating data demonstrated that the non-beneficial effect of APAP is mediated via its toxic metabolite NAPQI [21, 22]. At low levels, almost APAP is conjugated with glucuronic acid and sulfate in the liver before being excreted in the urine, only small fraction is oxidized by the enzyme cytochrome P450 2E1 (CYP2E1), forming NAPQI [19, 23, 24]. NAPQI always quickly detoxified via an interaction with glutathione (GSH) [19, 25]. However, at high levels of APAP, NAPQI production is

increased which can result in the cellular damage since NAPQI itself can bind with cellular proteins. Moreover, increase of NAPQI can induce the depletion of GSH as well [26, 27]. In the brain, the expression of the CYP2E1 enzyme has been demonstrated in several cells including neurons, astrocytes, and endothelial cells [19, 23, 24]. It is known that APAP can directly cross the blood brain barrier (BBB) [28]. This barrier is a neurovascular unit (NVU) comprising of different cell types including endothelial cells, astrocytes, pericytes, microglia, and neurons. Thus, after APAP reaching the cerebral circulation, it can be directly metabolized by the cells in the NVU, leading to NAPQI formation in the brain. As a result, in the case of long-term treatment or treatment with a high concentration of APAP, an abnormality of cells in the NVU can be expected.

Among the disorders for which APAP is commonly used as a treatment drug, migraine (a neurovascular disorder) is of particular interest to be studied due to its pathogenesis, which is tightly associated with the activation of the trigeminovascular system, either the trigeminal neurons or cerebral vessels [29, 30]. Studies in the migraine animal model have also revealed the alteration of BBB integrity induced by CSD activation [31, 32]. In addition, in migraine patients, increase of soluble ICAM-1 was detected after two hours after migraine attack [33]. Alterations of the cerebral vessels in these patients have been confirmed by findings that have demonstrated the association between migraine, particularly migraine with aura, and abnormalities in the cerebrovascular system [34, 35].

Moreover, it has been accepted that calcitonin gene related peptide (CGRP) is a key neuropeptide involved in migraine pathophysiology [36-38] since the clinical study in migraine patients revealed that the plasma CGRP was elevated during

migraine attack in the jugular venous blood [39]. Given the instability of the cerebral vessels in migraine patients, the addition of chronic APAP treatment might enhance the abnormalities in the cerebral microvessels of these patients. **However, the effect of chronic APAP treatment on the alteration of BBB integrity has never been explored**.

In order to clarify this hypothesis, the present study aimed to investigate the effects of chronic APAP treatment for the different time points (0, 15 and 30 days) on the alteration of BBB integrity in the condition with and without the activation of CSD. The following alterations of BBB integrity were monitored; the ultrastructural alteration of the NVU of the BBB (tight junction alignment, astrocytic foot-plate swelling, numbers of pinocytic vesicles and microvilli), the alteration of tight junction proteins (ZO-1, occludin, claudin-5, IgG extravasation), the expression of cell adhesion molecules (ICAM-1, VCAM-1), and the enzyme CYP2E1 activity in the cerebral cortex. The change in the expression of CGRP in TG was also studied.

Furthermore, the effect of chronic APAP treatment on the alteration of BBB integrity was confirmed by *in vitro* study in the brain endothelial cell line (bEnd.3).The alteration of tight junction proteins (ZO-1, occludin, claudin-5), the expression of cell adhesion molecules (ICAM-1, VCAM-1), and the enzyme CYP2E1 activity in cultured cell were studied in the condition either with and without CGRP activation. In this part of the study, besides the alteration in tight junction proteins, cell adhesion molecules, and enzyme CYP2E1 in the endothelial cells, the activation of the transcription factor (nuclear factor kappa-light-chain-enhancer of activated B cells, NF-**K**B) and cyclic AMP (cAMP)-dependent protein kinase (PKA) signaling pathways was monitored as well.

1.2 Key words

Paracetamol, blood brain barrier, cortical spreading depression, calcitonin gene related peptide, chronic treatment, NF-kB signaling pathway, PKA signaling pathway

1.3 Research design

Animal and cell culture experimental designs

1.4 Research questions

1.4.1 Does chronic APAP treatment alter the BBB integrity?

1.4.2 Does chronic APAP treatment enhance the effect of CSD activation on the alteration of the BBB integrity?

1.4.3 Does chronic APAP treatment increase the CSD-induced CGRP expression in the TG?

1.4.4 Does the activation of the NF-kB transcription factor involve in the alteration of the BBB integrity induced by chronic APAP treatment?

1.4.5 Does the activation of the PKA involve in the increase of the alteration of the BBB integrity induced by chronic APAP treatment?

1.5 Objectives

<u>Major objective</u>

To clarify the effect of chronic APAP treatment on the alterations of the cerebral vessels in the conditions with and without the activation of CSD.

<u>Minor objectives</u>

1. To investigate the effect of chronic APAP treatment on the ultrastructural changes of cerebral vessels in the brain.

2. To investigate the effect of chronic APAP treatment on the alteration of tight junction proteins in the brain and in the cultured endothelial cell.

3. To investigate the effect of chronic APAP treatment on the expression of cell adhesion molecules (ICAM-1, VCAM-1) in the brain and in the cultured endothelial cell.

4. To investigate the effect of chronic APAP treatment on the expression of CGRP in the TG.

5. To investigate the effect of chronic APAP treatment on the alteration of the CYP2E1 enzyme in the brain and in the cultured endothelial cell.

6. To investigate the effect of chronic APAP treatment on the activation of the NF-kB signaling pathway in the cultured endothelial cell.

7. To investigate the effect of chronic APAP treatment on the activation of the PKA enzyme in the cultured endothelial cell.

1.6 Hypothesis

Chronic APAP treatment will result in the increase in the NAPQI formation and the depletion of GSH in the brain. The accumulation of NAPQI and the increasing of oxidative stress from GSH depletion can lead to damage of the NVU of the BBB, which will finally cause the disturbance of BBB integrity. In combination with CSD activation, the disturbance of the BBB can become more severe due to the release of CGRP from the perivascular neurons caused by the activation of the trigeminovascular system. The mechanism underlying the alteration of the BBB integrity in chronic APAP treatment might mediate via the activation of both the NF-kB signaling pathway and PKA activity.

1.7 Conceptual framework
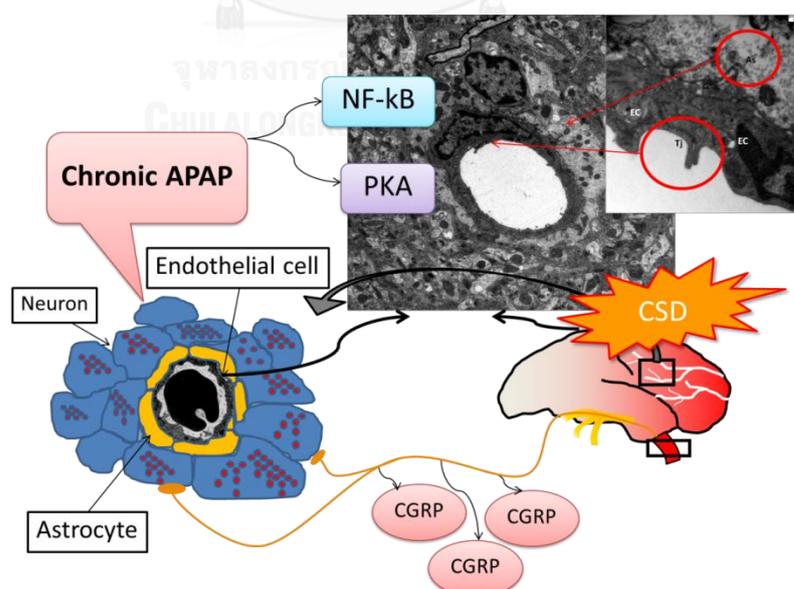
Figure 1 Schematic diagram of conceptual framework of chronic APAP treatment on the alteration of BBB integrity.

CHAPTER II
REVIEW LITERATURES

2.1 Blood brain barrier

The central nervous system (CNS) is an important system which controls most functions in the human body. The difference between the CNS and other systems is that CNS has a high activity, so it requires about 20% of oxygen consumption of cardiac output to regulate the normal function of neurons. Thus, the CNS is the most sensitive system to the imbalance of nutrients and toxic substances. In order to protect neurons from injury, the CNS has a special structure of cerebral microvessels called the blood brain barrier (BBB). It is a complex structure which interfaces between the blood and the brain parenchyma in the CNS. It acts as a controller in the exchanges of substances between those two compartments in order to maintain the homeostasis of the CNS. The components of the BBB are not only the endothelial cells but also consist of other cells and extracellular matrix that constitute the "neurovascular unit (NVU)" [40]. The major functions of BBB are:

1. control the ion balance

2. transport the essential nutrients

3. barrier for harmful molecules

4. introduce the inflammatory cells to the inflammation area of the brain

However, the brain might be damaged if the BBB turns into a pathological condition. This event results in the loss of BBB integrity and is the cause of many neurological disorders. The abnormality of the NVU's structure leads to the increase

of the number of the incidences in many diseases such as Alzheimer's disease, Parkinson's disease, infectious diseases, stroke and migraine headache [40].

Neurovascular unit of BBB

The NVU of the BBB composed of endothelial cells lining the cerebral capillaries and other elements that support the function of the NVU such as neurons, astrocytes, pericytes, and microglia. Moreover, the basement membrane that forms a barrier to control the transportation of the substances crossing between the blood and the brain also contribute the structure of this unit (Figure 2).
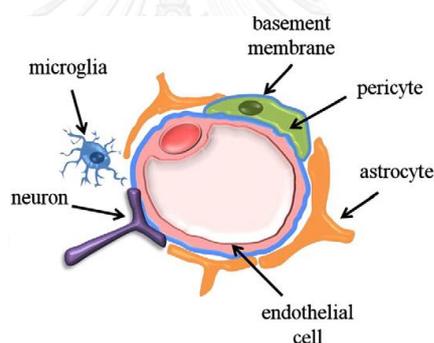
Figure 2-1

Figure 2 Neurovascular unit [41].

Endothelial cells

The brain capillary is a very special structure which has a unique type of endothelial cell that differ from the endothelial cell in other organs. It has a continuous basement membrane, absent of fenestrations, low pinocytic vesicles, high number of mitochondria, and the connection between cells are tighter (50-100 times more tight) than those in other capillaries because of which they are called

"tight junctions" [42, 43]. These characteristics of brain capillary result in the restriction of the paracellular diffusion and regulation of the passage of molecules from the circulation into the brain parenchyma [42, 44]. Thus, brain capillary is a very important structure to maintain the homeostasis of the brain, however the effect of this property will increase when combined with properties of other components [45].

Neurons

The effect of neurons involved in the formation of BBB is still unclear. It is known that brain endothelial cells receive either directly contact or indirectly contact via the astrocytic foot process from several types of neurons including noradrenergic, serotonergic, cholinergic, and GABAergic neurons [46]. The interactions between these neurotransmitters and their receptors distributed on the brain endothelial cells can result in a variety of the cerebrovascular responses.

Astrocytes

Astrocytes are glial cells that cover almost (>99%) all of the BBB endothelial cells by forming a lacework of fine lamellae. The interaction between these 2 cells affects the structure of each other. Astrocytes influence brain endothelial cells to develop the BBB phenotype by increasing in the property of the tight junction while endothelial cells also influence the up-regulation of aquaporin-4 expressed by astrocytes after co-culture together [40, 42, 47]. Moreover, astrocytes are important to the neuronal function because they enhance the communication between neurons and brain capillaries. Thus, the interaction of astrocytes and brain endothelial cells are essential for the neurovascular unit's function [48]. In addition,

astrocytes also play a major role in BBB functions by promoting proteoglycan synthesis which can increase the brain microvascular endothelial cells (BMVEC) electivity charges [49].

Microglia

Microglia are one of the cell types involve in the NVU of the BBB. They are located in the area of the perivascular space which have a very important role in maintaining BBB properties. The pivotal role of microglia involves the immune responses in the CNS [45]. Under normal condition, they supply neurons with trophic factors, contributes to the rearrangement of neural connections and plasticity of normal brain tissue. Under pathological condition, microglia are activated and result in the BBB instability. Thus, they have 2 forms, resting and activated forms. In the resting, they have small bodies and long thin processes. While the activated form has a phagocytic morphology which changes the morphology from long to short processes [50]. The activated microglia can released several mediators including pro-inflammatory cytokines which can affect the BBB integrity. However, the exact mechanisms of microglia associated with BBB properties are still unknown.

Tight junctions

The very important property of BBB is the regulation of paracellular permeability which strictly controls the substances crossing the BBB. The high electrical resistance of brain endothelial cells leads to the effective function of tight junctions to restrict paracellular movement. The effectiveness of the tight junctions is

supported by several tight junction proteins including claudins, occludin, and zona occludens (ZO) [51] (Figure 3).
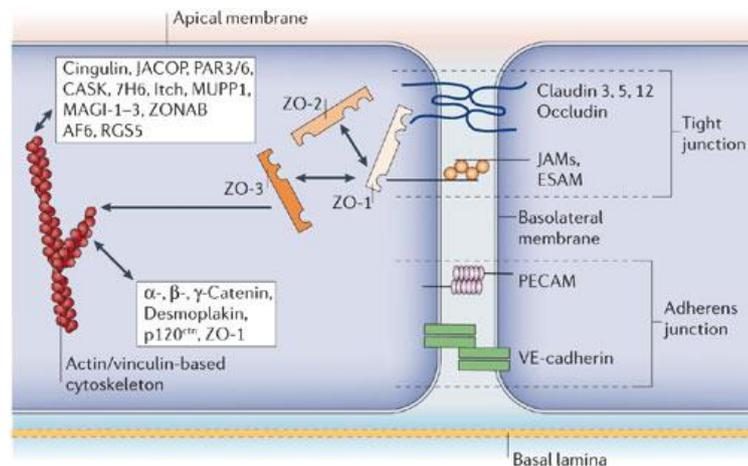
Figure 3 The molecular composition of endothelial tight junctions [52].

Occludin

Occludin is a 65 kDa transmembrane protein in tight junction that is composed of 4 transmembrane domains with the carboxyl and amino terminals in the cytoplasm and 2 extracellular loops in the intercellular cleft [53]. In between the brain endothelial cells, occludin expresses in high levels along the cell margins which ensures that it can decrease the paracellular permeability confirmed by the high electrical resistance of the tight junction [54]. The lower levels of occludin contribute to the dysfunction of the BBB in many neurological diseases [40].

Claudins

Claudins have approximately a weight of 20–27 kDa. There are 24 members of claudins in a family of tight junction proteins. They are integral membrane proteins that share the 4 transmembrane domains of occludin, but do not contain any

sequence homology to occludin [51]. Therefore, these 2 tight junctions, claudins and occludin, act in different roles in the BBB. Claudins form the primary seal of the tight junction while occludin support this structure but do not result in the tight junction formation [40]. Claudin-1 and claudin-5 are the predominant proteins in the tight junction that maintain the BBB function [55]. In particular, claudin-5 plays an important role in BBB permeability. The claudin-5 knockout mice demonstrated in a size-selective BBB defect and the disruption of this protein also detect in many cerebrovascular diseases [56].

<u>Zona occluden-1 and 2</u>

ZO proteins are the cytoplasmic proteins of tight junctions. The prominent members are ZO-1 and ZO-2. ZO-1 is a 220 kDa phosphoprotein that connects the transmembrane proteins in tight junction with the actin cytoskeleton [57]. Thus, the loss or disruption of ZO-1 from the junctional complexes resulted in the increase of BBB permeability (Mark and Davis 2002). ZO-2 is a 160 kDa phosphoprotein that has significant homology to ZO-1 [58]. However, few studies have been conducted on the ZO-2 function compared with studies on ZO-1 [59].

2.2 Migraine

Migraine is one of the disorders which has a high impact on the public health due to the disability of patient during migraine attack. It can be classified into 2 types depending on the symptoms called migraine with and without aura. Patients usually suffer from the migraine attack for 4-72 h in the unilateral side which is associated with nausea and vomiting including photophobia and phonophobia [60]. The

incidence of this disease is about 6–8% in men and 15–22% in women within Europe and the Americas and 29.1% in Thailand. Within this information it has also been reported that the peak of the prevalence is at the age of 40 and the incidence of this disease in the women is more than those in the men about 3 times [61-63]. Thus, the life of the patients who suffer from migraine will be highly effected and treatment will be costly.

Pathophysiology of migraine

Migraine is a very common chronic neurovascular disorder. It involves both of neuronal and vascular compartments. The pathogenesis of this disease first occurs in the CNS by activating the 'trigeminovascular nociceptive system'. This event leads to neurogenic vasodilatation within the dura mater which releases neuropeptides and pro-inflammatory cytokines that effect to the sensitization of peripheral and central neurons within the trigeminovascular system [29]. However, the exact mechanism of the etiology of migraine headache is still unknown (Figure 4).
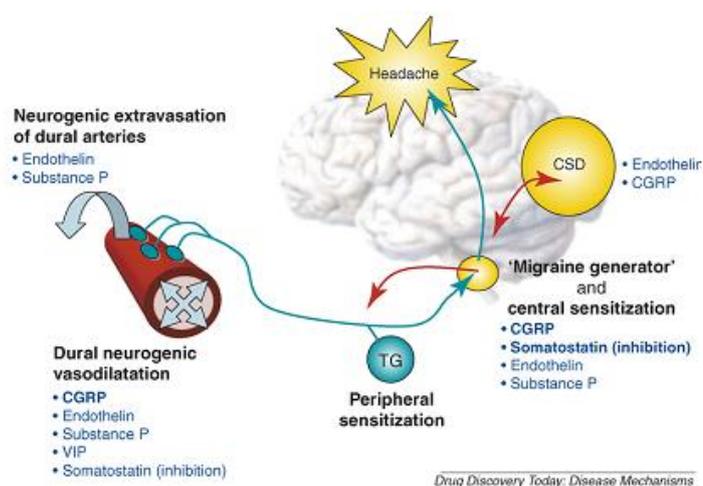
Figure 4 Role of neuropeptides in the pathophysiology of migraine [29].

Cortical spreading depression

Cortical spreading depression (CSD), which was discovered over 60 years ago by Leào [64], commonly occurs in migraine with aura. CSD, conducted by propagation of a depolarization wave, spreads over the cortex. The velocity of CSD that transverses the cerebral cortex is about 3–5 mm/min. During CSD, a short-lasting increase of cerebral blood flow arises and is followed by a long-lasting regional hyperemia [65]. Furthermore, CSD can be modulated by several vasoactive neuropeptides such as nitric oxide (NO), substance P, and calcitonin gene related peptide (CGRP). Among those neuropeptides, CGRP is the most potent neurogenic vasodilator which causes plasma protein extravasation and vasodilatation [66].

Calcitonin gene related peptide

Migraine is associated with the activation of the trigeminovascular system. This activation leads to the release of neuropeptides. CGRP is one of the neuropeptides involved in the dilation of cranial blood vessels and stimulation of the sensory nerve transmission [67]. CGRP is one of members of peptides in the calcitonin family. It is a 37-amino acid neuropeptide, which was first identified in 1983 [68]. CGRP is widely distributed in the peripheral and central nervous systems [69]. During a migraine attack, CGRP was elevated in the plasma concentrations in the jugular venous blood of patients [39]. This result is confirmed by the study in which the intravenous injection and infusion of CGRP produced a migraine-like headache [70, 71]. Furthermore, CGRP can lead to plasma protein extravasation and vasodilatation [72]. The cellular mechanisms of vasodilatation to CGRP have 2 pathways. The first one is endothelium-independent vasodilatation to CGRP.

Activation of CGRP receptors on smooth muscle cells is coupled to production of 3'-5'-cyclic adenosine monophosphate (cAMP) by adenylate cyclase. The increase in intracellular cAMP concentration then stimulates cAMP-dependent protein kinase A (PKA), which opens K^+ channels and activates Ca^{2+} sequestration mechanisms to cause smooth muscle relaxation. The second pathway is endothelium-dependent vasodilatation to CGRP. CGRP interacts with receptors on endothelial cells and stimulates production of nitric oxide (NO). This is also mediated via cAMP accumulation which leads to a direct effect of PKA on endothelial NO synthase (eNOS). Diffusion of NO into adjacent smooth muscle cells, activating guanylate cyclase, then leads to relaxation [73] (Figure 5).
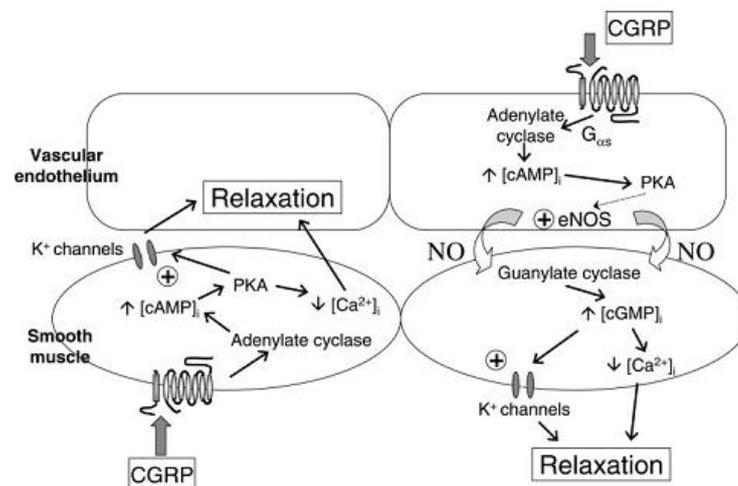
Figure 5 The cellular mechanisms of vasodilatation to CGRP [73].

CSD and neurogenic inflammation

In the CSD condition, the stimulation of the trigeminal ganglion results in the neuropeptide release from trigeminocervical nerve endings leading to the neurogenic inflammation. This inflammation can activate the trigeminal vascular nociceptive

system and cause a headache [74]. Furthermore, the endothelial cells are also playing an important role in the inflammation. They are essential for regulating vascular permeability and leukocyte migration by regulating the expression of cell adhesion molecule [75]. The two important cell adhesion molecules are intercellular adhesion molecule-1 (ICAM-1) and vascular cell adhesion molecule-1 (VCAM-1) that up-regulated during endothelial activation [76]. The involvement of neurogenic inflammation in migraine pathophysiology has been confirmed by the results from several studies. In 2006, Sarchielli and colleague had demonstrated that during a migraine attack, the increase of CGRP levels was detected in the jugular vein of migraine patients which was associated with the increase of pro-inflammatory cytokines IL-1β, IL-6, and TNF-α in the early hours of migraine attacks including the increase in ICAM-1 (sICAM-1) [33].

Migraine and cerebrovascular diseases

Migraine has become an important vascular risk factor during the past few years. It is considered as a risk factor for ischemic stroke [77]. A recent meta-analysis identified that all types of migraine headache were associated with an increased risk of stroke but this risk was double among migraine with aura patients [78]. An epidemiological study on brain abnormalities in migraine also supports the observation that 8.1% of patients with MA and 2.2% of patients with migraine without aura present subclinical brain lesions similar to strokes, even in the absence of a clinical history of stroke [79, 80]. Migraine can modify the homeostatic properties of the endothelium, favoring a prothrombotic, pro-inflammatory and proliferative condition that predisposes towards atherogenesis and the development of

thrombotic events other than migraine [81] [82]. Endothelial dysfunction is the result of (a) a reduction in the bioavailability of vasodilator substances (nitric oxide, for example) and an increase in contractile factors derived from the endothelium, causing an alteration in vascular reactivity (including the microvasculature), and (b) oxidative stress, which in turn promotes inflammatory processes. Oxidative stress markers are increased in migraine patients [83]. It is thought that prothrombotic, pro-inflammatory and other vasoactive peptides are released during migraine attacks, and that these could damage the vascular endothelium. On the other hand, cortical depression (CD) involves an alteration in the permeability of the BBB through the activation of metalloproteinases [31]. Their activation causes a direct cellular damage that, along with the release of vasoactive neuropeptides during migraine attacks, may stimulate inflammatory responses inside and outside of the brain [84].

2.3 Paracetamol

APAP is a common drug that became one of the most popular 'over-the-counter' medicines for fever, pain and headache due to several properties including: low price, abundant availability and safety. Even though it's widely used for over 60 years, the mechanism of action is still debated.

Mechanism of action

1. A central serotonergic mechanism

The modulation of the central serotonin system has been involved in the anti-nociceptive effect of APAP. The study in animals indicated that the 5-hydroxytryptamine type 3 (5-HT$_3$) receptors were involved in the analgesic effect of

this drug [85, 86] which correlated with the study in humans that confirmed by inhibiting with 5-HT$_3$ receptor antagonists [2]. Based on the results, it might be indicating that APAP can reduce serotonin which leads to the anti-nociceptive effect of this drug [87].

2. Prostaglandin H2 synthetase inhibition

The alternative pathway of the APAP mechanism is the inhibition of prostaglandin synthesis. APAP may be the cause of its ability to inhibit a specific site of the prostaglandin H2 synthase (PGHS) molecule. It has 2 isoforms, PGHS1 and PGHS2, which are commonly referred to as COX-1 and COX-2, respectively. In animal models, several reports have suggested that APAP could inhibit the other PGHS variant (COX-3) which exists in a high concentration in the CNS [88]. However, there is no evidence that COX-3 is expressed in humans [89].

3. Nitric oxide

Through the experiment in animals, it has been suggested that depolarization of afferent neurons by peripheral harmful stimuli leads to an activation of spinal N-methyl-D-Aspartate (NMDA) receptors and promote the synthesis of NO. APAP was considered in the involvement of the nociceptive process which occurs at the spinal level by inhibition of the NMDA receptor activation. This effect may be associated with an inhibition of NO mechanisms [90].

Metabolism of APAP

APAP is mainly metabolized in the liver by conjugating with glucuronic acid and sulfate after which those non-toxic products are excreted through the urine. About 5% of APAP is oxidized via the CYP2E1 enzyme forming a reactive metabolite, NAPQI, which is extremely toxic to the cells. NAPQI, after being produced, is rapidly detoxified by interaction with GSH to form a non-toxic metabolite that will be finally excreted through the urine [19, 25] (Figure 6).
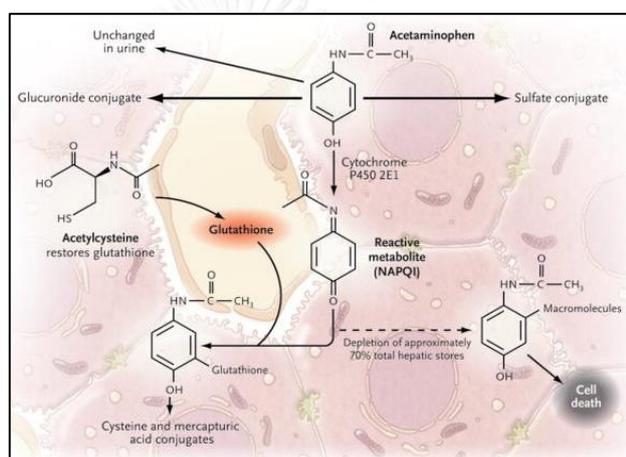
Figure 6 Metabolism of APAP [91].

Effects of APAP treatment

Beneficial effects

The accumulative evidences have confirmed that at therapeutic doses of APAP have protective effects to several pathological conditions. In the cerebral cortical cultured neurons, pretreatment with APAP (50 µM) increases the neuronal cell survival, and inhibits cytokines and chemokines after menadione exposure [9]. These results correlated with the results of the experiment in the brain endothelial

cell culture in which pretreatment with APAP (25-100 μM) has the protective effect against the oxidative stress [10].

<u>Adverse effects</u>

In the last decade, APAP treatment at a non-toxic dose to the liver has been demonstrated to have a toxic effect on several types of cells. The sub-toxic concentrations of APAP treatment decreased intracellular GSH in pulmonary macrophages and type II pneumocytes which might be a risk factor for asthma morbidity [92]. A relationship between APAP consumption and an increase in asthma prevalence was confirmed by the most recent study in 20,000 children and adolescents in Spain. APAP consumption was associated with a significant increase in asthma symptoms and the effect was more severe at a more frequent treatment with APAP [18]. Treatment with APAP at doses below those required to produce hepatotoxicity (250 and 500 mg/kg bw) caused an adverse effect to the CNS in the rat brain. They have demonstrated that APAP could produce the neurotoxic effect both *in vitro* and *in vivo* experiments [19]. The toxic of APAP to neurons was activated via the intrinsic pathway through a mechanism involving NF-kB which leads to an increase in IL-1β production

[93]. Based on those results, they suggested that the adverse effect of APAP treatment might be related to the activity of the CYP2E1 enzyme. In addition, NF-kB is a transcription factor which plays a key role in the regulation of many inflammatory genes. NF-kB dimmers are activated by phosphorylation of inhibitory IkB proteins and subsequently degraded by the ubiquitin-proteasome pathway. The active NF-kB subunits will translocate to the nucleus for regulating the cellular pro-

inflammatory and anti-inflammatory responses [94, 95] which lead to cell damages (Figure 7).
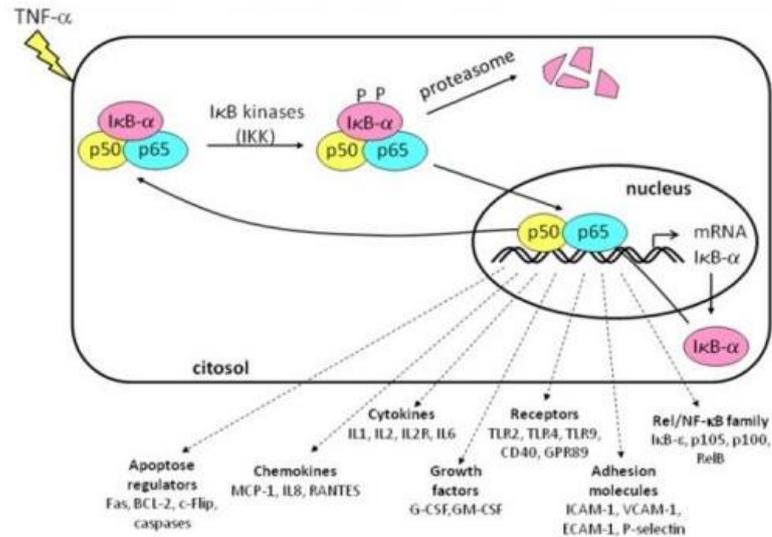
Figure 7 Classical pathway of NF-kB activation [96].

A study in pulmonary macrophages and type II pneumocytes has demonstrated that APAP treatment could decrease intracellular GSH at subtoxic and clinically relevant concentrations which might be a risk factor for asthma morbidity [97]. This result was confirmed by the most recent study from Gonzalez-Barcala and colleague (2012). In their study, 20,000 children and adolescents in Spain who had consumed APAP demonstrated a significant increase in asthma symptoms. Further, a positive relation between the severity of the effect and the frequency of drug intake was observed [18]. Concerning the effect of APAP in the circulatory system, long-term APAP treatment even used at the therapeutic doses revealed the increase of blood pressure which contributed to increase the risk of hypertension. Studies in both women and men who frequently took APAP at a dosage of 500 mg/day

demonstrated almost a 2-fold increase in the relative risk of incident hypertension than that observed in nonusers [12-14]. The effect of chronic APAP treatment has been confirmed by Sudano et al. that collateral treatment with APAP at a therapeutic dose (1 g/day) with standard cardiovascular therapy for 2 weeks in patients with coronary heart disease could induce an increase in both systolic and diastolic blood pressures [15].

At a high concentration of APAP, the toxic metabolite NAPQI will increase and lead to the depletion of GSH. The increase of NAPQI levels and the decrease of GSH results in cell damage and induces the hepatotoxicity. As I mention earlier, the CYP2E1 enzyme plays a key role in the production of the toxic metabolite NAPQI. Organs and tissues in which this enzyme is expressed will have the possibility to metabolite APAP and increase the accumulation of NAPQI formation. Based on the accumulative evidences, the CYP2E1 enzyme expression was also found in the lung, the kidney, and the brain [98]. In the brain, the expression of the CYP2E1 enzyme has been demonstrated in several cells including neurons, astrocytes, and endothelial cells [19, 23, 24]. It is known that APAP can directly cross the BBB which normally functions as a barrier to any substances in crossing between the blood and the brain in order to protect the brain cells. BBB is a NVU comprising of different cell types including endothelial cells, astrocytes, pericytes, microglia, and neurons. Thus, after APAP reaching the cerebral circulation, it can be directly metabolized by the cells in the NVU. Based on this, abnormality of cells in the NVU can be expected as a result of long term treatment or high concentration of APAP.

Furthermore, the studies in the CSD animal headache model have demonstrated that chronic treatment with APAP (200 mg/kg bw) could up-regulate

the 5-HT$_{2A}$ receptors in the brain. These results confirmed that the effect of chronic APAP could induce the hyperexcitability of cortical neurons [17]. However, the effects of chronic APAP treatment on the alteration of the BBB integrity have never been explored.

In order to clarify this hypothesis, the present study aims to investigate the effects of chronic APAP treatment for the different time points (0, 15 and 30 days) on the alteration of BBB integrity in the condition with and without the activation of CSD. The following alteration of BBB integrity will be monitored; the ultrastructural alteration of the neurovascular unit of BBB (tight junction alignment, astrocytic foot-plate swelling, numbers of pinocytic vesicles and microvilli), the alteration of tight junction proteins (ZO-1, occludin, claudin-5, IgG extravasation), the expression of cell adhesion molecules (ICAM-1, VCAM-1), and enzyme CYP2E1 activity in the cerebral cortex, and including the expression of CGRP in the trigeminal ganglion.

Furthermore, the effect of chronic APAP treatment on the alteration of BBB integrity will be confirmed by *in vitro* study in the bEnd3 brain endothelial cell line. In this part of the study, besides the alteration in tight junction proteins, cell adhesion molecules, and enzyme CYP2E1 in the endothelial cells, the activation of transcription factor NF-kB and PKA signaling pathways will be monitored as well.

CHAPTER III

MATERIALS AND METHODS

In order to investigate the effect of chronic APAP treatment on the CSD-induced the alteration of BBB integrity, the study was divided into 2 major parts (*in vivo* and *in vitro* studies) as follows:

3.1. *In vivo* study

3.1.1 Animals

Adult male Wistar rats weighing 200-250 g were obtained from National Animal Centre, Mahidol University, Thailand. They were housed five per cage in a room with controlled temperature and humidity with a 12-h dark/light cycle. Food and drink were fed *ad libitum*. The protocols of this study were executed according to the guidelines of the by the Ethical Committee of the Faculty of Medicine, Chulalongkorn University.

3.1.2 Study design

The experiment of *in vivo* study was divided into 3 experiments based on the experimental design as follows (n = 40, each):

Experiment I: The study of the effect of 0 day APAP treatment on the CSD induced the changes of BBB integrity

Experiment II: The study of the effect of 15 days APAP treatment on the CSD induced the changes of BBB integrity

Experiment III: The study of the effect of 30 days APAP treatment on the CSD induced the changes of BBB integrity
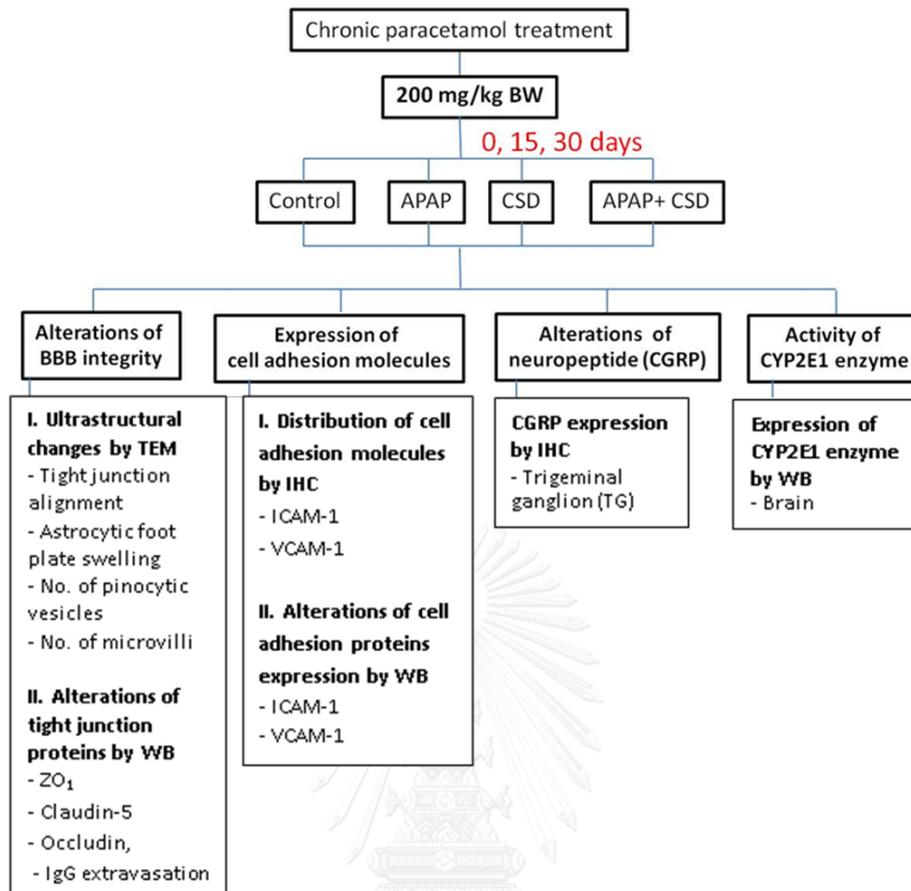
TEM = Transmission electron microscopic study

IHC = Immunohistochemical study

WB = Western blot analysis

Figure 8 Study design of *in vivo* experiment.

Experiment I: The study of the effect of 0 day APAP treatment on the CSD induced the changes of BBB integrity

Rats were separated into 2 groups; control and APAP treated group. A single dose of APAP (200 mg/kg bw, TP drug laboratories, Thailand) was injected (i.p.) into the rats in the APAP treated group while 0.9% normal saline at the same volume was given to the control group. After 1 hour of APAP treatment, each group of rats was

subdivided into 2 subgroups (CSD and without CSD group) and prepared for CSD induction.

Experiment II: The study of the effect of 15 days APAP treatment on the CSD induced the changes of BBB integrity

Rats were separated into 2 groups; control and APAP treated group. An equal dose of APAP and normal saline was given to the rats in a similar procedure as in experiment I **except** for the duration of treatment that was performed once daily for 15 days. After 24 hours of the last injection, each group of rats was subdivided into 2 subgroups (CSD and without CSD group) and prepared for CSD induction.

Experiment III: The study of the effect of 30 days APAP treatment on the CSD induced the changes of BBB integrity

Rats were separated into 2 groups; control and APAP treated group. An equal dose of APAP and normal saline was given to the rats in a similar procedure as the experiment I **except** for the duration of treatment that was performed once daily for 30 days. After 24 hours of the last injection, each group of rats was subdivided into 2 subgroups (CSD and without CSD group) and prepared for CSD induction.

3.1.3 Surgical procedure and CSD induction

After the last injection of APAP or saline, each group of rats from the experiments I-III was subdivided into 2 subgroups as follows: CSD and without CSD group. All rats were anaesthetized by an intraperitoneal injection of sodium pentobarbital (60 mg/kg bw) to maintain the surgical anesthesia. They were firmly

fixed to the head holder of a stereotaxic frame. After the skin and soft tissue were removed, a craniotomy (2 mm in diameter) was made in the right parietal bone at 7 mm posterior and 1 mm lateral to bregma. The dura mater was then removed and CSD was induced by the application of solid KCl (3 mg) onto the surface of the right parietal cortex in the CSD induced groups while NaCl (3 mg) was used in the non-CSD induced groups as in a similar procedure as in previous studies [16, 17].

3.1.4 Immunohistochemical and transmission electron microscopic studies

<u>Sample collection</u>

Two hours after the KCl or NaCl application, rats were deeply anesthetized with an overdose of sodium pentobarbital followed by transcardial perfusion with 250 ml of 0.1 M phosphate buffered saline (PBS) and 250 ml of 4% paraformaldehyde in 0.1 M PBS, pH7.4, respectively. Then, the right TG was collected while 3 mm thick brain slice was cut at 3 mm anterior to the bregma. Both of them were immediately fixed in 4% paraformaldehyde at 4 °C for overnight before being further processed for embedding in the paraffin for immunohistochemical study. In addition, the frontal cortex ipsilateral to the CSD activation at the area 6 mm anterior to the bregma was cut into small cubes (1 mm^3) before submerging into 3% glutaraldehyde for transmission electron microscopic study.

<u>Immunohistochemistry</u>

For the detection of CGRP, 3 μm thick longitudinal serial sections of the TG were cut by using a microtome. The sections were collected in series of 1 in 8 and placed on Superfrost plus slides (Thermoscientific, Portsmouth, New Hampshire, USA). In total, 4 sections were selected from each animal (n = 5 for each group). All sections were deparaffinized and incubated with antigen retrieval solution (citrate buffer pH 6.0, Dako, Glostrup, Denmark), 3% Hydrogen peroxide, and 3% normal horse serum (PAN Biotech GmbH, Aidenbach, Germany) in PBS. Sections were labeled by incubating with rabbit anti-CGRP (1:6,000; Sigma, St. Louis, Missouri, USA) at 37°C for 30 min. CGRP immunoreactivity was detected using an ultraView Universal DAB Detection Kit (Ventana Medical Systems, Inc., Arizona, USA). The entire process was conducted with an automatic slide staining machine (Benchmark XT, Ventana Medical Systems, Inc., USA). All slides were dehydrated in ethanol, mounted, and cover-slipped with a mounting medium. All sections were scanned using a slide scanner (Aperio ScanScope, Aperio, Vista, California, USA). To determine the number of CGRP-immunoreactive (CGRP-IR) neurons in the TG, only sections with an average of 800-1,000 ganglion cells were used for evaluation. The data are presented as the percentage of CGRP-IR cells per section. During analysis, investigators were blinded as to the identity of all samples.

In addition, 5 μm thick coronal serial sections of the brain were cut for ICAM-1 and VCAM-1 detection. Each detection was collected in 1 in 10 series. In total, 4 sections were collected from each animal (n = 5 for each group). The selected sections were placed on the super-frost plus slide (Thermoscientific, Portsmouth,

New Hampshire, USA) and heated at 60°C overnight before processing for deparaffinization. The immunoreactivity of ICAM-1, and VCAM-1 was detected by using an ultraView Universal DAB Detection Kit (Ventana, USA). The whole process will be operated on the automatic machine for slide staining (Ventana, USA). The stained sections will be dehydrated, cleared with xylene, and cover slipped. The slides will be examined under light microscope. All slides were then incubated with citrate buffer pH 6.0 (antigen retrieval solution, Dako, Glostrup, Denmark), 3% H_2O_2 (endogeneous peroxidase blocking), and 3% normal horse serum (PAN Biotech GmbH, Aidenbach, Germany) in PBS. The immunoreactivities of ICAM-1 and VCAM-1 were labeled by incubating the sections with mouse anti-ICAM-1 (1:100 dilution; BD Bioscience Pharmingen, California, USA) and rabbit anti-VCAM-1 (1:100 dilution; Santa Cruz Biotechnology, California, USA) at 37 °C for 30 min. Immunoreactivities were detected with the ultraView Universal DAB Detection Kit (Ventana Medical Systems, Inc., Arizona, USA). This whole process was performed by an automatic slide staining machine (Benchmark XT, Ventana Medical Systems, Inc., USA). All slides were dehydrated in a graded series of ethanol, mounted, cover-slipped, and scanned with a slide scanner (Aperio ScanScope, Aperio, Vista, California, USA).

To determine the number of ICAM-1 and VCAM-1 immunoreactive microvessels, a 1,000 x 600 μm grid was drawn in the area of lamina I-VI of the brain ipsilateral to the site of KCl or NaCl application. The numbers of ICAM-1 or VCAM-1 immunopositive microvessels in 8 randomly selected areas were counted. The results are reported as the average numbers of ICAM-1 or VCAM-1 immunopositive vessels per 5 mm^2. The counting process was blinded from the treatment group classification.

Ultrastructural study

Transmission electron microscopy was used to determine the effect of APAP on the cerebral microvessel ultrastructure. All 1 mm^3 frontal cortex cubes were post-fixed with 1% osmium tetroxide, and dehydrated through a graded series of ethanol. They were passed through propylene oxide and embedded in Epon (Epon 812; Electron Microscopy Sciences, Ft. Washington, USA). Semi-thin and ultra-thin sections were cut by the ultramicrotome. Semi-thin sections (0.5 μm thick) were stained with toluidine blue in order to select the suitable area. The ultra-thin sections (70-90 nm thick) were further cut with a diamond knife, placed on a copper grid and stained with uranyl acetate and lead citrate. The stained sections were examined under the transmission electron microscope (JEM 1210; JEOL, Tokyo, Japan).

The parameters of ultrastructural change of the cerebral microvessel; the number of microvilli, the number of endothelial pinocytic vesicles, astrocytic foot plate swelling assessment, and tight junction alignment were examined. Fifteen capillaries (diameter: 8-10 μm) per sample were randomly selected. Tight junction alignment was measured the angle to the basement membrane (0-20°=normal, >20°=abnormality). The number of microvilli was counted and reported as the average number of microvilli per vessel. For the number of pinocytic vesicles, two electron micrographs which cover the area of endothelial cells were taken from each capillary at a final magnification of 80,000x. The number of pinocytic vesicles was counted and reported as the average number of pinocytic vesicles per μm^2. For the astrocytic foot plate swelling, every vessel was photographed at a final magnification of 12,000x and evaluated the degree of the astrocytic foot plate swelling based on the following criteria: *normal*-no astrocytic foot plate swelling observed around the

blood vessel, *moderate*-less than 50% of the astrocytic foot plates around the blood vessel were swollen, and *severe*-more than 50% of the astrocytic foot plates around the blood vessel were swollen.

3.1.5 Western blot analysis

<u>Sample collection</u>

Two hours after the KCl or NaCl application, rats were deeply anesthetized with an excessive dose of sodium pentobarbital followed by transcardial perfusion with normal saline before decapitation and brain was removed immediately. The frontal cortex ipsilateral to the CSD activation was rapidly dissected on ice at 3 mm anterior to bregma and frozen in liquid nitrogen and stored at -80°C until extraction. Each sample was homogenized and sonicated in ice-cold RIPA lysis buffer (Cell Signaling Technology®, Massachusetts, USA), containing 20 mM Tris-HCl (pH 7.5), 150 mM NaCl, 1 mM Na_2EDTA, 1 mM EGTA, 1% NP-40, 1% sodium deoxycholate, 2.5 mM sodium pyrophosphate, 1 mM b-glycerophosphate, 1 mM Na_3VO_4, 1 μg/ml leupeptin and a protease/phosphatase inhibitor cocktail (Cell Signaling Technology®, Massachusetts, USA). The samples were then centrifuged at 12,000 x g, 4 °C for 15 min. The supernatants were collected and protein concentrations were measured by using the Pierce™ BCA protein assay kit (Thermo Scientific, Illinois, USA) with bovine serum albumin (BSA) as standard before electrophoresis.

<u>Western blotting</u>

The expressions of tight junction proteins (ZO-1, occludin, claudin-5, IgG extravasation), cell adhesion molecules (ICAM-1, VCAM-1), and enzyme CYP2E1, were

detected from the proteins of the frontal cortex. Equal amounts of protein samples (10-60 μg/μl) were denatured in 95°C for 5 min and loaded on 7.5-12.5% SDS polyacrylamide gel at 80-100 volts constant and transferred onto the nitrocellulose membranes at 0.35 Amp constant using a Mini Trans-Blot® Electrophoresis Transfer Cell (BioRad, California, USA). The membranes were blocked non-specific binding of proteins with 5% non-fat dry milk or 5% BSA in Tris-buffered saline containing with 0.1% Tween -20 (TBST) for 1 hour at room temperature. The membranes were incubated with rabbit anti-ZO-1 (1:1,000 dilution; Invitrogen, USA), rabbit anti-occludin (1:500 dilution; Invitrogen, USA), rabbit anti-claudin-5 (1:500 dilution; Santa Cruz Biotechnology, California, USA), rabbit anti-VCAM-1 (1:1,000 dilution; Santa Cruz Biotechnology, California, USA) or mouse anti-ICAM-1 (1:1,000 dilution; BD Bioscience Pharmingen, California, USA), and rabbit anti-CYP2E1 (1:2,500 dilution; Abcam) antibody at 4°C overnight to detect the expressions of ZO-1, occludin, claudin-5, VCAM-1, ICAM-1, and CYP2E1, respectively. After washing the membranes for 5 minutes for 3 times, an anti-mouse or rabbit secondary antibody conjugated with horse radish peroxidase (HRP) (Sigma, St. Louis, Missouri, USA) was incubated to the membrane for 1 hour at room temperature. For the detection of IgG extravasation, only rat anti-IgG conjugated with HRP link was applied to the membrane (1:1,000 dilution; Cell Signaling, USA). After washing each membrane, Immunoreactive bands were visualized using a chemiluminescence system (Amersham™ ECL™ Prime Western Blotting Detection Reagent, GE Healthcare Life Sciences, Buckinghamshire, UK) and exposed onto film. The intensities of the immunoreactive bands were analyzed with Image J software (National Institutes of Health, Bethesda, Maryland,

USA). The results are reported as the ratios of the densities of ZO-1, occludin, claudin-5, IgG, VCAM-1, ICAM-1, or CYP2E1 to β-actin.

3.2 *In vitro* study

In order to confirm the effect of chronic APAP treatment on the alteration of BBB integrity, the study was performed with *in vitro* study in the brain endothelial cell line.

3.2.1 Cell culture

Mouse brain endothelial cell line (bEnd.3) was purchased from the American Type Culture Collection (ATCC), USA. Cells were cultured in Dulbecco's Modified Eagle's Medium (Hyclone, USA) supplemented with 10% (v/v) heat-inactivated fetal bovine serum (FBS) (Hyclone, USA), 100 U/ml penicillin and 100 mg/ml streptomycin, and HEPES (Hyclone, USA). Cells were maintained at 37°C in a saturated humidity atmosphere containing 95% air and 5% CO_2 after which they were incubated and sub-cultured according to recommendation of ATCC. For the experiment, bEnd.3 cells were used before passage 30.

3.2.2 Cytotoxicity of APAP by MTS assay

In order to select the dose for chronic APAP treatment to bEnd.3 cell, the IC_{50} was performed using CellTiter 96® AQueous One Solution Cell Proliferation Assay (MTS assay; Promega, Wisconsin, USA). The MTS assay is a colorimetric method for determining the number of viable cells in proliferation or cytotoxicity assays. The MTS tetrazolium compound (Owen's reagent) is bioreduced by cells into a colored

formazan product that is soluble in tissue culture medium. This conversion is presumably accomplished by NADPH or NADH produced by dehydrogenase enzymes in metabolically active cells.

bEnd.3 cells were seeded at a density of $5x10^3$ cells in 96-well plate for 12 hours. After cell attachment, 100 µl of various concentrations of APAP between 0-10,000 µM were replaced and cells were incubated at 37°C in a saturated humidity atmosphere containing 95% air and 5% CO_2 for 24 hours. After that, media was removed and replaced with fresh media followed by adding 20 µl of MTS reagent. Cells were further incubated for 2 hours before recording the absorbance at 490 nm using a 96-well plate reader and the data were presented as the percentage of cell viability.

3.2.3 Study design

The experiment of *in vitro* study was divided into 2 experiments based on the experimental design as follows:

Experiment I: The study of the effect of acute APAP treatment on the CGRP induced changes of endothelial cell properties

Experiment II: The study of the effect of chronic APAP treatment (2 and 4 weeks) on the CGRP induced changes of endothelial cell properties
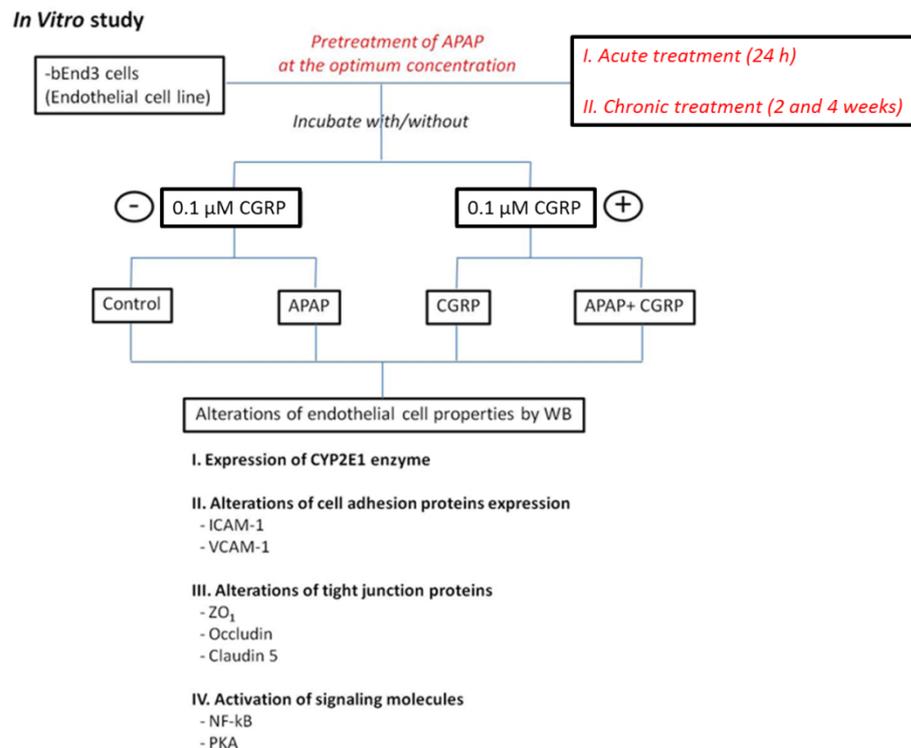
Figure 9 Study design of *in vitro* experiment.

APAP treatment

Experiment I: The study of the effect of acute APAP treatment on the CGRP induced changes of endothelial cell properties

bEnd.3 cells were seeded at the density of 2.5×10^5 into 75 cm^2 tissue culture flasks for 24 hours in a completed media containing 10% FBS at 37°C in an incubator with a saturated humidity atmosphere containing 95% air and 5% CO_2. The culture flasks were divided into 2 groups; control and APAP treated groups. After 24 hours, old culture media was removed. Fresh media was refilled in the control group while 100 µM of APAP was refilled in the APAP treated group. After 24 hours of treatment, cells from each flask were further prepared for CGRP activation.

Experiment II: The effect study of the of chronic APAP treatment (2 and 4 weeks) on the CGRP induced changes of endothelial cell properties

bEnd.3 cells were seeded at the density of 5×10^5 into 75 cm^2 tissue culture flasks for 24 h in a completed media containing 10% FBS at 37°C in an incubator with a saturated humidity atmosphere containing 95% air and 5% CO_2. bEnd.3 cells were cultured and the experiment were designed in a similar setup as with the experiment I **except** for the duration of treatment that was performed for 2 and 4 weeks as in a similar procedures as in previous studies [63]. For chronic APAP treatment, the fresh completed media was refilled in the control group while the 100 µM of APAP was refilled in the APAP treated group for 72 hours. The cells in each flask were sub-cultured and allowed to adhere overnight (24 hours) before retreatment with the same concentration of test agent. This process was continued with the same protocol for 2 and 4 weeks before CGRP activation (Figure 10).
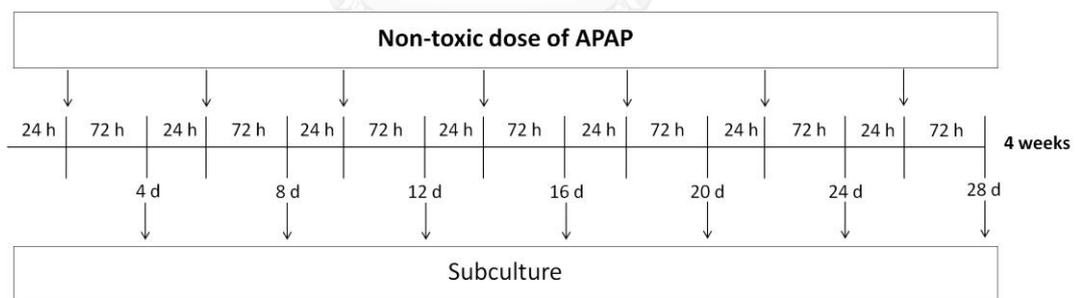

Figure 10 Schedule for chronic APAP treatment in bEnd3 cells.

<u>CGRP activation</u>

After APAP treatment, bEnd.3 cells were subdivided into 2 subgroups; with and without CGRP activation. The culture media was removed and 0.1 µM CGRP (Sigma, Israel) in the fresh media was replaced into the CGRP activated groups while only media was replaced into the non-CGRP activated groups for 1 hour. After CGRP activation, cells in all groups were collected to be examined by western blot analysis.

3.2.3 Western blot analysis

<u>Sample collection</u>

bEnd3 cells in the 75 cm^2 tissue culture flasks were washed with sterile PBS and trypsinized with 0.25% trypsin/EDTA before centrifugation at 5,000 x g, 4°C for 5 min. Cell pellet was washed with PBS followed by replacing with ice-cold RIPA lysis buffer (Cell Signaling Technology®, Massachusetts, USA), containing a protease/phosphatase inhibitor cocktail (Cell Signaling Technology®, Massachusetts, USA). Cells were sonicated and centrifuged at 12,000xg, 4°C for 15 min. The supernatants were collected and stored at -80°C until the electrophoresis was performed. Protein concentrations were measured by using the Pierce™ BCA protein assay kit (Thermo Scientific, Illinois, USA) with BSA as standard before electrophoresis.

<u>Western blotting</u>

The expression of enzyme CYP2E1, cell adhesion molecules (ICAM-1, VCAM-1), the alteration of tight junction proteins (ZO-1, occludin, claudin-5) including signaling pathway (NF-**K**B, PKA) of the proteins from the *in vitro* experiment were

detected. The protocols of western blot analysis were performed according the same design as that of the experiment in the *in vivo* study. The dilutions of primary antibodies were prepared as follows: rabbit anti-CYP2E1 (1:2,500 dilution; Abcam), rabbit anti-ZO-1 (1:1,000 dilution; Invitrogen, USA), rabbit anti-occludin (1:500 dilution; Invitrogen, USA), rabbit anti-claudin-5 (1:500 dilution; Santa Cruz Biotechnology, California, USA), rabbit anti-VCAM-1 (1:1,000 dilution; Santa Cruz Biotechnology, California,, USA) or mouse anti-ICAM-1 (1:1,000 dilution; BD Bioscience Pharmingen, California, USA), rabbit anti-phospho-NF-κB-p65 or NF-κB -p65 antibody (1:1,000 dilution; Cell Signaling Technology®, Massachusetts, USA), and rabbit anti-phospho-PKA C or PKA C$_\alpha$ antibody (1:1,000 dilution; Cell Signaling Technology®, Massachusetts, USA).

3.3. Data Analysis

The results are presented as means ± the standard error of mean (S.E.M.). Statistical analyses were performed using one-way ANOVA followed by Bonferroni's test for multiple comparison tests (Graphpad Prism 5). Probability values (*P*) values of less than 0.05 were considered statistically significant.

CHAPTER IV
RESULTS

4.1 Study I: The effect of acute and chronic APAP treatment on the alterations of the cerebral vessels in the conditions with and without the activation of CSD

In this study, APAP at the dose of 200 mg/kg bw was used as a drug treatment. The results demonstrated that neither acute nor chronic treatment affected the rats' body weights. There was no significant difference in the average body weights between the control and 30-day APAP-treated groups. The results also confirmed that 30 days of APAP treatment had no effect on liver since which evaluated by no change in level of three major functional enzymes of the liver (alanine aminotransferase; AST, aspartate aminotransferase; ALT, alkaline phosphatase; ALP) observed in the rats with 30-day APAP treatment. Moreover, the morphological study of the liver revealed no significant differences between the APAP-treated and non-APAP treated rats (data not shown).

Effect of APAP treatment on the CSD-induced ultrastructural alterations of cerebral endothelial cells

The results revealed that the CSD induction caused the alteration in the ultrastructure of the cerebral microvessels as indicated by the increase in the numbers of microvilli and pinocytic vesicles in the endothelial cells obtained from the CSD group as compared with those observed in the control group ($P<0.05$). Astrocytic foot plate swelling around the cerebral vessels was clearly demonstrated in the animals that underwent CSD activation.

Single (0-day) APAP treatment

The results revealed that pretreatment with APAP for one hour could attenuate the alterations of cerebral microvessels induced by CSD. The numbers of microvilli and pinocytic vesicles in the APAP pretreatment group were significantly lower than those observed in the CSD group (Figure 11B, Figure 11C and Table 1).

Acute APAP treatment also had a protective effect against the astrocytic foot plate swelling induced by CSD. The proportion of astrocytic foot plate swelling in the perivascular areas of the vessels obtained from the APAP pretreated group was decreased when compared to the CSD group (Figure 11, Figure 13A). No significant difference was observed in the ultrastructural alterations (astrocytic foot plate swelling and formation of microvilli and pinocytic vesicle) between the cerebral microvessels obtained from the acute APAP treatment group and the control group.

Moreover, the alteration of the tight junction alignment was evaluated based on the angle between the tight junction plane of the endothelium and the vessel lumen. Tight junction alignment was classified into following criteria: *normal*-less than 20°, and *abnormality (high angle)*-between 21°-90°. The results demonstrated that the proportion of normal angle tight junction was observed in the control and APAP-treated with or without CSD activation. However, the high angle was observed in the CSD group (Figure 13B).
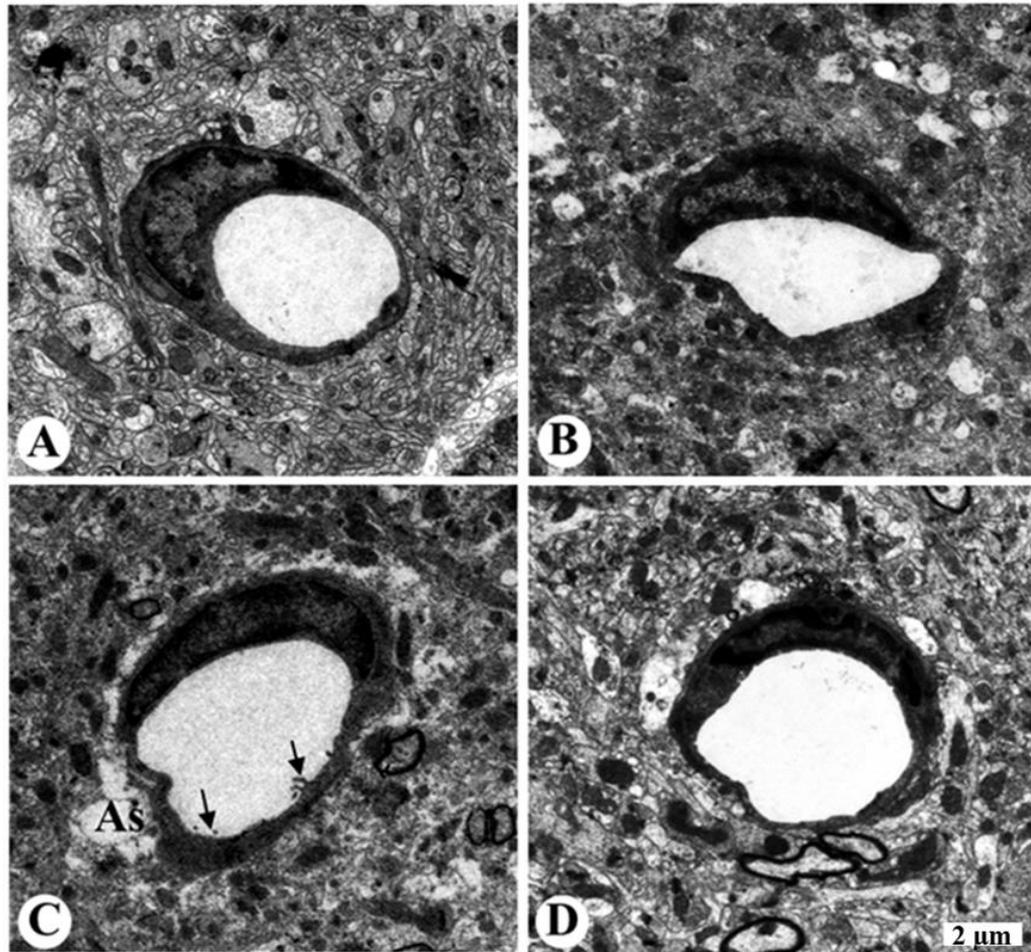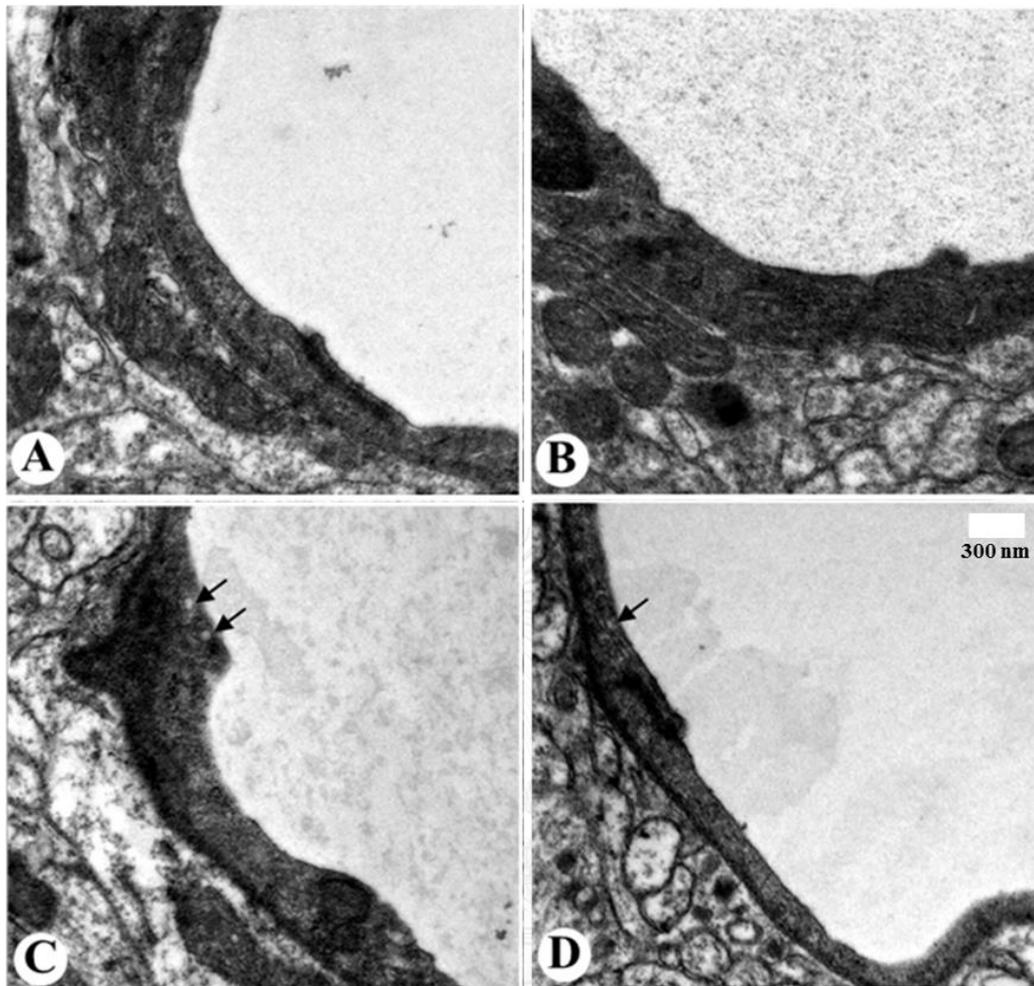
Figure 11 Effects of 0-day of APAP treatment on CSD-induced ultrastructural changes of microvillous formation and astrocytic foot plate swelling in cerebral endothelial cells.

Electron micrographs showing the ultrastructures of cerebral microvessels obtained from the control (A), APAP-treated without CSD (B), CSD (C), and APAP-treated with CSD (D) groups. Microvillous formation (arrow); Swelling of the astrocytic foot plate (As). Scale bar = 2 μm.

Figure 12 Effects of 0-day of APAP treatment on CSD-induced ultrastructural changes of pinocytic vesicles in cerebral endothelial cells.

Electron micrographs showing pinocytic formations in the endothelial cells obtained from the control (A), APAP-treated without CSD (B), CSD (C), and APAP-treated with CSD (D) groups. Pinocytic vesicle (arrow). Scale bar = 200 nm.
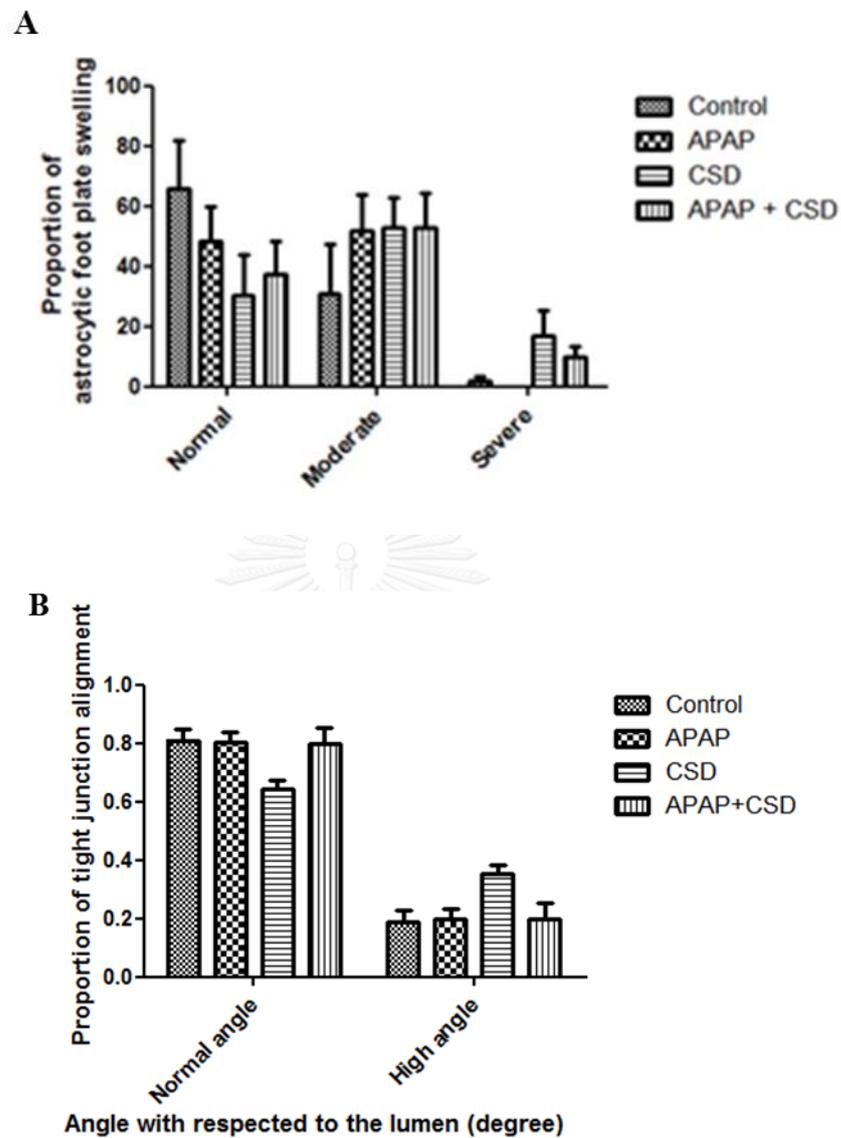
Figure 13 Effects of 0-day of APAP treatment on CSD-induced ultrastructural changes in astrocytes and tight junction.

Histograms showing the proportions of astrocytic foot plate swelling (A) and tight junction alignment (B) observed in the control, APAP-treated without CSD, CSD, and APAP-treated with CSD groups

15-day of APAP treatment

In contrast, chronic APAP treatment for 15 days revealed the opposite effect on the on the ultrastructural alterations against CSD activation. The results obtained from chronic APAP treatment exhibited a significant increase in the number of microvilli and pinocytic vesicles comparing with those of the control group. These abnormalities of cerebral microvessels were higher in combination with CSD activation. The data are shown in Figure 14, Figure 15 and Table 1. The astrocytic foot plate swelling in the perivascular areas of the cerebral microvessels obtained from the chronic APAP-treated with or without CSD activation group was also demonstrated the moderate degree when compared with the control group. The data are shown in Figure 14, Figure 16A. Moreover, the measurement of the tight junction alignment also demonstrated the proportion of tight junction with high angle in the animals with APAP treatment (Figure 16B).
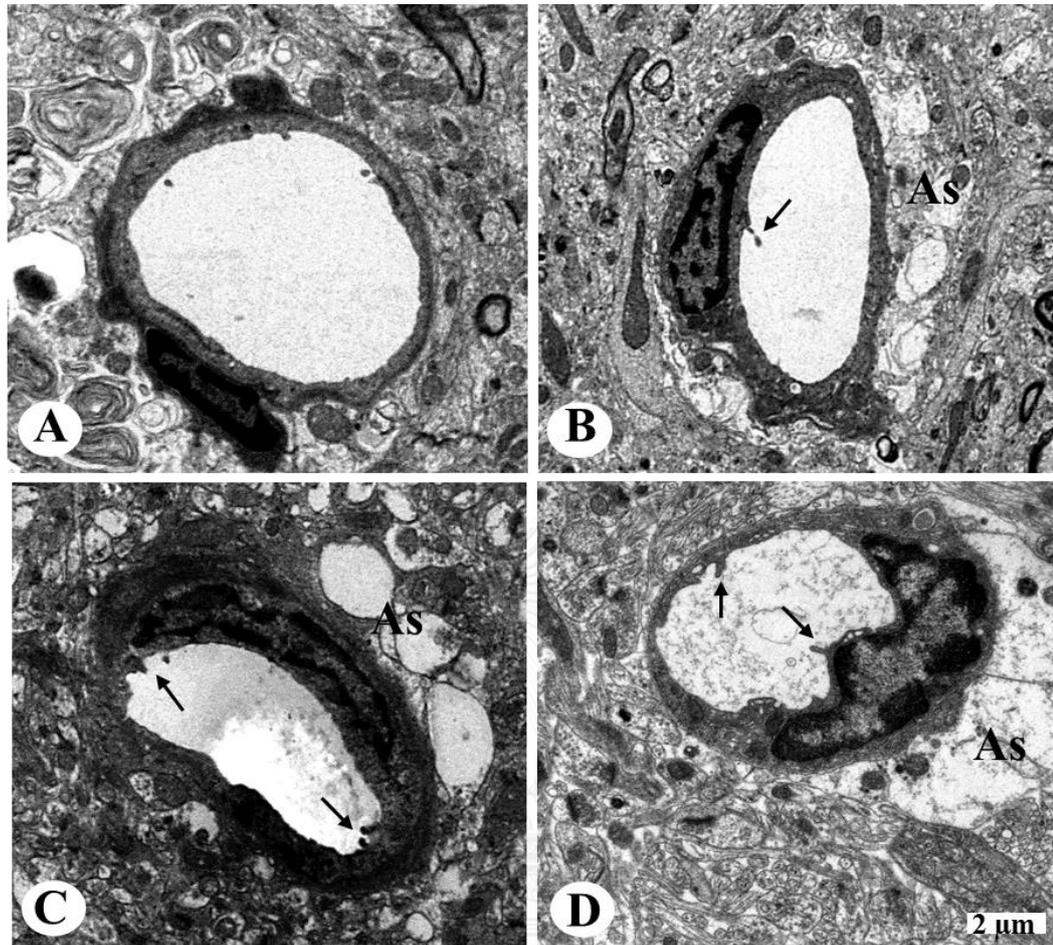
Figure 14 Effects of 15-day of APAP treatment on CSD-induced ultrastructural changes of microvillous formation and astrocytic foot plate swelling in cerebral endothelial cells.

Electron micrographs showing the ultrastructures of cerebral microvessels obtained from the control (A), APAP-treated without CSD (B), CSD (C), and APAP-treated with CSD (D) groups. Microvillous formation (arrow); Swelling of the astrocytic foot plate (As). Scale bar = 2 μm.
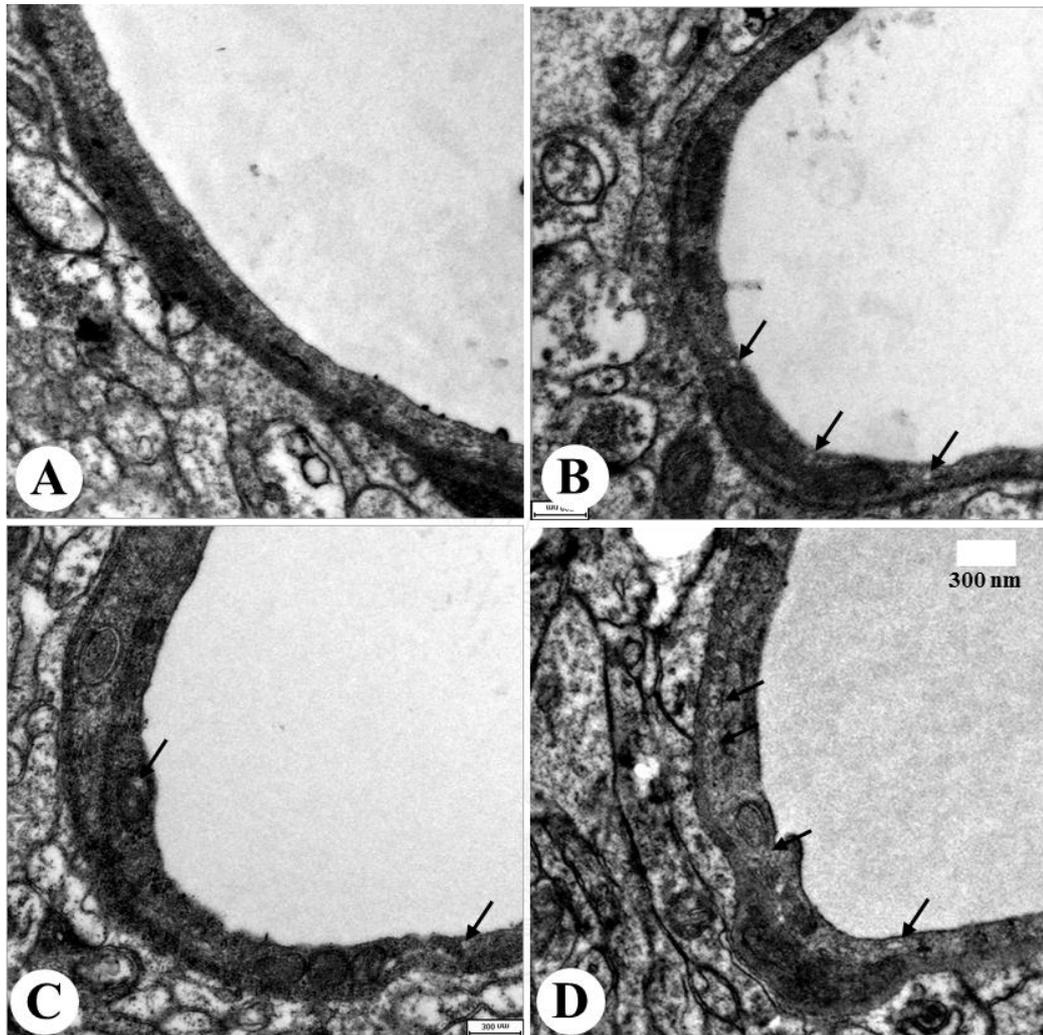
Figure 15 Effects of 15-day of APAP treatment on CSD-induced ultrastructural changes of pinocytic vesicles in cerebral endothelial cells.

Electron micrographs showing pinocytic formations in the endothelial cells obtained from the control (A), APAP-treated without CSD (B), CSD (C), and APAP-treated with CSD (D) groups. Pinocytic vesicle (P). Scale bar = 200 nm.
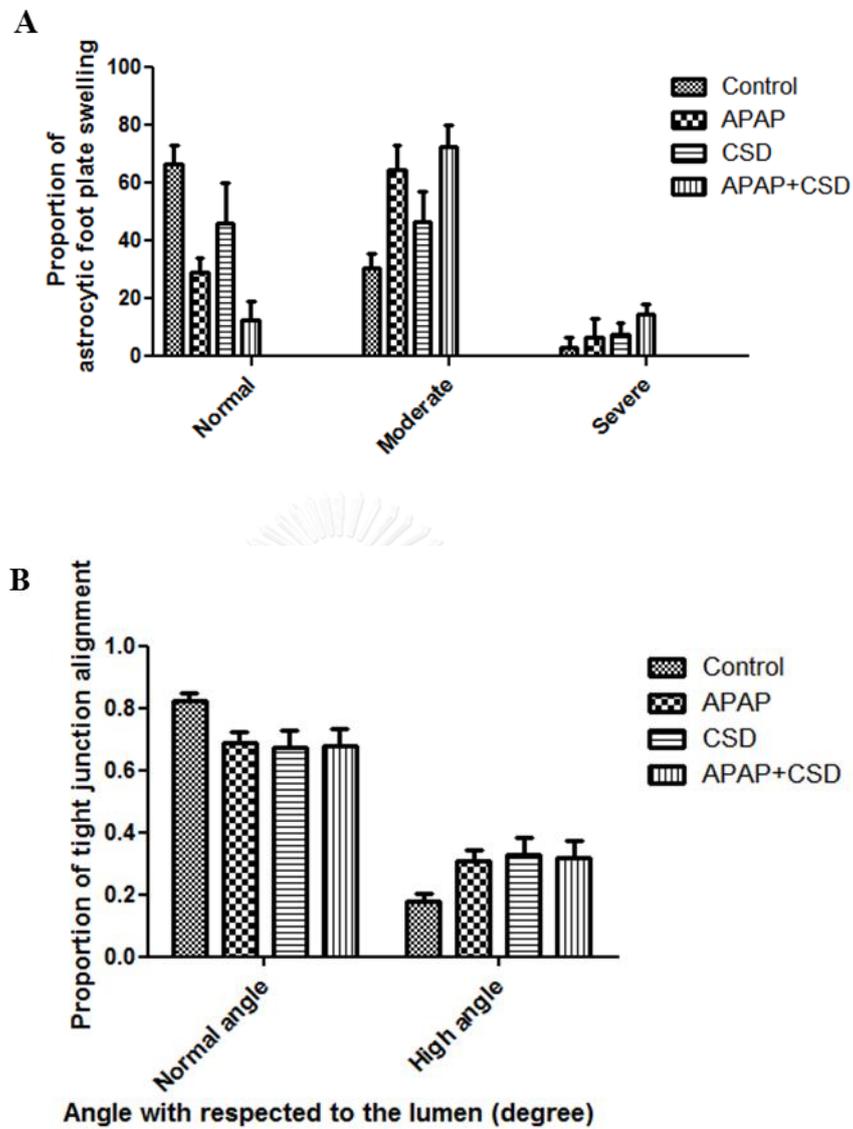
Figure 16 Effects of 15-day of APAP treatment on CSD-induced ultrastructural changes in astrocytes and tight junction.

Histograms showing the proportions of astrocytic foot plate swelling (A) and tight junction alignment (B) observed in the control, APAP-treated without CSD, CSD, and APAP-treated with CSD groups

30-day of APAP treatment

Interestingly, the ultrastructural alterations of the rats that received chronic APAP treatment for30 days were significant higher than thoseobserved in 15 days of APAP treatment. The results demonstrated that a significant increase in the number of microvilli and pinocytic vesicles was observed in the APAP-treated group as compared with those from the control group ($P<0.01$). These data are shown in Figure 17, Figure 18 and Table 1. These alterations of the cerebral microvessels, including astrocytic foot plate swelling, were more severe in chronic APAP treatment with CSD activation. In combination with CSD activation, the number of pinocytic vesicles in the endothelial cells was significant higher than that observed in the CSD group. With CSD activation, the swelling of astrocytic foot plate around the cerebral microvessels in the chronic APAP treatment were more prominent than those observed in the animal without treatment. These data are shown in Figure 17, Figure 19A.

Additionally, the evaluation of the tight junction alignment demonstrated that the proportion of normal angle tight junction was observed only in the control group. While the CSD and APAP-treated with or without CSD group demonstrated the high degree of angle (Figure 19B).
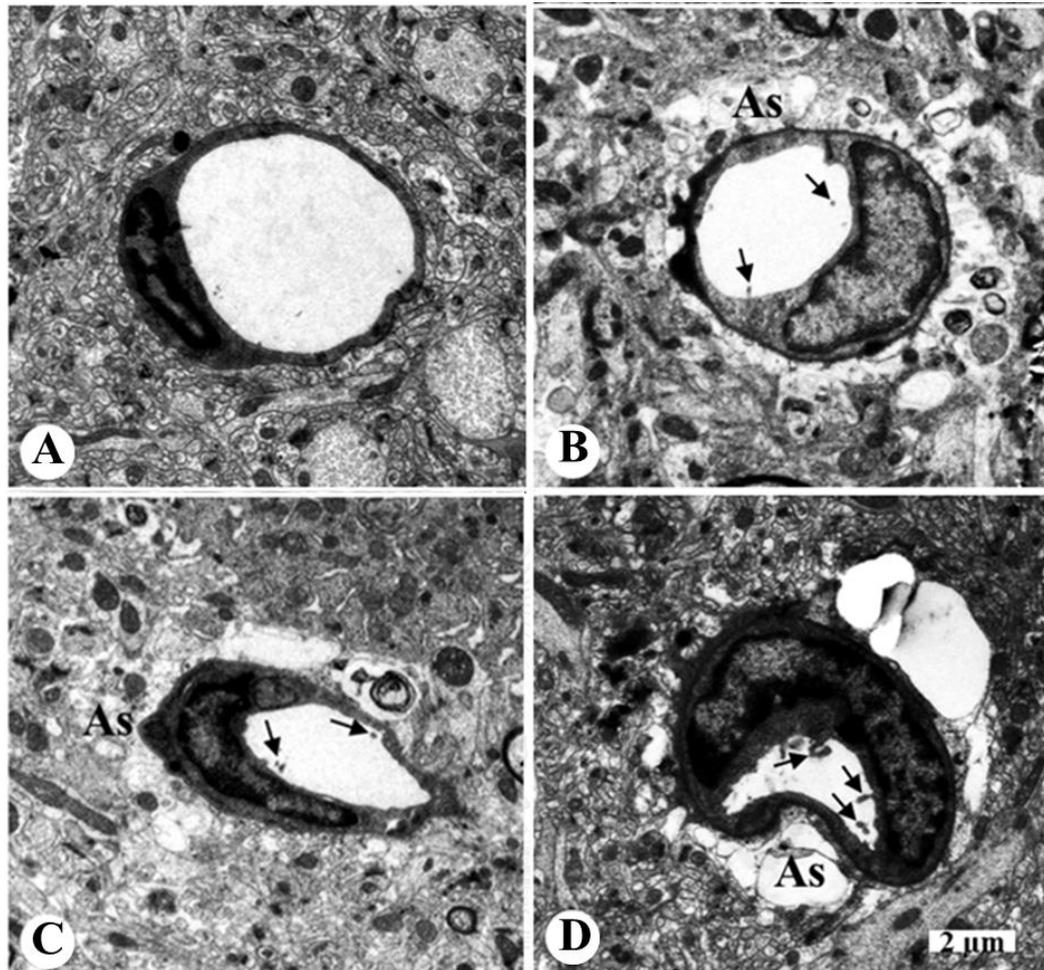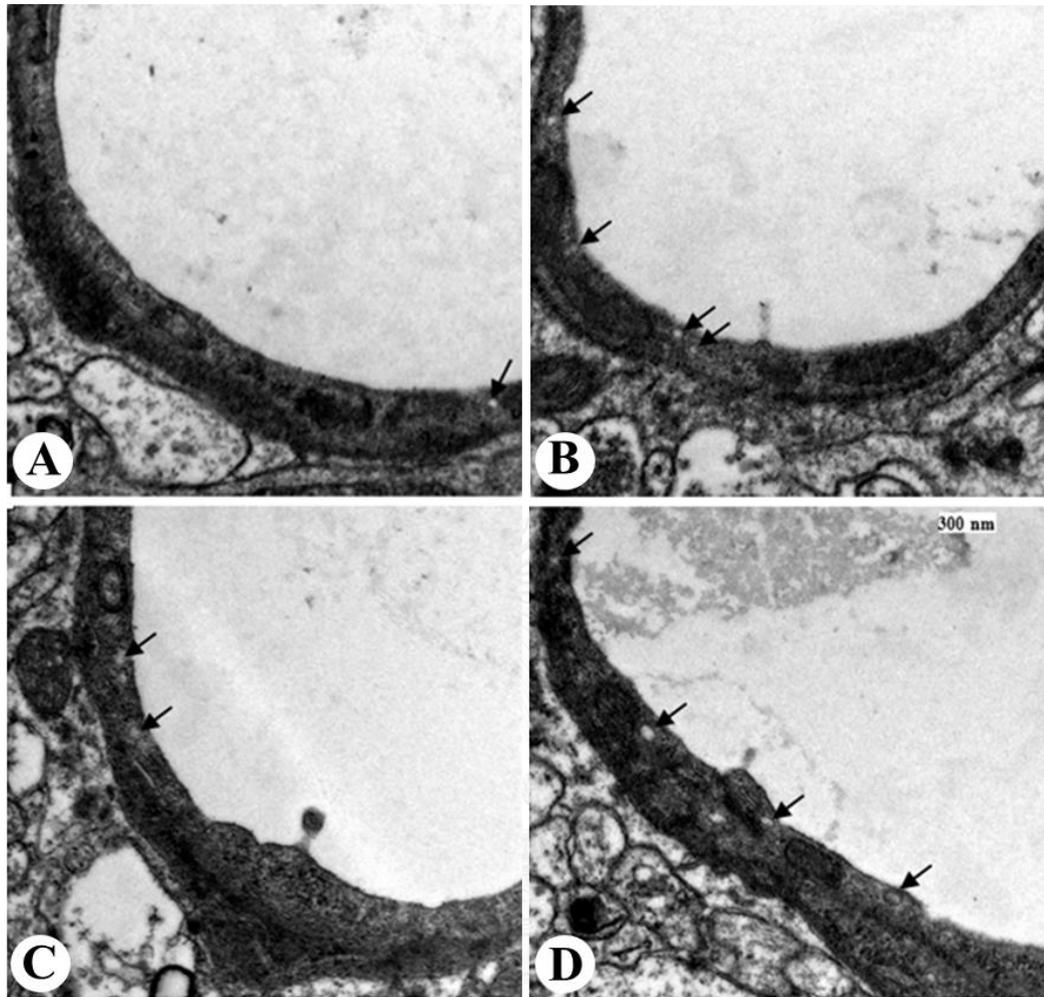
Figure 17 Effects of 30-day of APAP treatment on CSD-induced ultrastructural changes of microvillous formation and astrocytic foot plate swelling in cerebral endothelial cells.

Electron micrographs showing the ultrastructures of cerebral microvessels obtained from the control (A), APAP-treated without CSD (B), CSD (C), and APAP-treated with CSD (D) groups. Microvillous formation (arrow); Swelling of the astrocytic foot plate (As). Scale bar = 2 μm.

Figure 18 Effects of 30-day of APAP treatment on CSD-induced ultrastructural changes of pinocytic vesicles in cerebral endothelial cells.

Electron micrographs showing pinocytic formations in the endothelial cells obtained from the control (A), APAP-treated without CSD (B), CSD (C), and APAP-treated with CSD (D) groups. Pinocytic vesicle (P). Scale bar = 200 nm.
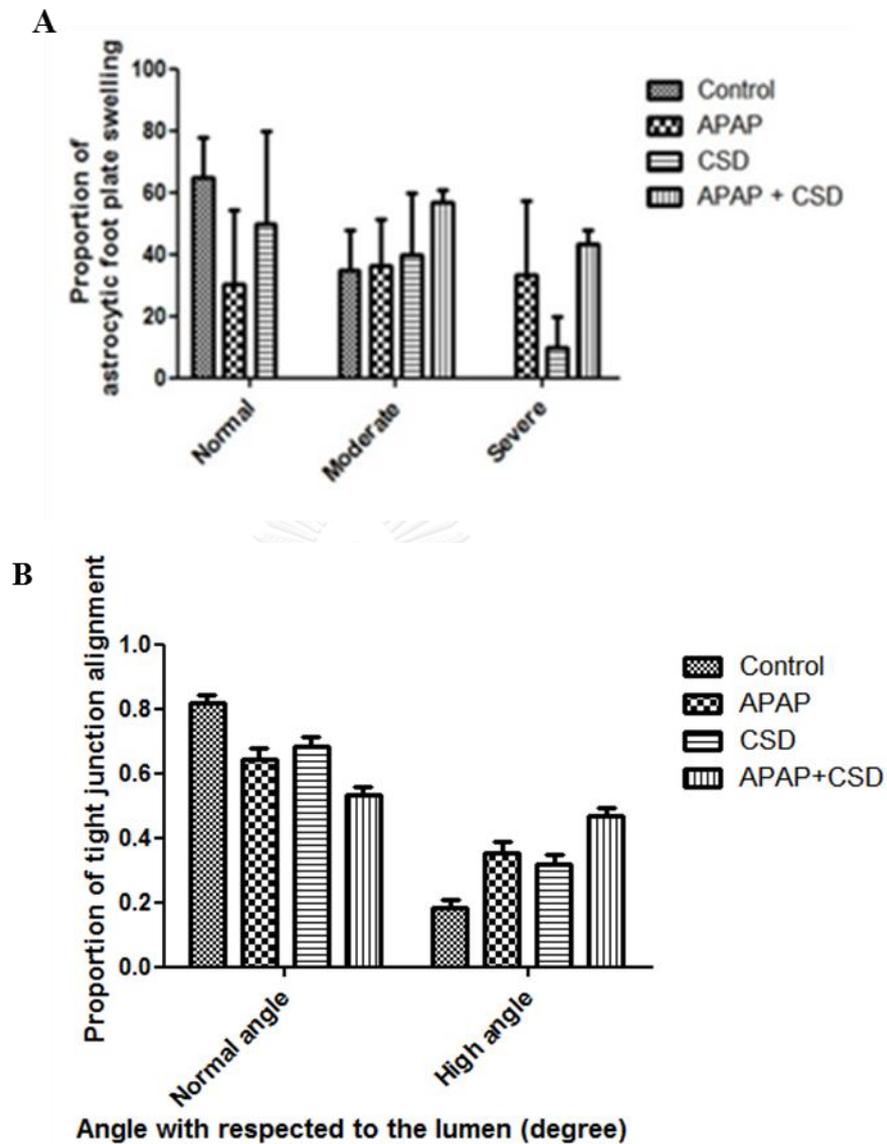
Figure 19 Effects of 30-day of APAP treatment on CSD-induced ultrastructural changes in astrocytes and tight junction.

Histograms showing the proportions of astrocytic foot plate swelling (A) and tight junction alignment (B) observed in the control, APAP-treated without CSD, CSD, and APAP-treated with CSD groups

Table 1 Effects of 0-, 15-, and 30-day of APAP treatments on CSD-induced ultrastructural changes in cerebral endothelial cells.

Variables	Control group	APAP-treated group	CSD group	APAP-treated with CSD group
0-day of APAP treatment				
Pinocytic vesicles (number per μm^2)	16.89±0.92	18.13±0.58	22.96±1.26*	19.12±0.89
Microvilli (number per vessel)	1.20±0.19	1.32±0.32	2.54±0.41*	1.38±0.21
15-day of APAP treatment				
Pinocytic vesicles (number per μm^2)	16.11±0.42	23.64±2.06*	22.18± 0.99	26.77±1.55**
Microvilli (number per vessel)	0.7133±0.13	2.070±0.21**	2.890±0.12**	2.233±0.10**
30-day of APAP treatment				
Pinocytic vesicles (number per μm^2)	17.16±0.48	30.15±2.25**	23.35±0.55	33.54±1.82***[#]
Microvilli (number per vessel)	0.86±0.35	2.60±0.27**	2.80±0.15**	2.98±0.18***

* *P* <0.05 compared with the control group.

** *P* <0.01 compared with the control group.

*** *P* <0.001 compared with the control group.

[#] *P* <0.05 compared with the CSD group.

Effect of APAP treatment on the CSD-induced alterations of tight junction proteins on cerebral endothelial cells

ZO-1

In order to investigate the effect of chronic APAP treatment on BBB integrity, the expression of the tight junction protein ZO-1 (220 kDa) was detected in the cerebral cortex obtained from all experimental groups. When compared with the control group, the CSD-activated group demonstrated the decrease of ZO-1 level in all experiments. Pretreatment with acute APAP treatment could elevate the level of ZO-1expression against CSD activation (Figure 20). However, 2 weeks of APAP treatment, the expression of ZO-1 was significant decreased in the APAP-treated with CSD activation group ($P<0.05$; Figure 21). Moreover, 4 weeks of APAP treatment, the alteration of ZO-1 levels was significant decreased when compared with the control, APAP-treated alone, and CSD groups ($P<0.001$; Figure 22).
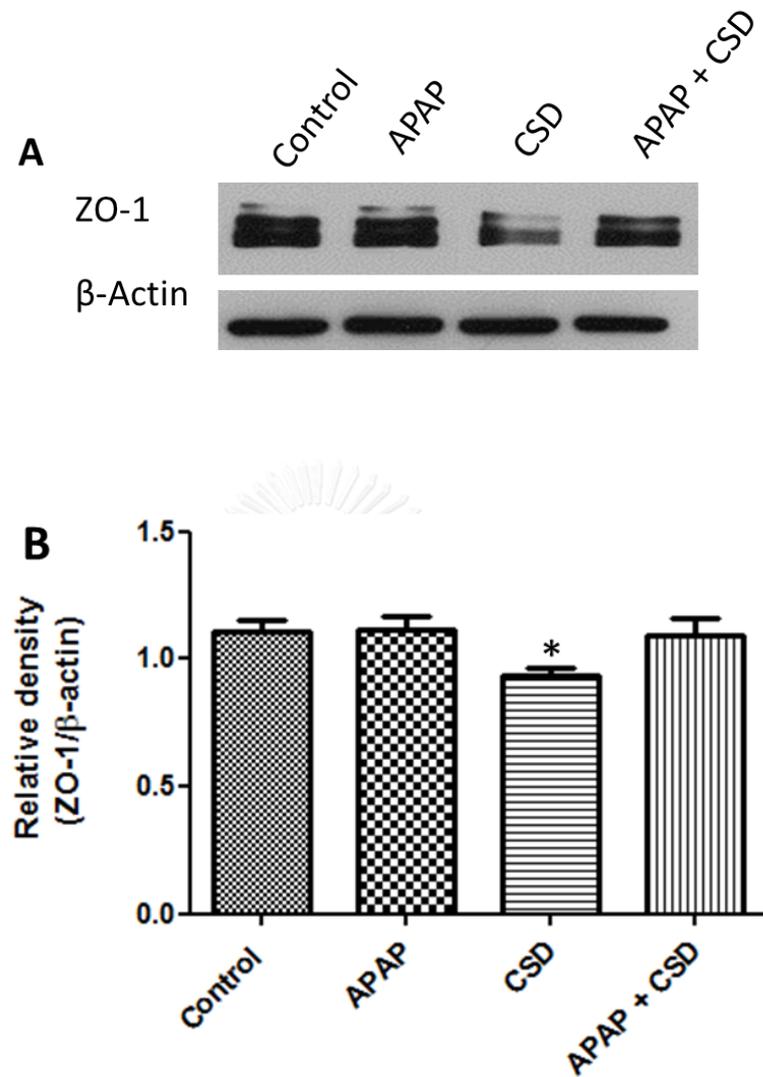
Figure 20 Effect of 0-day of APAP treatment on the CSD-induced alterations of ZO-1 expression on cerebral endothelial cells.

(A) The ZO-1 protein levels were analyzed by western blotting and are shown for the control, APAP-treated without CSD, CSD, and APAP-treated with CSD groups.

(B) The quantitative data are expressed as relative densities compared to β-actin.

Figure 21 Effect of 15-day of APAP treatment on the CSD-induced alterations of ZO-1 expression on cerebral endothelial cells.

(A) The ZO-1 protein levels were analyzed by western blotting and are shown for the control, APAP-treated without CSD, CSD, and APAP-treated with CSD groups.

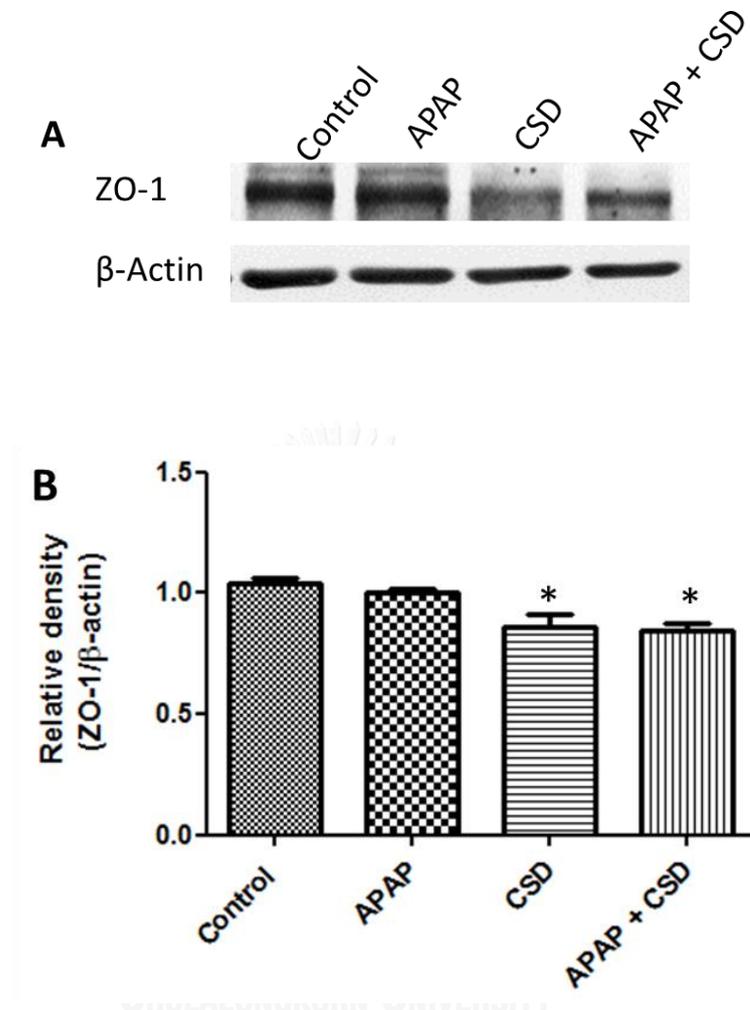(B) The quantitative data are expressed as relative densities compared to β-actin.

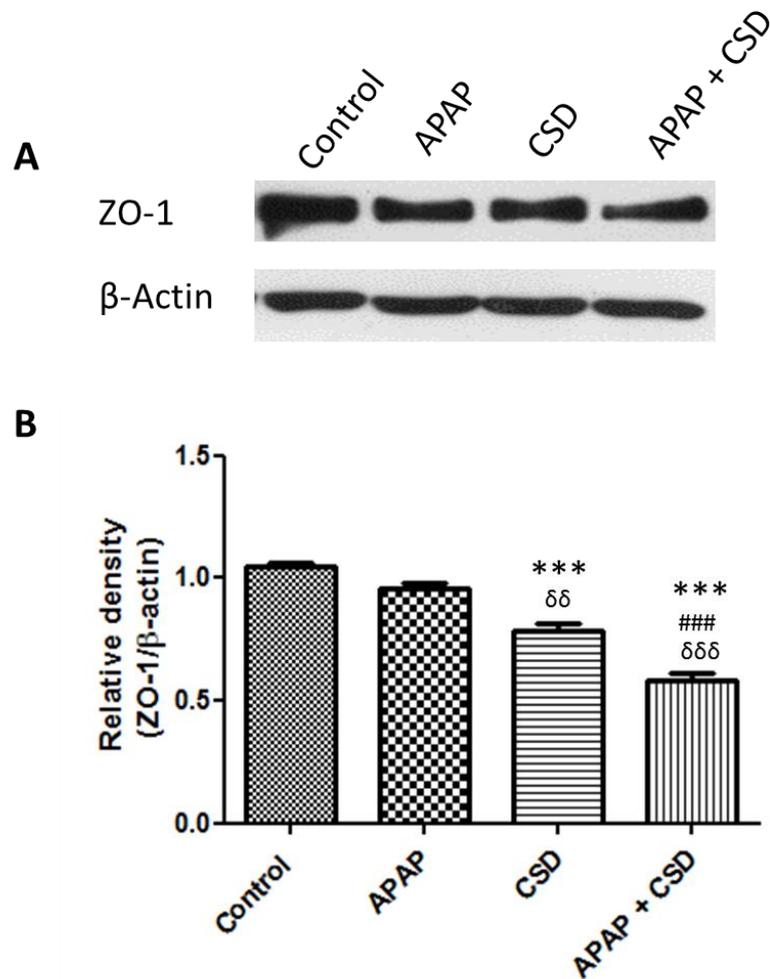*$P<0.05$ compared to the control group.

Figure 22 Effect of 30-day of APAP treatment on the CSD-induced alterations of ZO-1

expression on cerebral endothelial cells.

(A) The ZO-1 protein levels were analyzed by western blotting and are shown for the

control, APAP-treated without CSD, CSD, and APAP-treated with CSD groups.

(B) The quantitative data are expressed as relative densities compared to β-actin.

***$P<0.001$ compared to the control group, [###]$P<0.001$ compared to the CSD group,

[δδ]$P<0.01$ compared to the APAP-treated without CSD group, [δδδ]$P<0.001$ compared

to the APAP-treated without CSD group.

Occludin

To evaluate the effect of chronic APAP treatment on the expression of tight junction proteins, occludin (65 kDa) was detected in the cerebral cortex obtained from all experimental groups. The results revealed that induction of CSD could decrease the expression of occludin as compared with the control group. With acute APAP treatment, either alone or combination with CSD, the level of occludin expression did not differ from the control group (Figure 23). However, after 2 weeks of APAP treatment, the expression of occludin was decrease when combined with CSD activation as compared with the control (Figure 24). Moreover, the decrease of this tight junction protein was more severe after chronic APAP treatment for 4 weeks (Figure 25).

Figure 23 Effect of 0-day of APAP treatment on the CSD-induced alterations of

occludin expression on cerebral endothelial cells.

(A) The occludin protein levels were analyzed by western blotting and are shown for

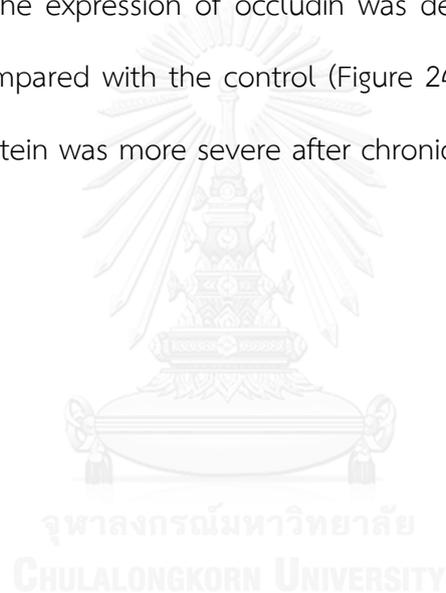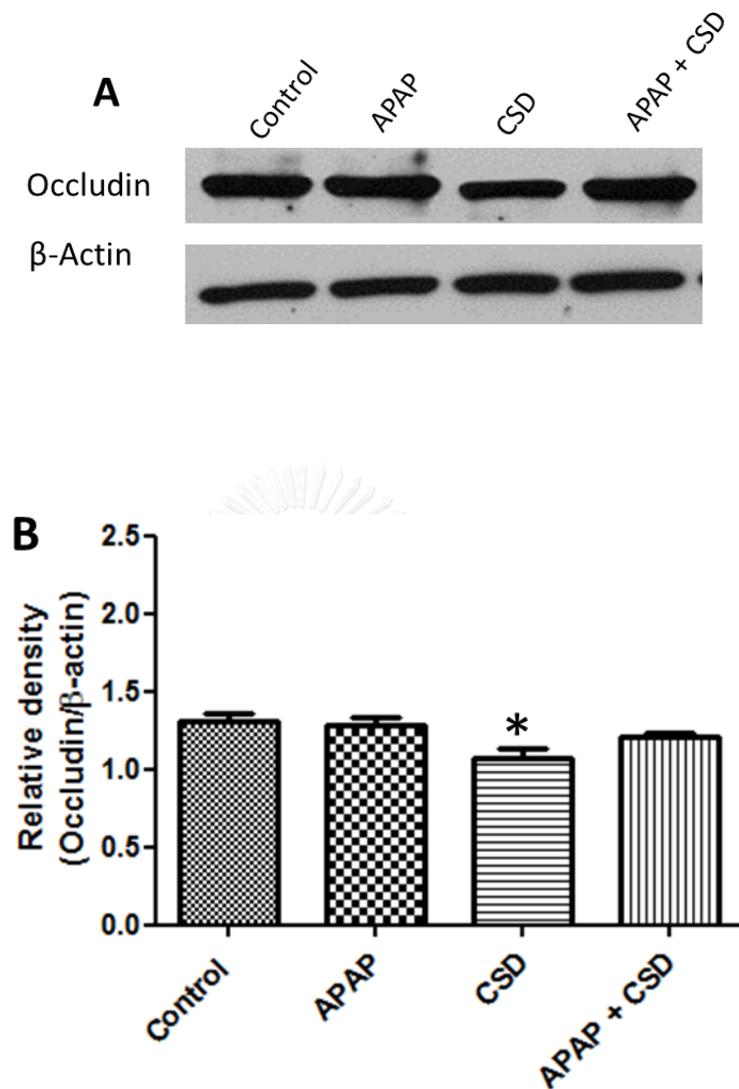the control, APAP-treated without CSD, CSD, and APAP-treated with CSD groups.

(B) The quantitative data are expressed as relative densities compared to β-actin.

*$P<0.05$ compared to the control group, #$P<0.05$ compared to the CSD group,

$\delta$$P<0.05$ compared to the APAP-treated without CSD group.

Figure 24 Effect of 15-day of APAP treatment on the CSD-induced alterations of
occludin expression on cerebral endothelial cells.
(A) The occludin protein levels were analyzed by western blotting and are shown for

the control, APAP-treated without CSD, CSD, and APAP-treated with CSD groups.

(B) The quantitative data are expressed as relative densities compared to β-actin.

*$P<0.05$ compared to the control group, #$P<0.05$ compared to the CSD group,

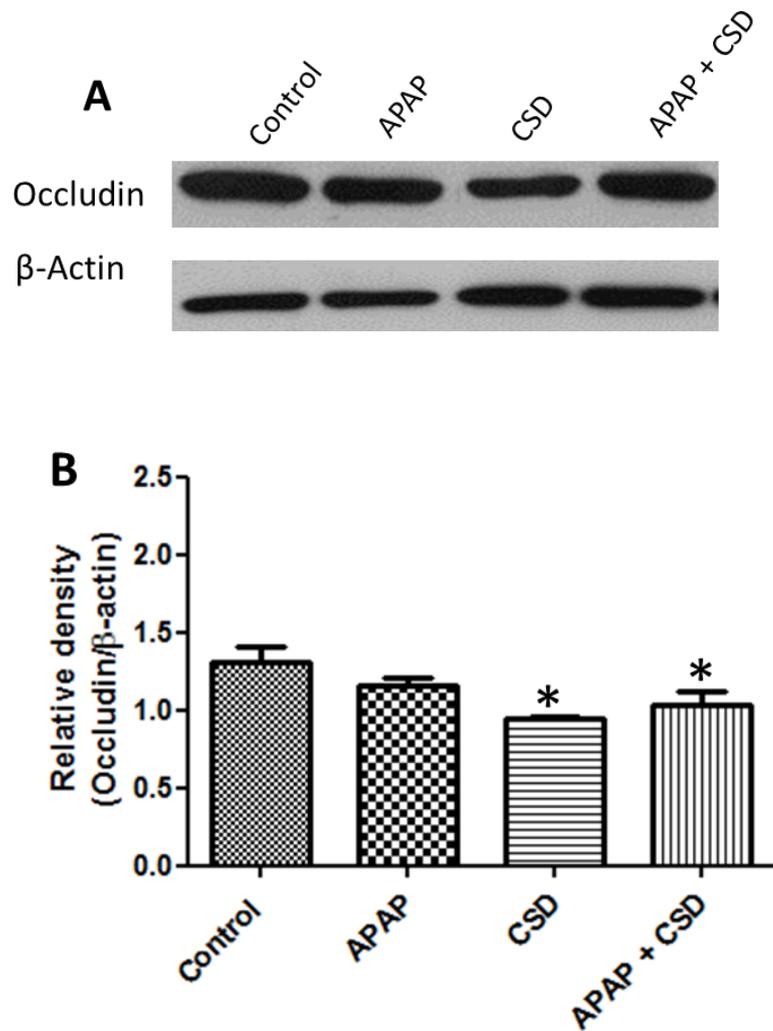$\delta$$P<0.05$ compared to the APAP-treated without CSD group.

Figure 25 Effect of 30-day of APAP treatment on the CSD-induced alterations of occludin expression on cerebral endothelial cells.

(A) The occludin protein levels were analyzed by western blotting and are shown for

the control, APAP-treated without CSD, CSD, and APAP-treated with CSD groups.

(B) The quantitative data are expressed as relative densities compared to β-actin.

*P<0.05 compared to the control group

Claudin-5

In order to investigate the effect of chronic APAP treatment on the BBB integrity, the expression of the tight junction protein claudin-5 (23 kDa) was also observed in the cerebral cortex obtained from all experimental groups. The results demonstrated that acute APAP treatment had no effect on the expression of claudin-5. Moreover,   pretreatment with APAP for 1 h could protect cerebral vessels against CSD activation (Figure 26). In contrast, chronic APAP treatment (≥2 weeks) demonstrated the opposite effect of this drug to the expression of caludin-5. The results revealed that chronic APAP treatment alone or in combination with CSD activation resulted in the significant decrease when compared with the control groups (Figure 27 Figure 28).
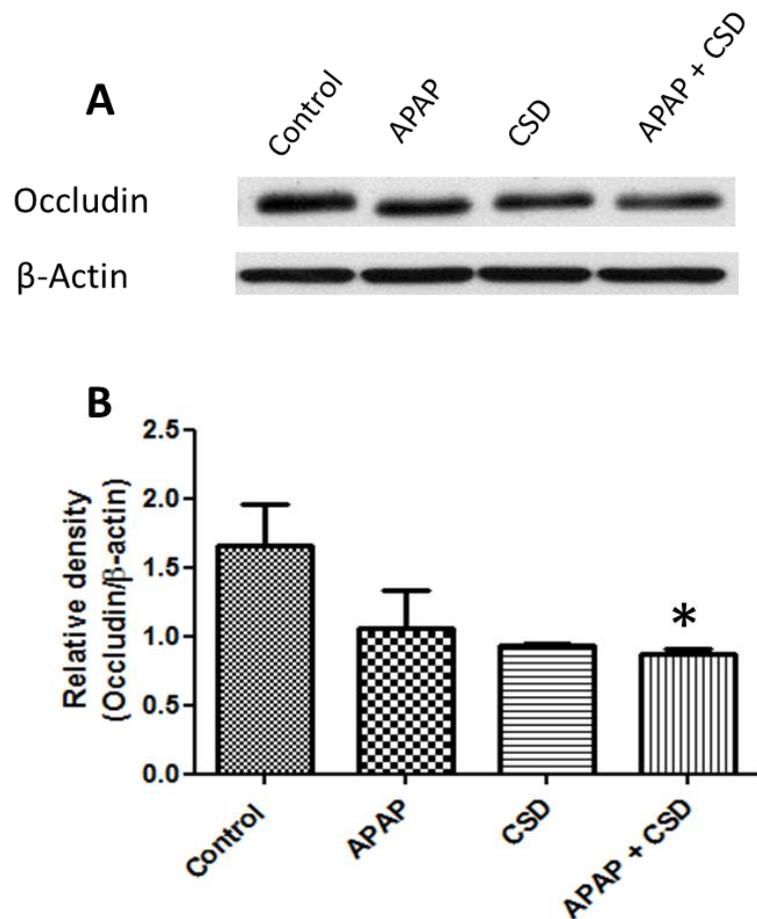
Figure 26 Effect of 0-day of APAP treatment on the CSD-induced alterations of

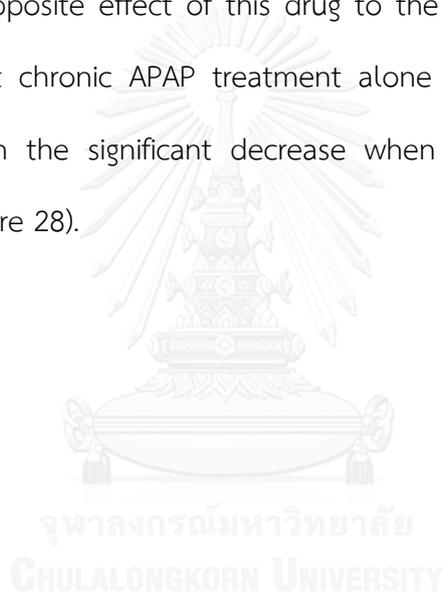claudin-5 expression on cerebral endothelial cells.

(A) The claudin-5 protein levels were analyzed by western blotting and are shown for

the control, APAP-treated without CSD, CSD, and APAP-treated with CSD groups.

(B) The quantitative data are expressed as relative densities compared to β-actin.

*P<0.05 compared to the control group, #P<0.05 compared to the CSD group,

δP<0.05 compared to the APAP-treated without CSD group.

Figure 27 Effect of 15-day of APAP treatment on the CSD-induced alterations of claudin-5 expression on cerebral endothelial cells.

(A) The claudin-5 protein levels were analyzed by western blotting and are shown for the control, APAP-treated without CSD, CSD, and APAP-treated with CSD groups.

(B) The quantitative data are expressed as relative densities compared to β-actin.

*$P<0.05$ compared to the control group, #$P<0.05$ compared to the CSD group, $^{\delta}P<0.05$ compared to the APAP-treated without CSD group.
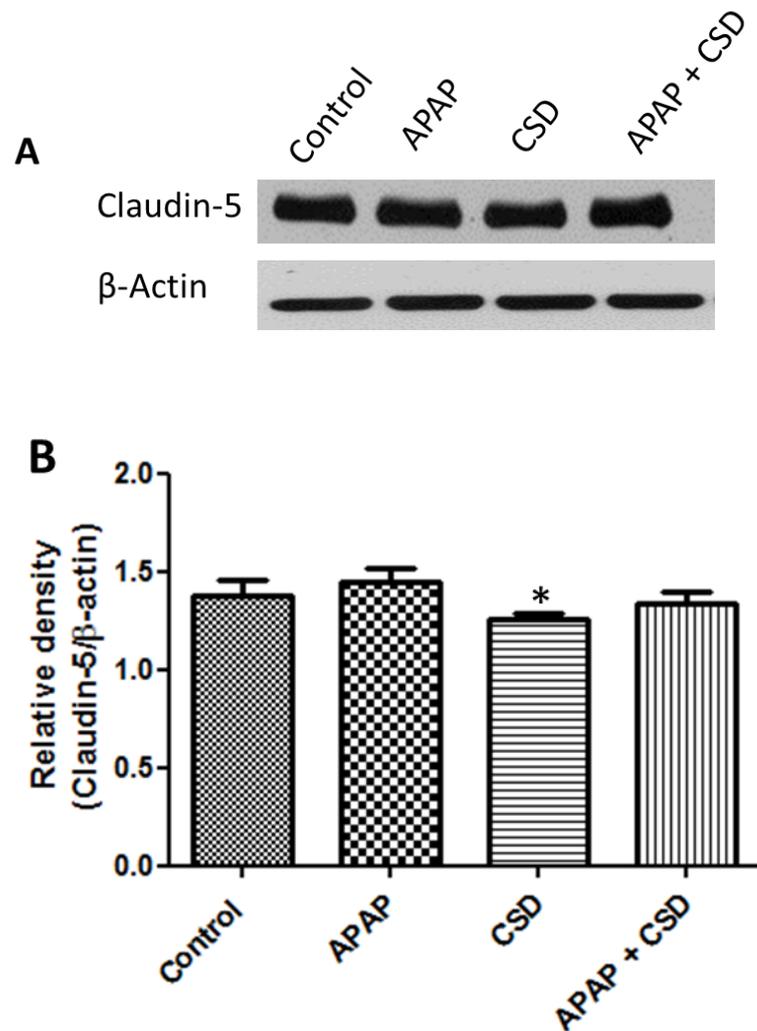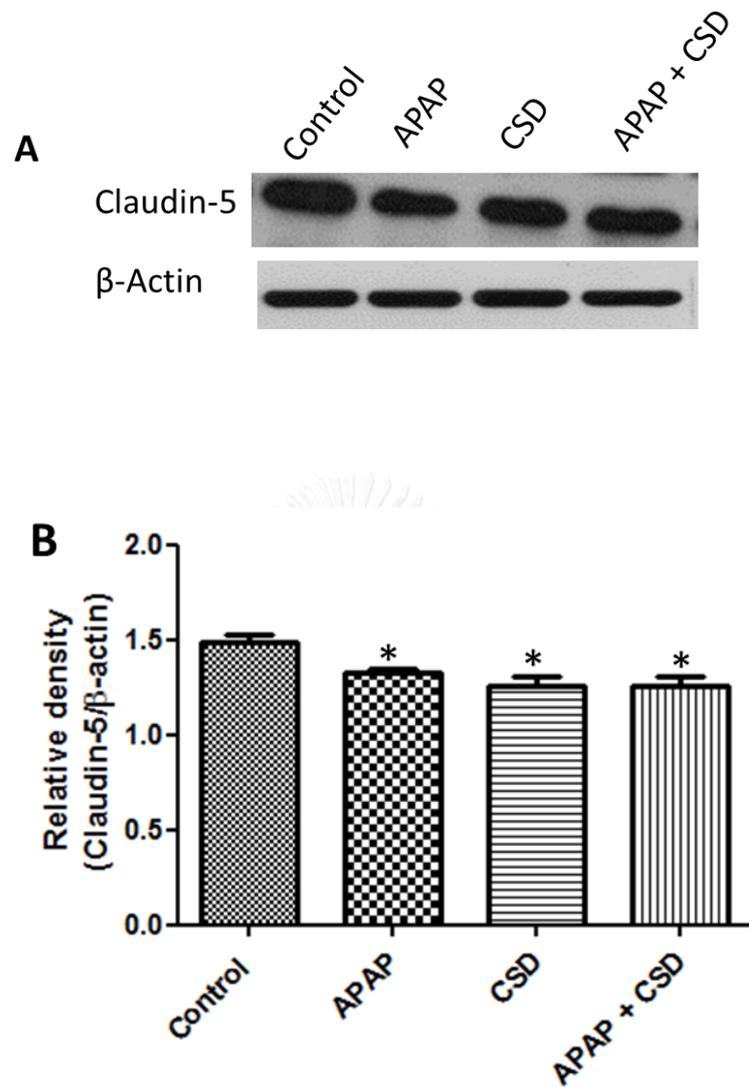
Figure 28 Effect of 30-day of APAP treatment on the CSD-induced alterations of claudin-5 expression on cerebral endothelial cells.

(A) The claudin-5 protein levels were analyzed by western blotting and are shown for the control, APAP-treated without CSD, CSD, and APAP-treated with CSD groups.

(B) The quantitative data are expressed as relative densities compared to β-actin.

*P<0.05 compared to the control group, #P<0.05 compared to the CSD group, δP<0.05 compared to the APAP-treated without CSD group.

IgG extravasation
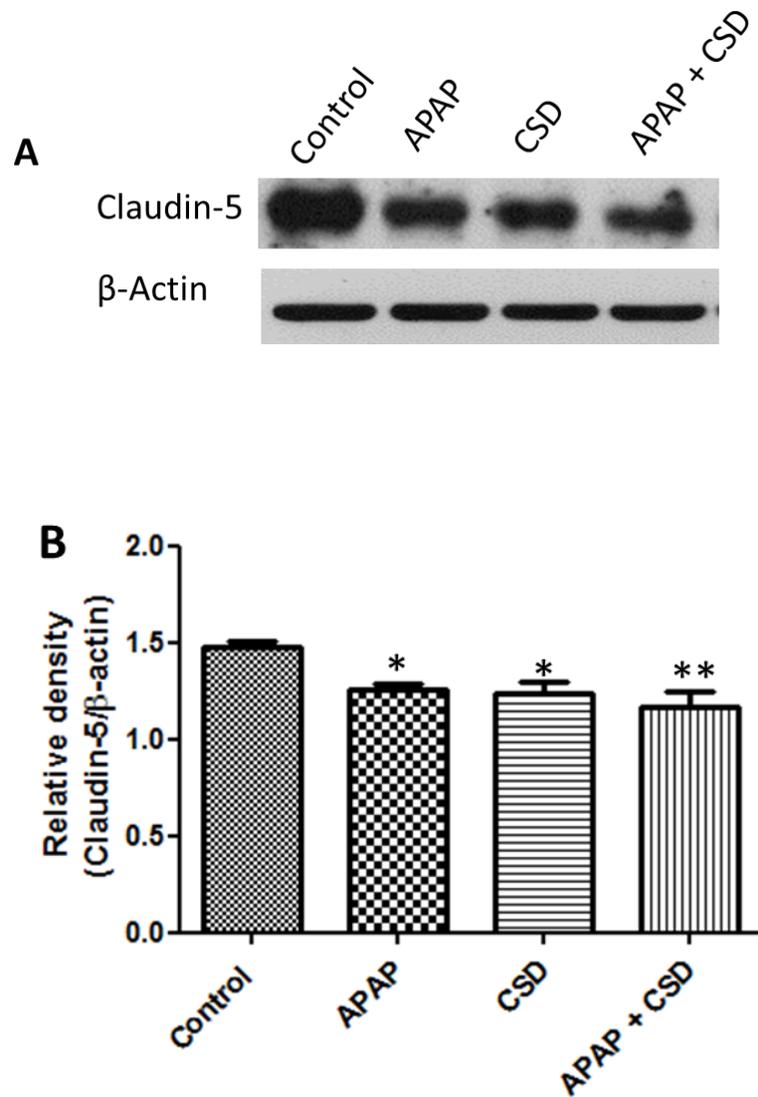
IgG extravasation is an indicator which indicates the damage of BBB integrity. In this study, the expression of IgG light chain (25 kDa) was analyzed in the cerebral cortex obtained from all experimental groups. The results demonstrated that the induction of CSD could induce an increase of IgG level as compared with that in the control group. With acute APAP treatment, there was no change in the level of IgG and still protected cerebral vessels from CSD activation (Figure 29). At 2 weeks of treatment, the level of IgG was increase either in the APAP-treated alone or in combination with CSD activation (Figure 30). Interestingly, the increase in abnormality of IgG level was observed in the animal-treated with APAP for 4 weeks. The results demonstrated that chronic APAP treatment alone increased the level of IgG in the brain as compared with the control group. When combined with CSD activation, the level of IgG was significantly higher than those observed in the other groups (Figure 31).

Figure 29 Effect of 0-day of APAP treatment on the CSD-induced alterations of IgG extravasation on cerebral endothelial cells.

(A) The IgG extravasation protein levels were analyzed by western blotting and are shown for the control, APAP-treated without CSD, CSD, and APAP-treated with CSD groups.

(B) The quantitative data are expressed as relative densities compared to β-actin.

*$P<0.05$ compared to the control group, #$P<0.05$ compared to the CSD group, $\delta P<0.05$ compared to the APAP-treated without CSD group.

Figure 30 Effect of 15-day of APAP treatment on the CSD-induced alterations of IgG extravasation on cerebral endothelial cells.

(A) The IgG extravasation protein levels were analyzed by western blotting and are shown for the control, APAP-treated without CSD, CSD, and APAP-treated with CSD groups.

(B) The quantitative data are expressed as relative densities compared to β-actin.

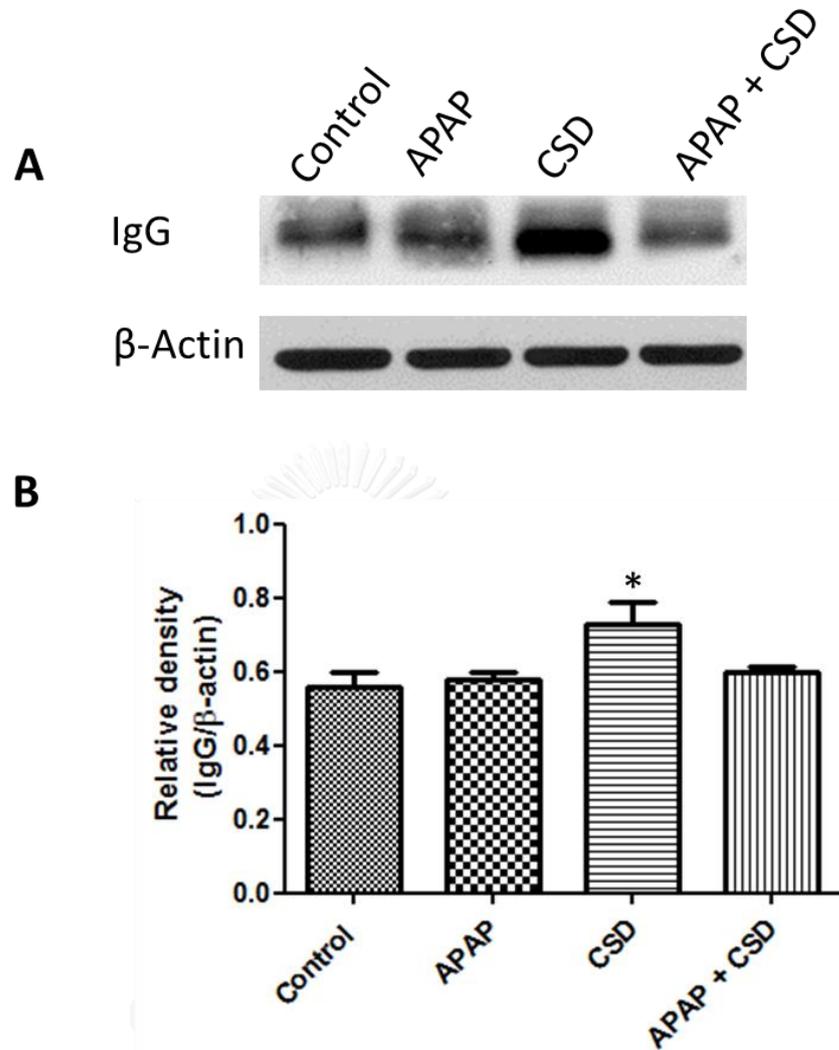*P<0.05 compared to the control group.

Figure 31 Effect of 30-day of APAP treatment on the CSD-induced alterations of IgG extravasation on cerebral endothelial cells.

(A) The IgG extravasation protein levels were analyzed by western blotting and are shown for the control, APAP-treated without CSD, CSD, and APAP-treated with CSD groups.

(B) The quantitative data are expressed as relative densities compared to β-actin.

***$P<0.001$ compared to the control group, [#]$P<0.05$ compared to the CSD group, [δ]$P<0.05$ compared to the APAP-treated without CSD group.
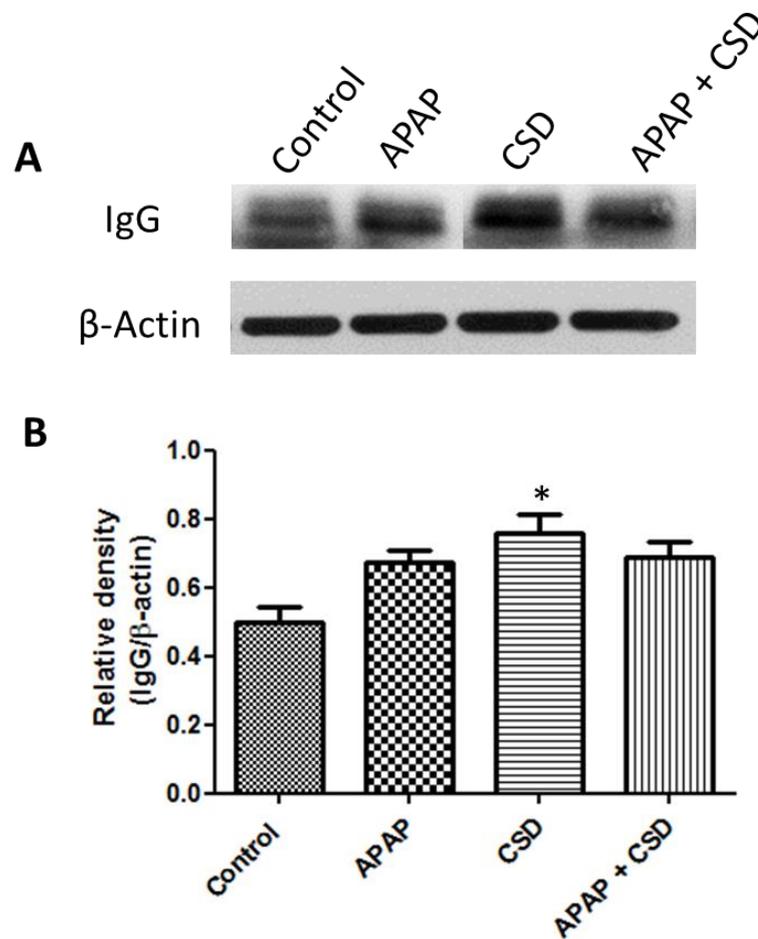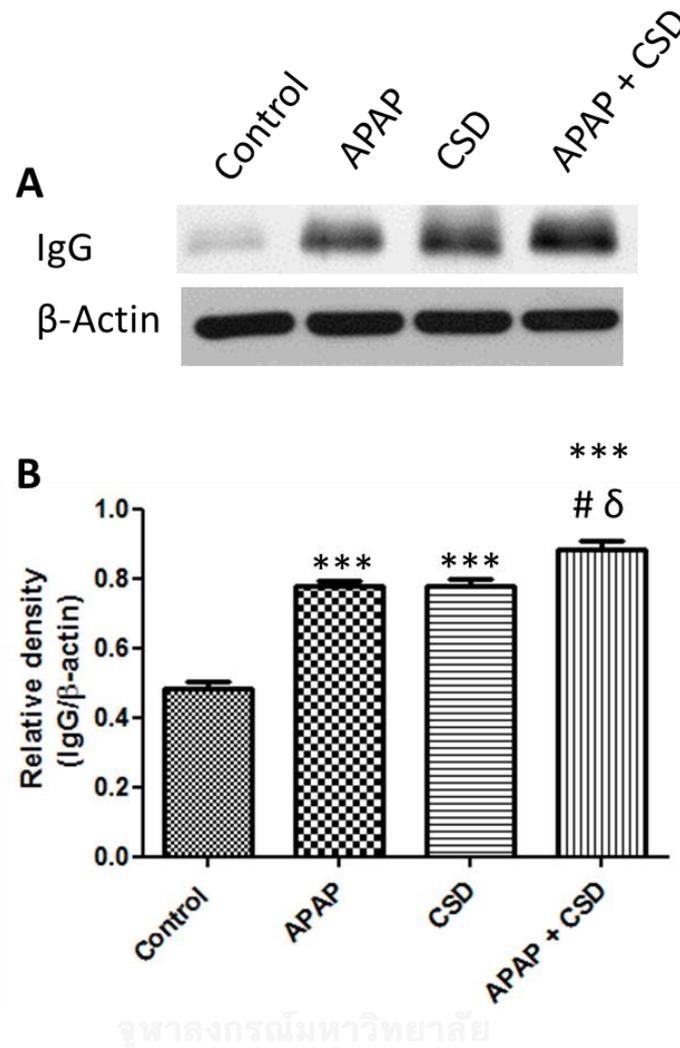
Effect of APAP treatment on the CSD-induced expression of cell adhesion molecules on cerebral microvessels

The expressions of cell adhesion molecule proteins (ICAM-1 and VCAM-1) in the cerebral cortex were evaluated by using western blotting. The results revealed that the level of ICAM-1 expression observed in the CSD group was significantly increased those observed in the control group ($P<0.05$). However, pretreatment with APAP one hour could attenuate the expression of ICAM-1 induced by CSD as demonstrated in Figure 32. No differences in the expression of VCAM-1 were observed in any experimental group as shown in Figure 35.

Interestingly, the results reveal that chronic APAP treatment for 15 and 30 days had the opposite effect of this drug on the expressions of cell adhesion molecules in the rats. Compared with those from the control group, chronic APAP treatment either alone or in combination with CSD significantly increased the expression of ICAM-1 (Figure 34, Figure 36). Additionally, the results demonstrated that the level of VCAM-1 protein expression was significantly higher in 30-day of APAP treated with CSD group than that observed in the control group ($P<0.01$). These data are shown in Figure 42.

The results obtained from immunohistochemical study also correlate well with the results of western blot analyses. In CSD group, the numbers of ICAM-1- and VCAM-1-immunopositive vessels were significantly higher than that observed in the control group.. Pretreatment with acute APAP treatment could attenuate the numbers of ICAM-1- and VCAM-1-immunopositive vessels induced by CSD (Figure 33, Figure 39). However, chronic APAP treatment (15 and 30 days) with CSD activation caused a significant increase in the number of those immunopositive vessels

compared to the CSD group. These data are shown in Figure 35, Figure 37, Figure 41, Figure 43.

Figure 32 Effects of 0-day of APAP treatment on CSD-induced the expression of ICAM-1 in the cerebral cortex.

(A) The ICAM-1 protein levels were analyzed by western blotting and are shown for the control, APAP-treated without CSD, CSD, and APAP-treated with CSD groups.

(B) Quantitative data are expressed as relative densities compared to β-actin.

*$P<0.05$ compared to the control group.

Figure 33 Effects of 0-day of APAP treatment on CSD-induced ICAM-1 expression in the cerebral cortex.

Photomicrographs showing ICAM-1-immunoreactive cells (arrows) in the cerebral cortices obtained from the control (A), APAP-treated without CSD (B), CSD (C), and APAP-treated with CSD (D) groups. Scale bar = 200 μm.
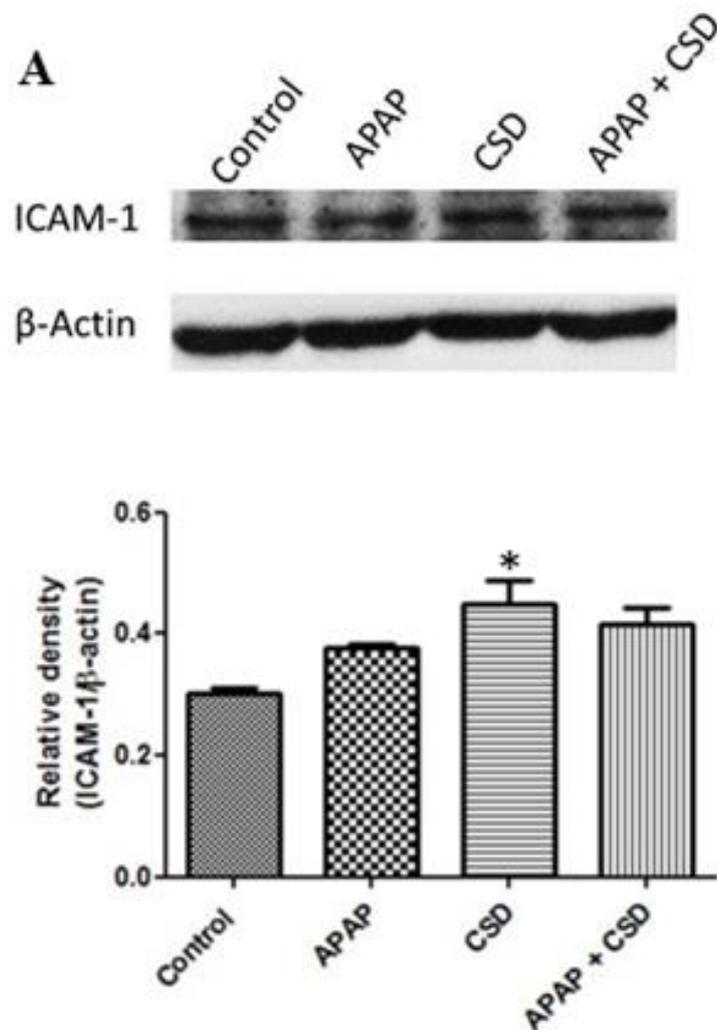
Figure 34 Effects of 15-day of APAP treatment on CSD-induced the expression of

ICAM-1 in the cerebral cortex.

(A) The ICAM-1 protein levels were analyzed by western blotting and are shown for

the control, APAP-treated without CSD, CSD, and APAP-treated with CSD groups.

(B) Quantitative data are expressed as relative densities compared to β-actin.

*$P<0.05$ compared to the control group, *** $P<0.001$ compared to the control group'

$P<0.01$ compared to the CSD group.

Figure 35 Effects of 15-day of APAP treatment on CSD-induced ICAM-1 expression in the cerebral cortex.

Photomicrographs showing ICAM-1-immunoreactive cells (arrows) in the cerebral cortices obtained from the control (A), APAP-treated without CSD (B), CSD (C), and APAP-treated with CSD (D) groups. Scale bar = 200μm.

Figure 36 Effects of 30-day of APAP treatment on CSD-induced the expression of
ICAM-1 in the cerebral cortex.

(A) The ICAM-1 protein levels were analyzed by western blotting and are shown for

the control, APAP-treated without CSD, CSD, and APAP-treated with CSD groups.

(B) Quantitative data are expressed as relative densities compared to β-actin.

*P<0.05 compared to the control group, *** P<0.001 compared to the control group,

P<0.01 compared to the CSD group, δδδ P<0.001 compared to the APAP-treated
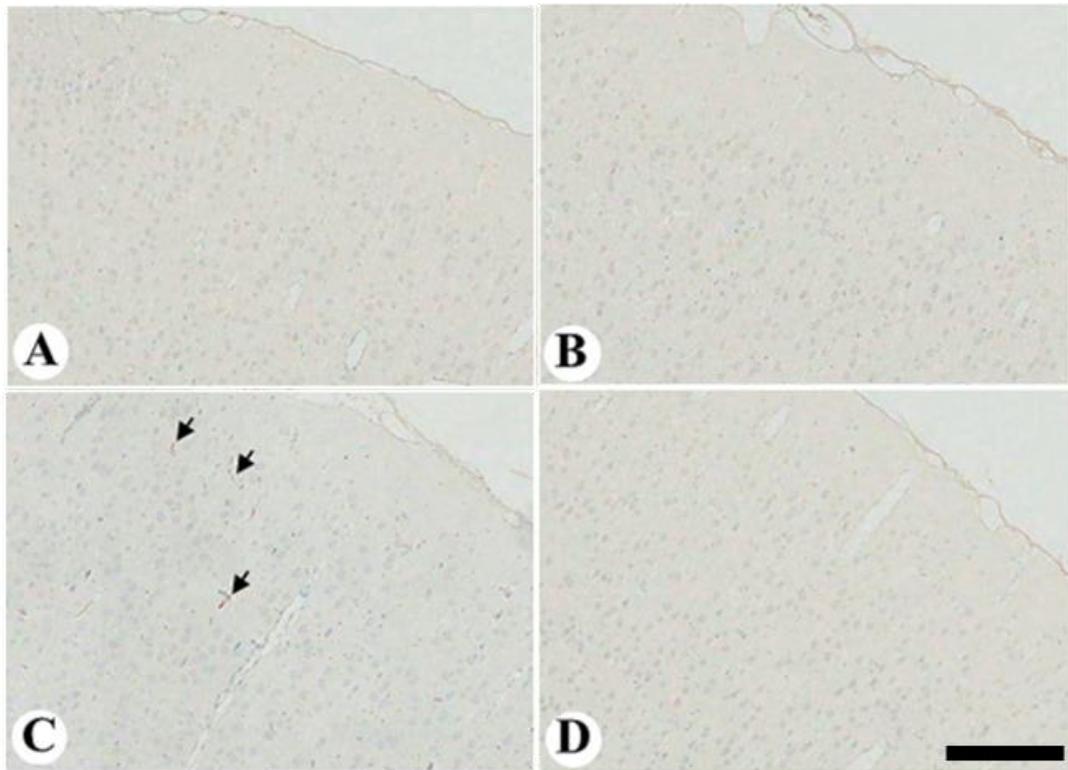
without CSD group.

Figure 37 Effects of 30-day of APAP treatment on CSD-induced ICAM-1 expression in the cerebral cortex.

Photomicrographs showing ICAM-1-immunoreactive cells (arrows) in the cerebral cortices obtained from the control (A), APAP-treated without CSD (B), CSD (C), and APAP-treated with CSD (D) groups. Scale bar = 200 μm.
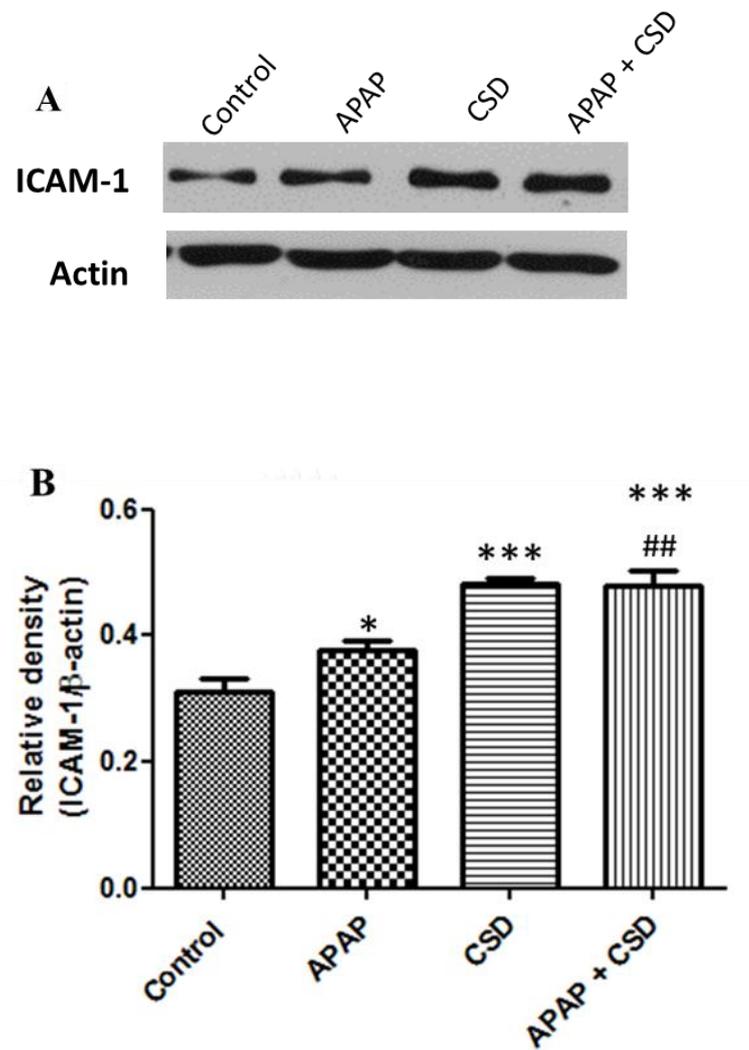
Figure 38 Effects of 0-day of APAP treatment on CSD-induced the expression of

VCAM-1 in the cerebral cortex.

(A) The VCAM-1 protein levels were analyzed by western blotting and are shown for

the control, APAP-treated without CSD, CSD, and APAP-treated with CSD groups.

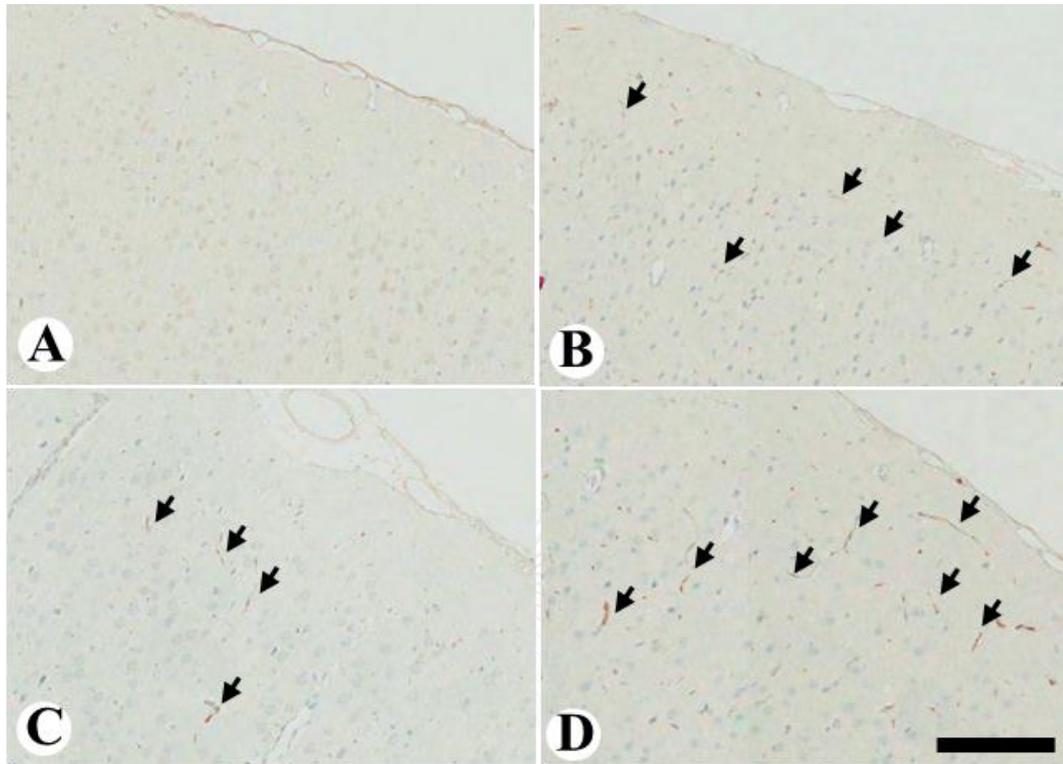(B) Quantitative data are expressed as relative densities compared to β-actin.

Figure 39 Effects of 0-day of APAP treatment on CSD-induced VCAM-1 expression in the cerebral cortex.

Photomicrographs showing VCAM-1-immunoreactive cells (arrows) in the cerebral cortices obtained from the control (A), APAP-treated without CSD (B), CSD (C), and APAP-treated with CSD (D) groups. Scale bar = 200 μm.
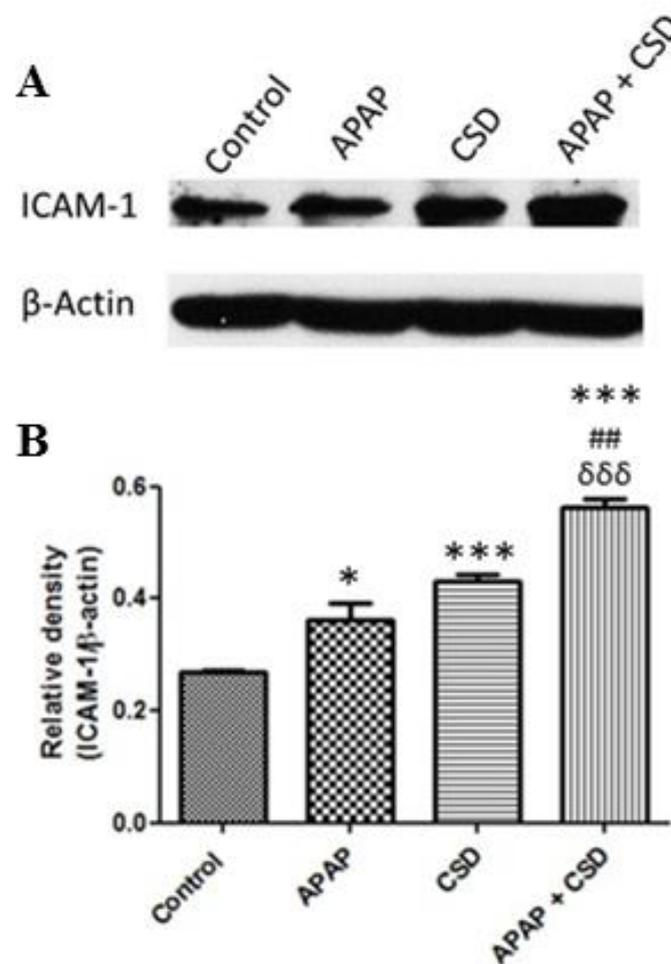
Figure 40 Effects of 15-day of APAP treatment on CSD-induced the expression of
VCAM-1 in the cerebral cortex.

(A) The VCAM-1 protein levels were analyzed by western blotting and are shown for

the control, APAP-treated without CSD, CSD, and APAP-treated with CSD groups.

(B) Quantitative data are expressed as relative densities compared to β-actin.

Figure 41 Effects of 15-day of APAP treatment on CSD-induced VCAM-1 expression in the cerebral cortex.

Photomicrographs showing VCAM-1-immunoreactive cells (arrows) in the cerebral cortices obtained from the control (A), APAP-treated without CSD (B), CSD (C), and APAP-treated with CSD (D) groups. Scale bar = 200μm.
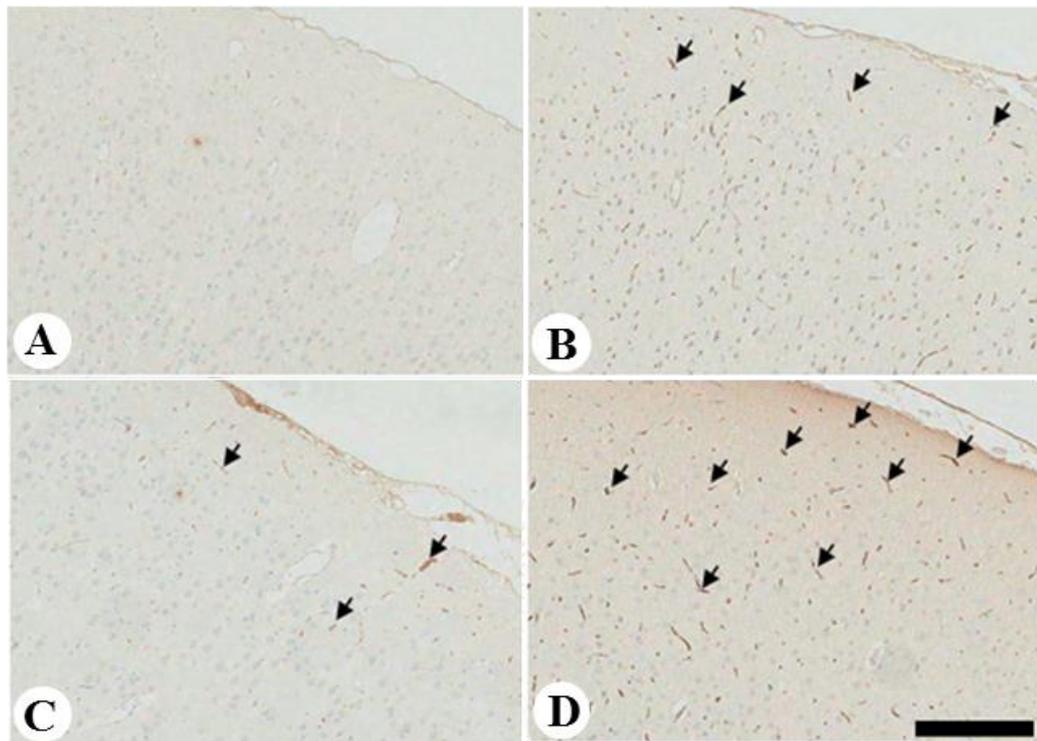
A

B

Figure 42 Effects of 30-day of APAP treatment on CSD-induced the expression of VCAM-1 in the cerebral cortex.

(A) The VCAM-1 protein levels were analyzed by western blotting and are shown for the control, APAP-treated without CSD, CSD, and APAP-treated with CSD groups.

(B) Quantitative data are expressed as relative densities compared to β-actin.

**P<0.01 compared to the control group.
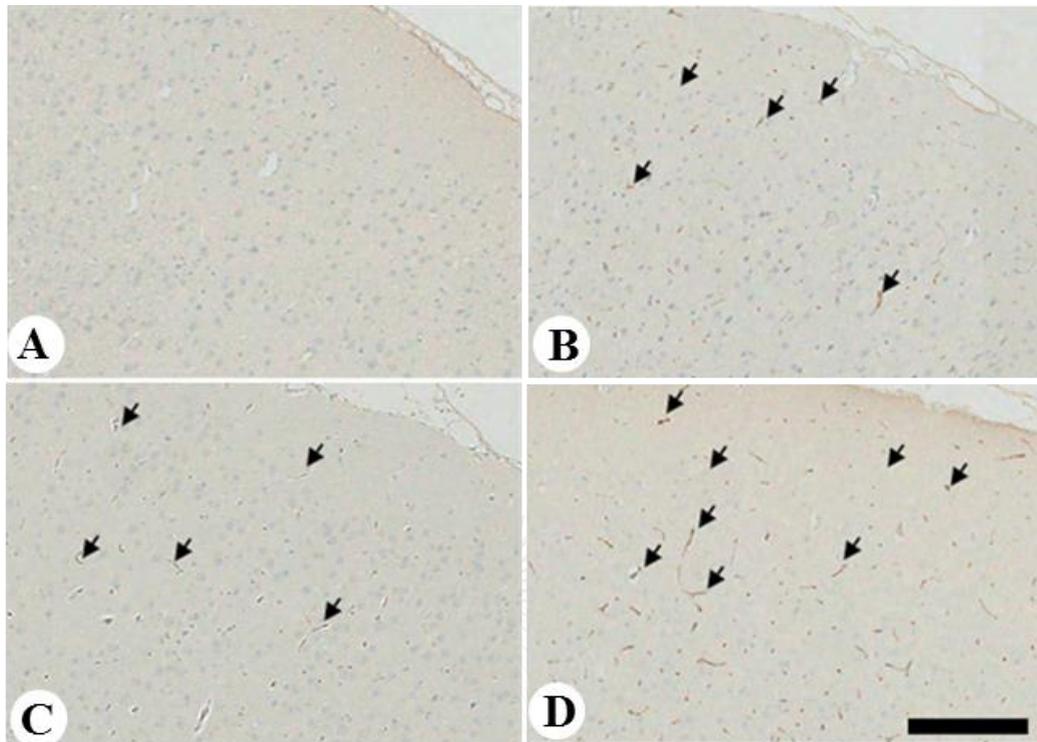
Figure 43 Effects of 30-day of APAP treatment on CSD-induced VCAM-1 expression in the cerebral cortex.

Photomicrographs showing VCAM-1-immunoreactive cells (arrows) in the cerebral cortices obtained from the control (A), APAP-treated without CSD (B), CSD (C), and APAP-treated with CSD (D) groups. Scale bar = 200μm.

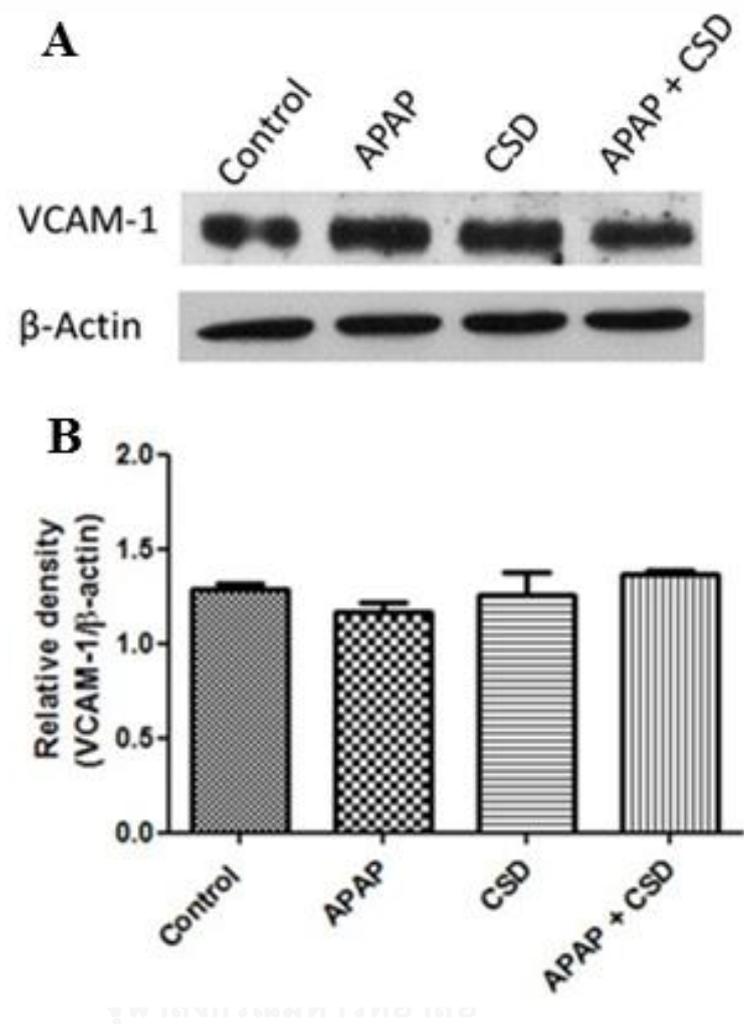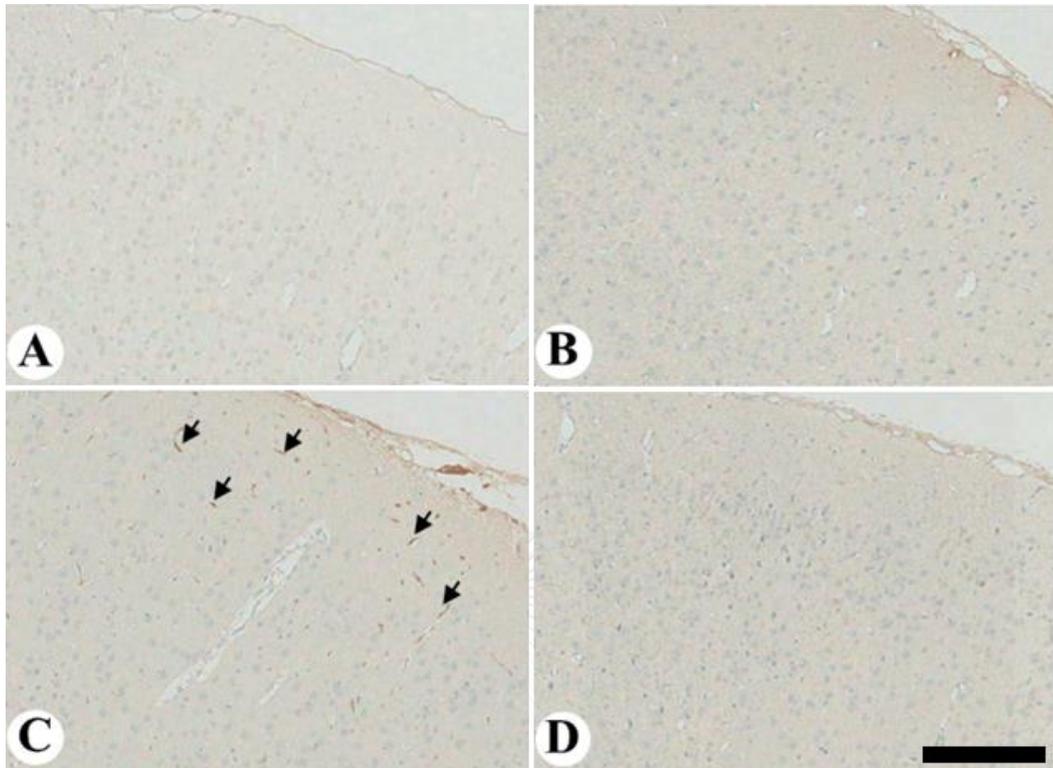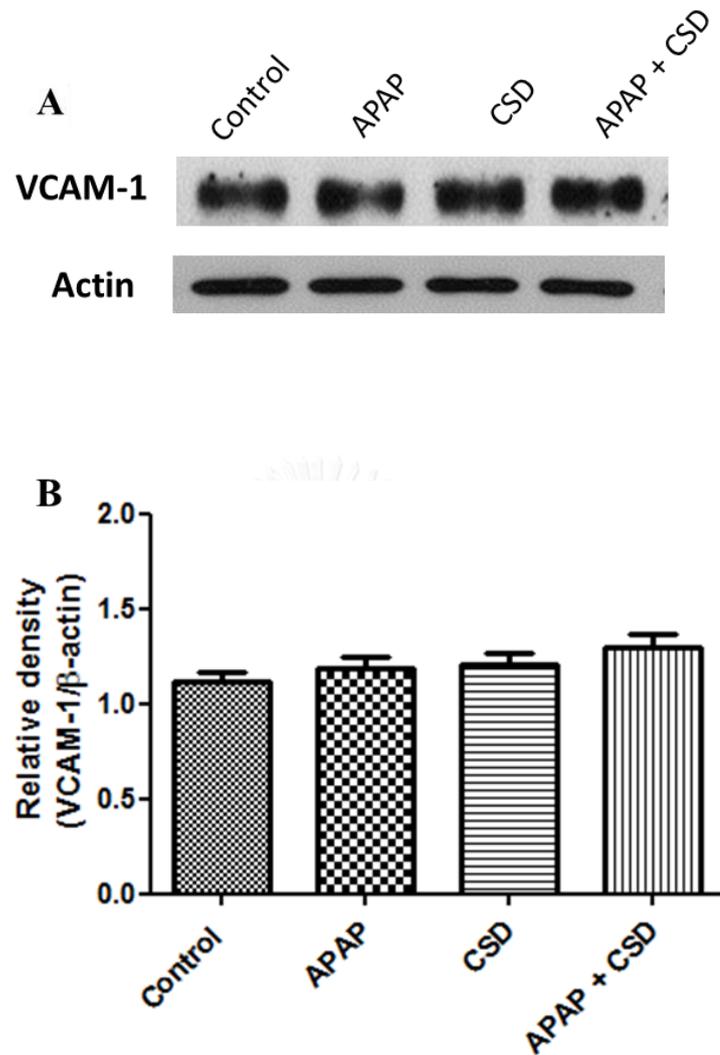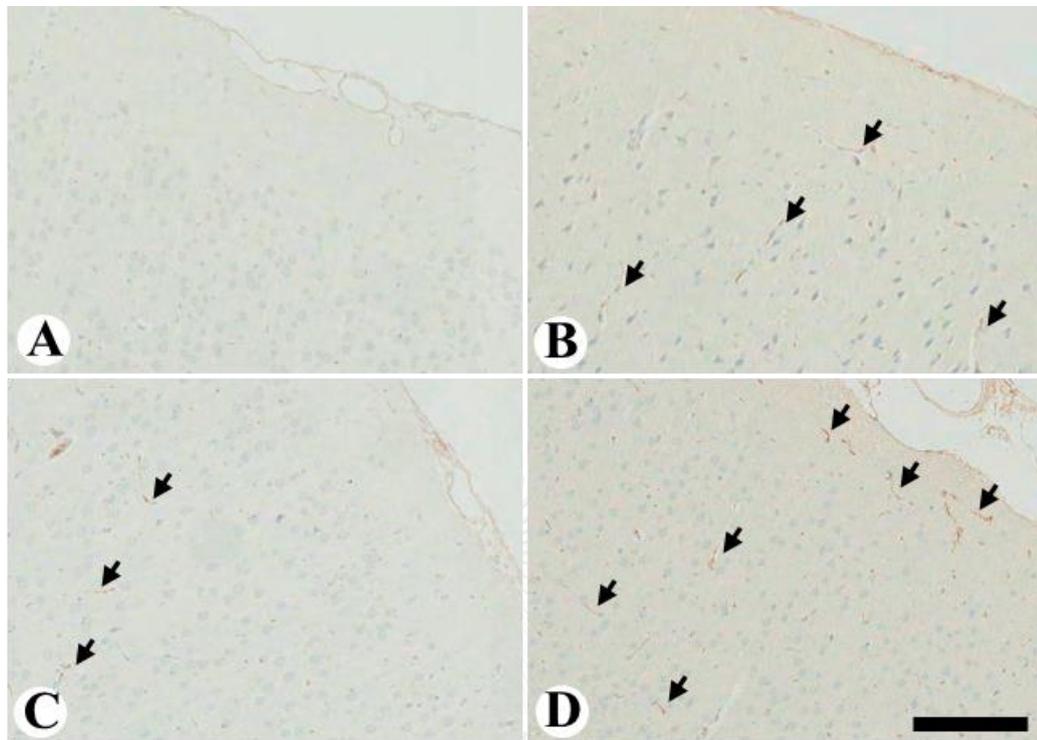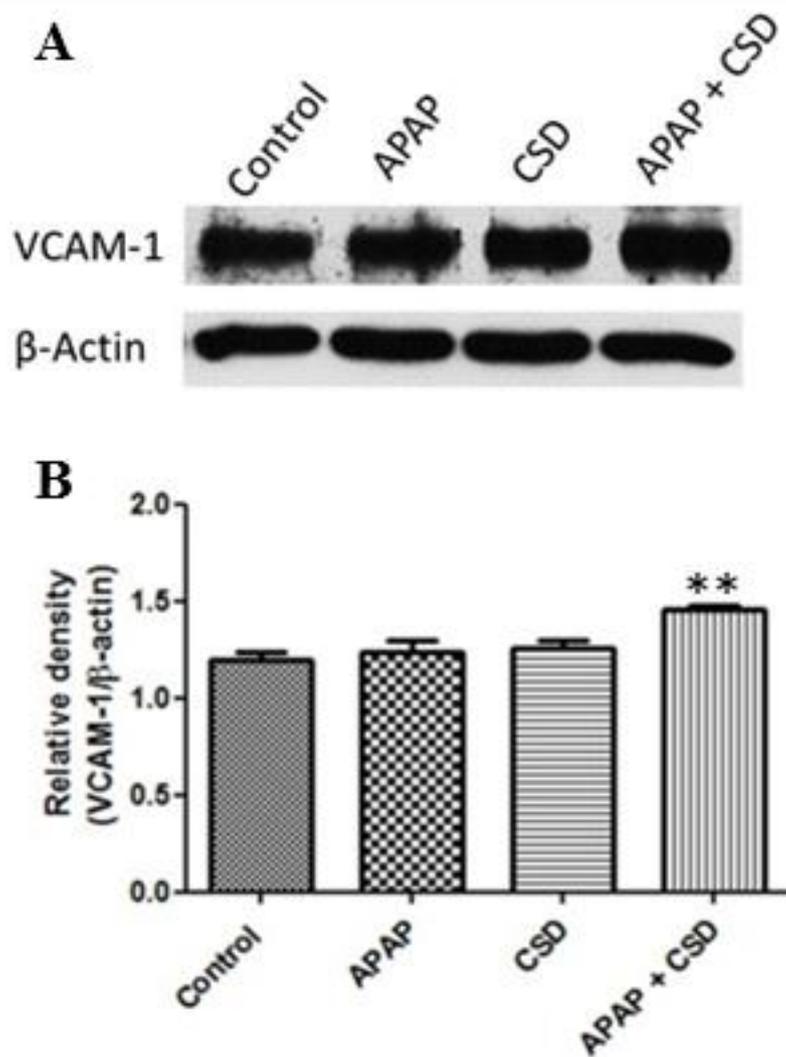**Effect of APAP treatment on CSD-induced CGRP expression in the TG**

To determine the effect of chronic APAP treatment on the CGRP expression, TGs with 800-1,000 neurons were selected from each animal. Statistical analyses did not reveal any significant differences among experimental groups in the total number of TG neurons. Immunohistochemistry revealed that CGRP is mainly localized in small to medium sized neurons (up to 30 µm in diameter). In this study, the total number of CGRP-IR cells was expressed the data as the average percentage of the total number of CGRP-IR neurons in the TG for each experimental group.

The results revealed that the induction of CSD significantly increased the average percentage of total CGRP-IR neurons compared with the control groups (Figures 44, Figure 45, Figure 46 and Table 2, P <0.001). This is consistent for every time point analyzed (0, 15, and 30 days). A single injection of APAP prior to CSD induction attenuated the total number CGRP-IR cells in the TG (27.62±0.77) compared with those from the CSD group (41.12±1.49) (Figures 44, and Table 2, P <0.001).

In the experiment with 15-days treatment, APAP treatment alone or in combination with CSD exhibited a significant higher percentage of total CGRP-IR cells when compared with controls (33.62±1.00, 33.85±1.12 and 26.93±0.88 for APAP treatment alone, APAP treatment with CSD, and control groups, respectively, P <0.001). However, those numbers were significantly lower than that of the CSD group (41.31±1.29) (Figures 45 and Table 2, P <0.001).

Results from the 30-day treatment groups demonstrated that the average percentage of total CGRP-IR cells in APAP (42.56±1.24) or APAP with CSD (48.68±0.83) treated groups were significantly higher than those obtained from the control group

(28.10±1.25) (*P* <0.001). No difference in the total number of CGRP immunopositive neurons was observed when comparing between the APAP and CSD groups (Figures 46 and Table 2).

Long-term treatment with APAP enhances CGRP expression in the TG. This effect is time-dependent because the average percentage of total CGRP-IR cells after the 30-day treatment was significantly higher than those observed in the 15-day treatment. The same pattern of this alteration is observed as well in the animal with APAP treatment and CSD activation.
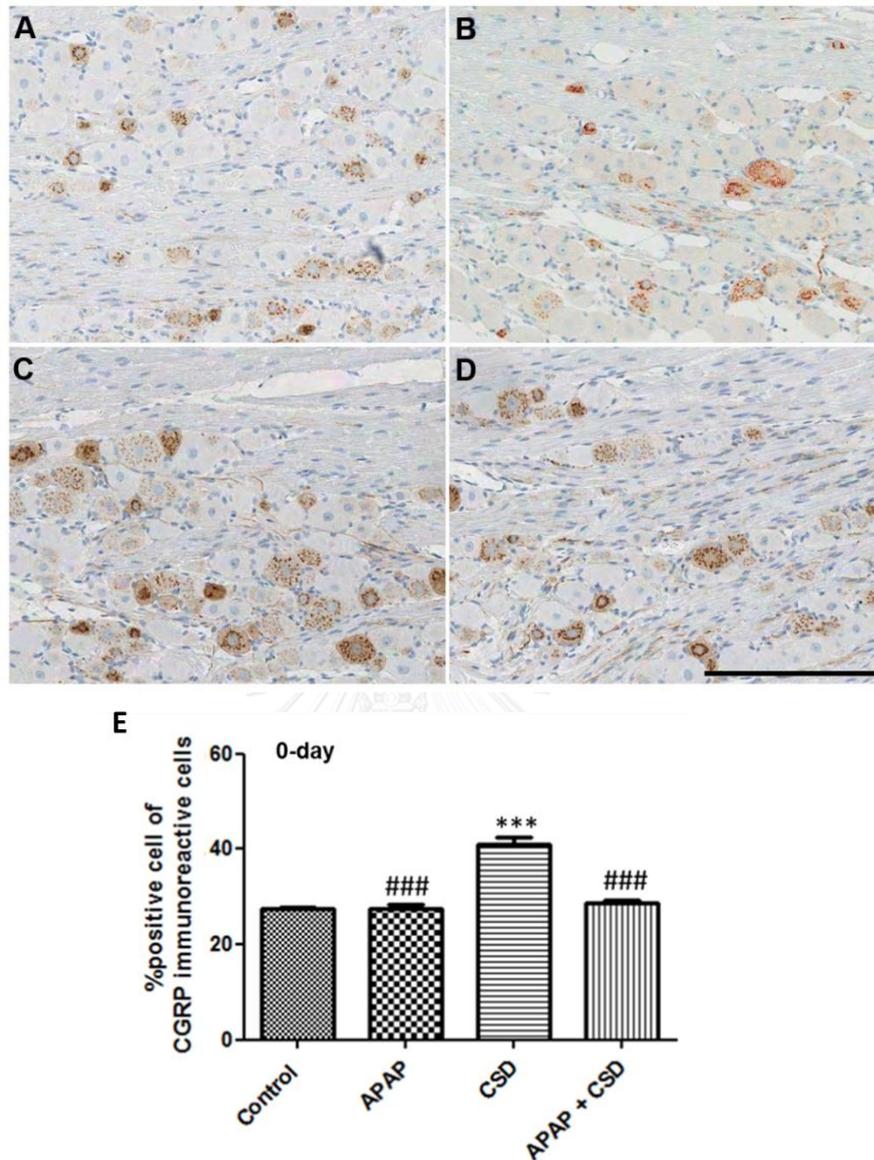
Figure 44 Effect of 0-day of APAP treatment on CSD-induced CGRP expression in the TG.

The photomicrographs show the CGRP-IR neurons in the TG ipsilateral to the site of KCl or NaCl application obtained from the control (A), APAP-treated without CSD (B), CSD (C), and APAP-treated with CSD (D) groups. Scale bar = 200 µm.

(E) Histograms showing the average percentage of CGRP-IR cells per total cells.

*** $P<0.001$ compared to the control group, ### $P<0.001$ compared to the CSD group.
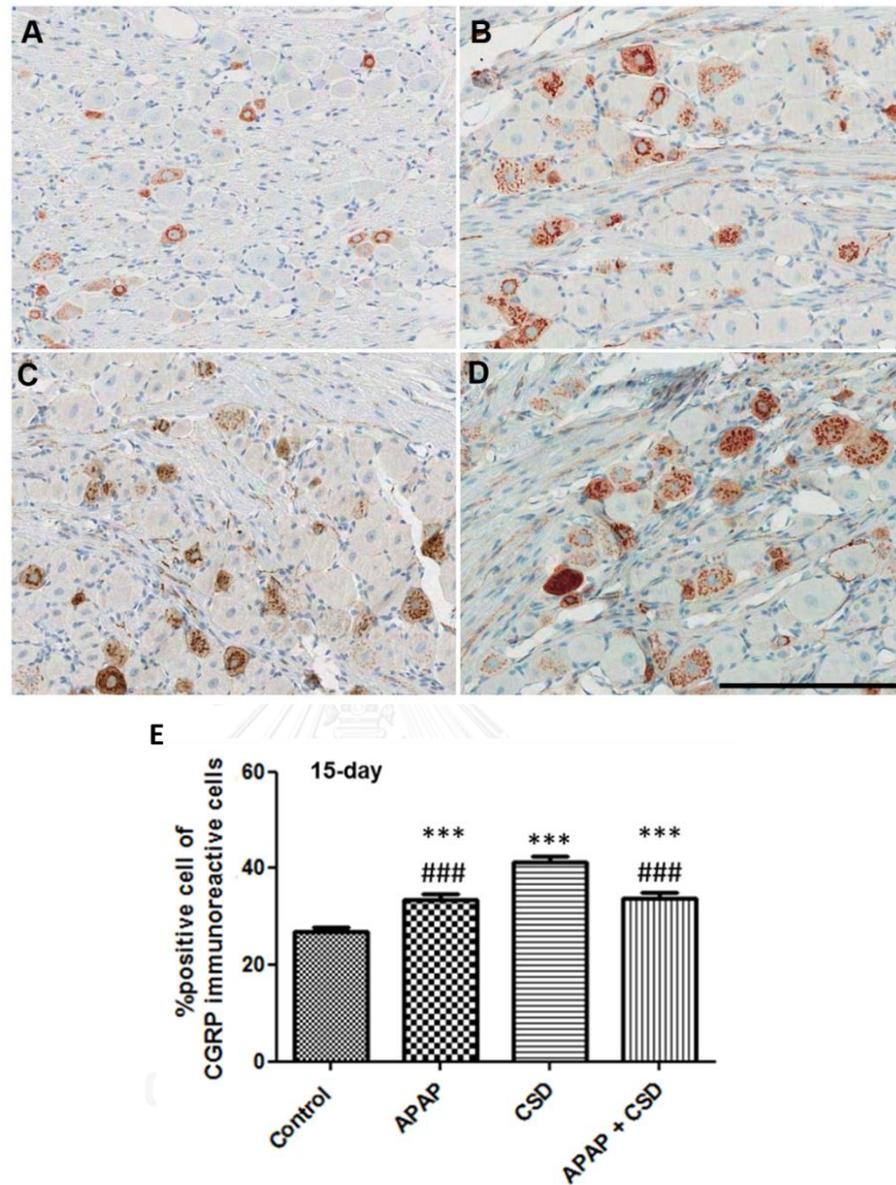
Figure 45 Effect of 15-day of APAP treatment on CSD-induced CGRP expression in the TG.

The photomicrographs show the CGRP-IR neurons in the TG ipsilateral to the site of KCl or NaCl application obtained from the control (A), APAP-treated without CSD (B), CSD (C), and APAP-treated with CSD (D) groups. Scale bar = 200 μm.

(E) Histograms showing the average percentage of CGRP-IR cells per total cells.

*** $P<0.001$ compared to the control group, ### $P<0.001$ compared to the CSD group.
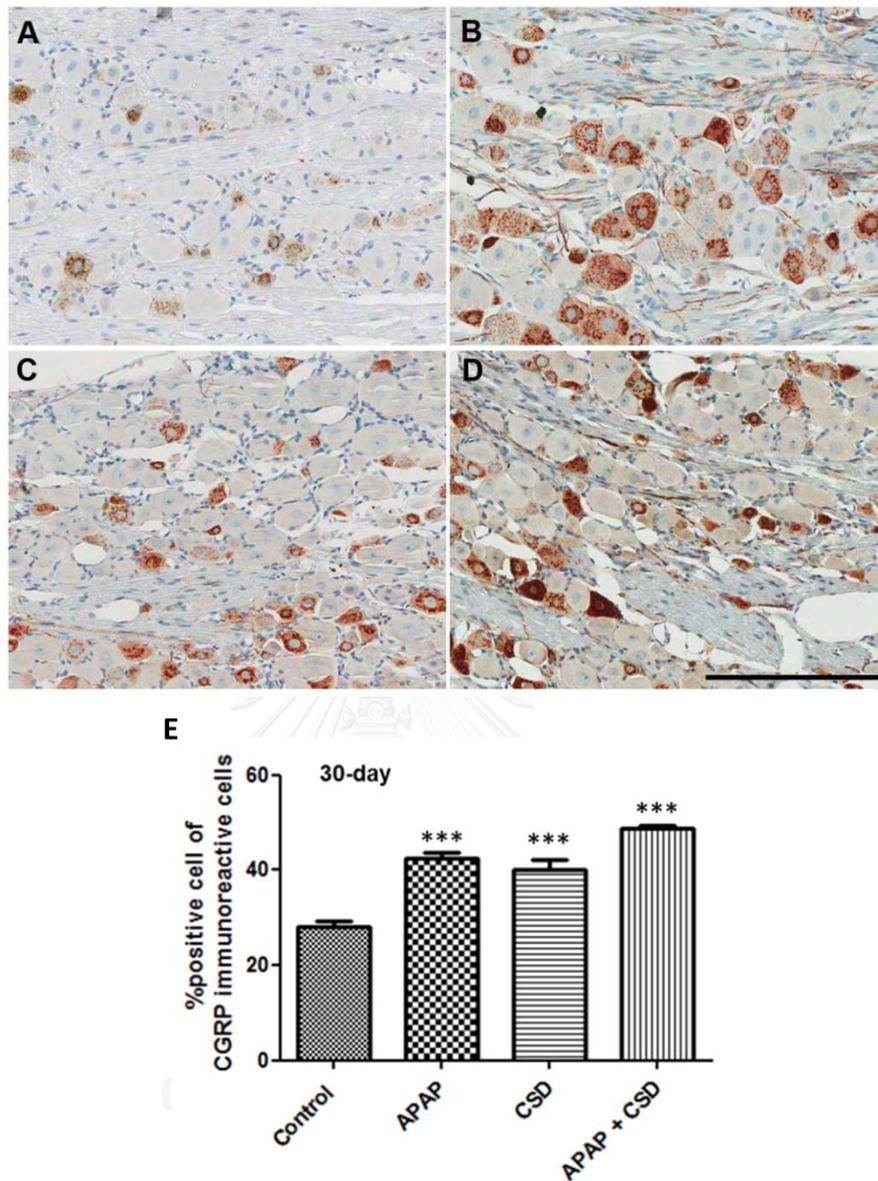
Figure 46 Effect of 30-day of APAP treatment on CSD-induced CGRP expression in the TG.

The photomicrographs show the CGRP-IR neurons in the TG ipsilateral to the site of KCl or NaCl application obtained from the control (A), APAP-treated without CSD (B), CSD (C), and APAP-treated with CSD (D) groups. Scale bar = 200 μm.

(E) Histograms showing the average percentage of CGRP-IR cells per total cells.

*** $P<0.001$ compared to the control group.

Table 2 Effect of APAP treatment on CSD-induced CGRP expression in the TG

Measure variables	Control group	APAP-treated group	CSD group	APAP-treated with CSD group
% of total CGRP-immunopositive neurons in the TG				
0-day	27.40±0.41	27.62±0.77[###]	41.12±1.49[***]	28.84±0.60[###]
15-day	26.93±0.88	33.62±1.00[***###]	41.31±1.29[***]	33.85±1.12[***###]
30-day	28.10±1.25	42.56±1.24[***]	40.02±2.11[***]	48.68±0.83[***]

[***] *P* <0.001 compared with the control group.

[###] *P* <0.001 compared with the CSD group.

Effect of APAP treatment on the alteration of the CYP2E1 enzyme in the brain

In the brain, cell components in the NVU have been reported their ability in the expression of enzyme CYP2E1. The important of this enzyme involves in the metabolism of APAP which lead to the accumulation of NAPQI and finally damage to the cells. This study aimed to investigate the alteration of the enzyme CYP2E1 activity in the brain after rats received acute and chronic APAP treatment.

The results demonstrated that there was no different between the control and CSD groups in all experimental periods. At 0-day of APAP treatment, rats in the APAP-treated with and without CSD groups exhibited the increase of enzyme CYP2E1 levels when compared with the control and CSD groups ($P<0.01$; Figure 47). This alteration of this enzyme was also detected in the 15-day of treatment as well ($P<0.001$; Figure 48). However, the level of enzyme CYP2E1 was extremely increased in the 30-day of APAP treatment, either with or without CSD activation ($P<0.001$; Figure 49).
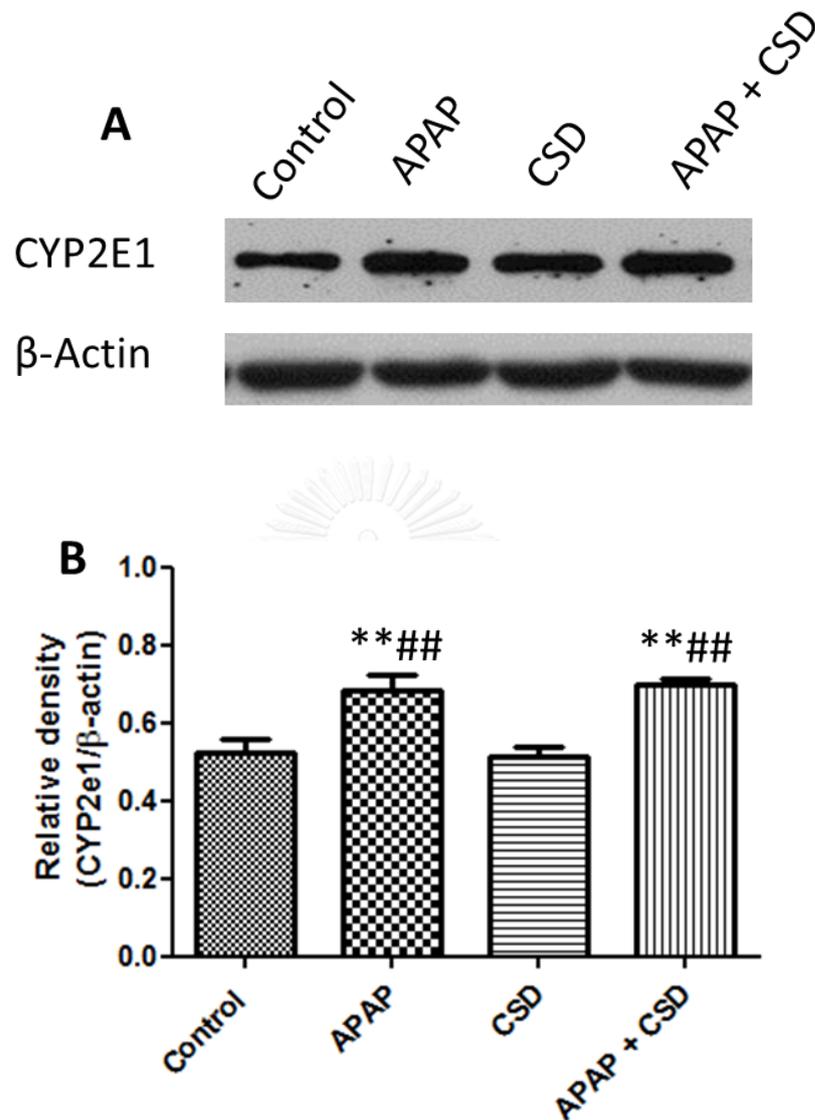
Figure 47 Effects of 0-day of APAP treatment on the alteration of the CYP2E1 enzyme

in the brain.

 (A) The CYP2E1 protein levels were analyzed by western blotting and are shown for

the control, APAP-treated without CGRP, CGRP, and APAP-treated with CGRP groups.

(B) Quantitative data are expressed as relative densities compared to β-actin.

** $P<0.01$ compared to the control group, [##] $P<0.01$ compared to the CSD group.
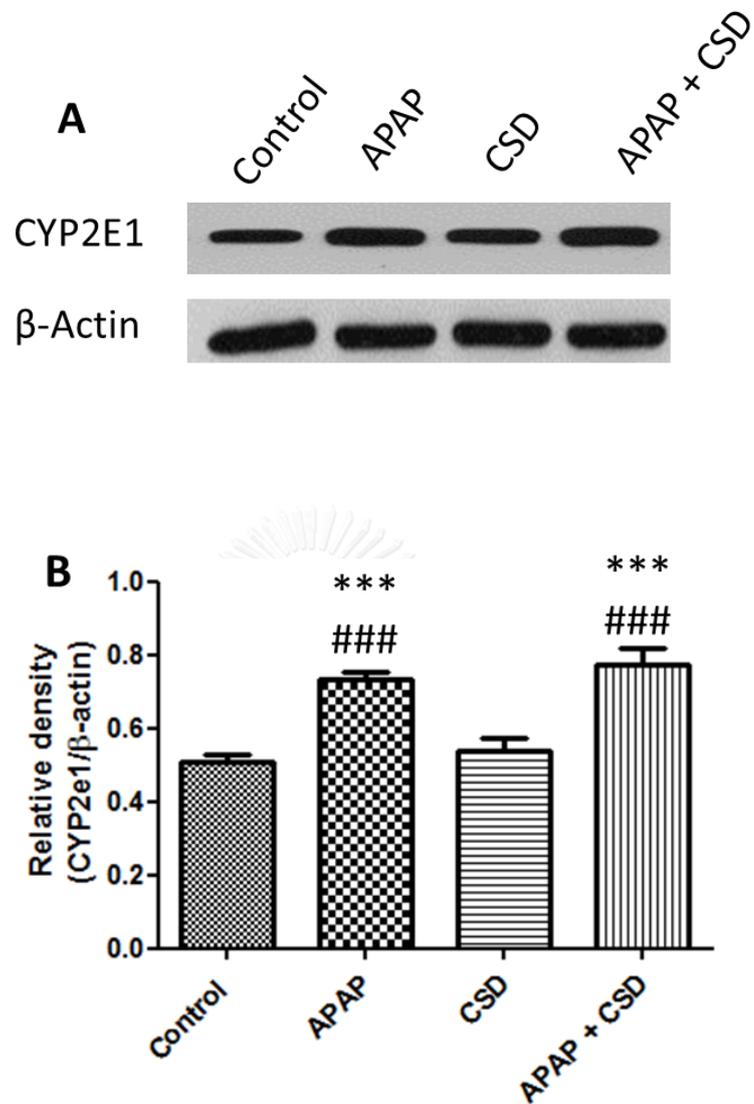
Figure 48 Effects of 15-day of APAP treatment on the alteration of the CYP2E1 enzyme in the brain.

(A) The CYP2E1 protein levels were analyzed by western blotting and are shown for the control, APAP-treated without CGRP, CGRP, and APAP-treated with CGRP groups.

(B) Quantitative data are expressed as relative densities compared to β-actin.

*** $P<0.001$ compared to the control group, ### $P<0.001$ compared to the CSD group.
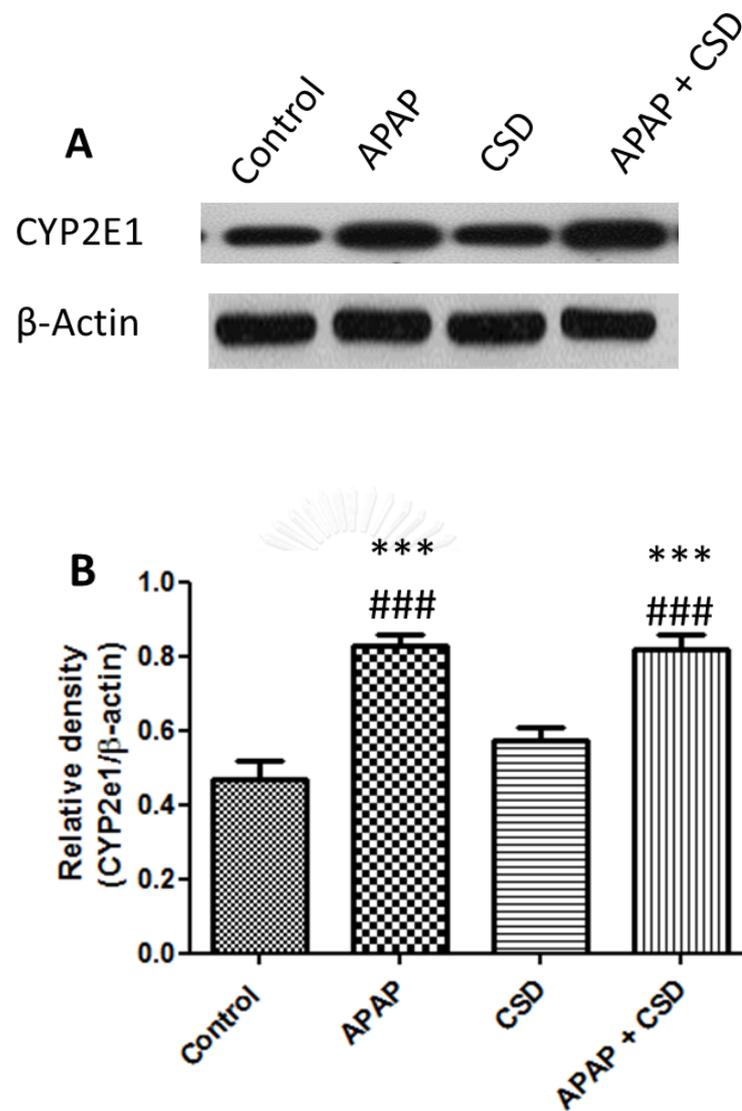
Figure 49 Effects of 30-day of APAP treatment on the alteration of the CYP2E1 enzyme in the brain.

(A) The CYP2E1 protein levels were analyzed by western blotting and are shown for the control, APAP-treated without CGRP, CGRP, and APAP-treated with CGRP groups.

(B) Quantitative data are expressed as relative densities compared to β-actin.

*** $P<0.001$ compared to the control group, ### $P<0.001$ compared to the CSD group.

The results obtained from *in vivo* study demonstrated that acute and chronic treatment with APAP resulted in different responses of the cerebral microvessels to CSD activation. The induction of CSD alone induced increases in ultrastructural alterations, cell adhesion molecule expression, and IgG extravasation on the cerebral microvessels. These alterations are parallel with the decrease in expression of the tight junction proteins. While acute APAP treatment attenuated those alterations of cerebral microvessels induced by CSD, the opposite response was observed in the rats that received chronic APAP treatment. Moreover, the expression of CGRP in the TG was enhanced after chronic APAP treatment as well.

4.2 Study II: The study of the effect of acute and chronic APAP treatment on the alteration of BBB integrity in the cultured brain endothelial cell line (bEnd.3 cell).

Cytotoxic assay of APAP in bEnd.3 cell

In order to select the dose of APAP for treatment, the bEnd.3 cell was incubated with the different concentrations of this drug and the result was detected by MTS assay. The results demonstrated that IC_{50} of this drug which induced 50% of cell death was 6,000 µM. Moreover, the result of MTS assay demonstrated that at the concentration of APAP lower than 1,000 µM could induce cell death less than 10% (Figure 50). Based on the previous study by [10], the concentration of APAP was used in the treatment of rat brain endothelial cell was 100 µM and the results demonstrated the protective effect of this drug to the cell from oxidative stress. Thus, in this study, 100 µM of APAP concentration was selected because this concentration was also in range between 0-1,000 µM that induced 10% of cell death.
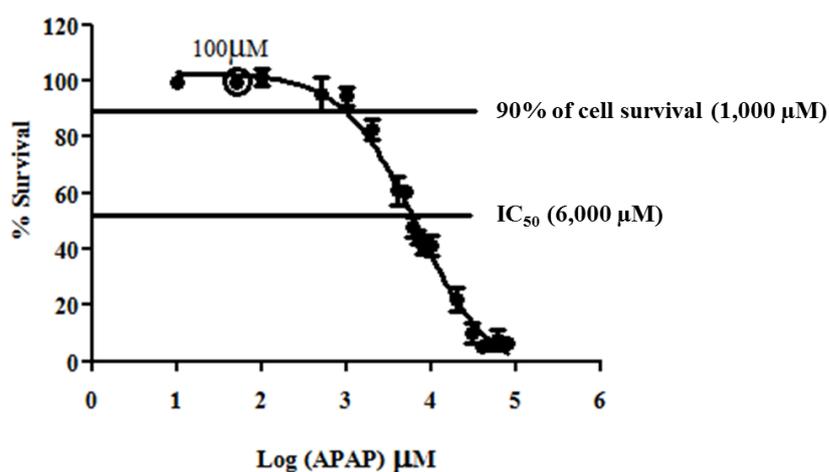
Figure 50 Cytotoxicity of APAP to bEnd.3 cells determined by MTS assay.

Effect of APAP treatment on the CGRP-induced alterations of tight junction proteins expression in cultured brain endothelial cell line (bEnd.3 cell)

In order to confirm the effect of APAP treatment on the CGRP-induced the alterations of BBB integrity in brain endothelial cell, the 3 different time points of APAP treatment were studied in bEnd.3 cell in the condition with and without CGRP activation. The expression of tight junction proteins was investigated by western blotting.

In the CGRP-activated groups, the levels of tight junction proteins (ZO-1, occludin, and claudin-5) significantly decreased when compared with the control group. These alterations were consistent for all 3 different durations of experiment.

With acute APAP treatment for 24 h, there was no significant difference observed in those of tight junction proteins. In combination with CGRP activation, pretreatment with APAP could attenuate the decrease of tight junction proteins of bEnd.3 cell induced by CGRP (Figure 51-Figure 59). However, the expression of tight junction proteins obtained from the bEND3 cell with chronic APAP treatment (2, 4 weeks of APAP treatment) demonstrated the significant lower levels of ZO-1, occludin, and claudin-5 than those observed in the control group. The expression of tight junction proteins (ZO-1) was further decreased in the chronic APAP-treated cells with CGRP activation (Figure 53).

Figure 51 Effects of APAP treatment for 24 h on CGRP-induced the expression of ZO-1 in the bEnd.3 cell.

(A) 10 ug total protein extracts were separated on 7.5% SDS- PAGE before transferred onto nitrocellulose membrane. Anti-ZO-1 and goat anti-rabbit-HRP were used for detection.

(B) Quantitative data are expressed as relative densities compared to β-actin.

The experiment was under taken in 3 dependent times with duplicated assay. Data represented as mean ± SEM. [#]$P<0.05$ compared to the CGRP-treated cells.

Figure 52 Effects of APAP treatment for 2 weeks on CGRP-induced the expression of

ZO-1 in the bEnd.3 cell.

(A) 10 ug total protein extracts were separated on 7.5% SDS- PAGE before transferred

onto nitrocellulose membrane. Anti-ZO-1 and goat anti-rabbit-HRP were used for

detection.

(B) Quantitative data are expressed as relative densities compared to β-actin.

The experiment was under taken in 3 dependent times with duplicated assay. Data

represented as mean ± SEM.

[#]$P<0.05$ compared to the CGRP-treated cells.

Figure 53 Effects of APAP treatment for 4 weeks on CGRP-induced the expression of ZO-1 in the bEnd.3 cell.

(A) 10 ug total protein extracts were separated on 7.5% SDS- PAGE before transferred onto nitrocellulose membrane. Anti-ZO-1 and goat anti-rabbit-HRP were used for detection.

(B) Quantitative data are expressed as relative densities compared to β-actin.

The experiment was under taken in 3 dependent times with duplicated assay. Data represented as mean ± SEM. [#]$P<0.05$ compared to the CGRP-treated cells.

A

Occludin

β-Actin

B

Figure 54 Effects of APAP treatment for 24 h on CGRP-induced the expression of occludin in the bEnd.3 cell.

(A) 10 ug total protein extracts were separated on 10% SDS-PAGE before transferred onto nitrocellulose membrane. Anti-occludin and goat anti-rabbit-HRP were used for detection.

(B) Quantitative data are expressed as relative densities compared to β-actin.

The experiment was under taken in 3 dependent times with duplicated assay. Data represented as mean ± SEM. *P<0.05 compared to the control-treated cells.

Figure 55 Effects of APAP treatment for 2 weeks on CGRP-induced the expression of occludin in the bEnd.3 cell.

(A) 10 ug total protein extracts were separated on 10% SDS-PAGE before transferred onto nitrocellulose membrane. Anti-occludin and goat anti-rabbit-HRP were used for detection.

(B) Quantitative data are expressed as relative densities compared to β-actin.

The experiment was under taken in 3 dependent times with duplicated assay. Data represented as mean ± SEM. *$P<0.05$ compared to the control-treated cells.
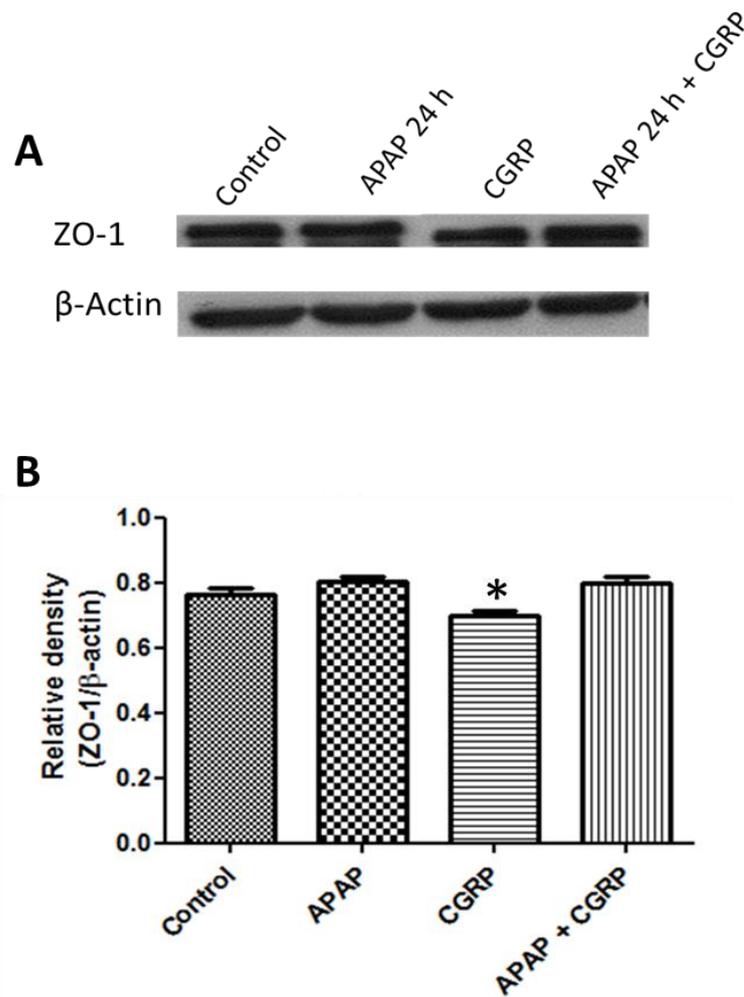
Figure 56 Effects of APAP treatment for 4 weeks on CGRP-induced the expression of occludin in the bEnd.3 cell.

(A) 10 ug total protein extracts were separated on 10% SDS-PAGE before transferred onto nitrocellulose membrane. Anti-occludin and goat anti-rabbit-HRP were used for detection.

(B) Quantitative data are expressed as relative densities compared to β-actin.

The experiment was under taken in 3 dependent times with duplicated assay. Data represented as mean ± SEM. $^*P<0.05$ compared to the control-treated cells.
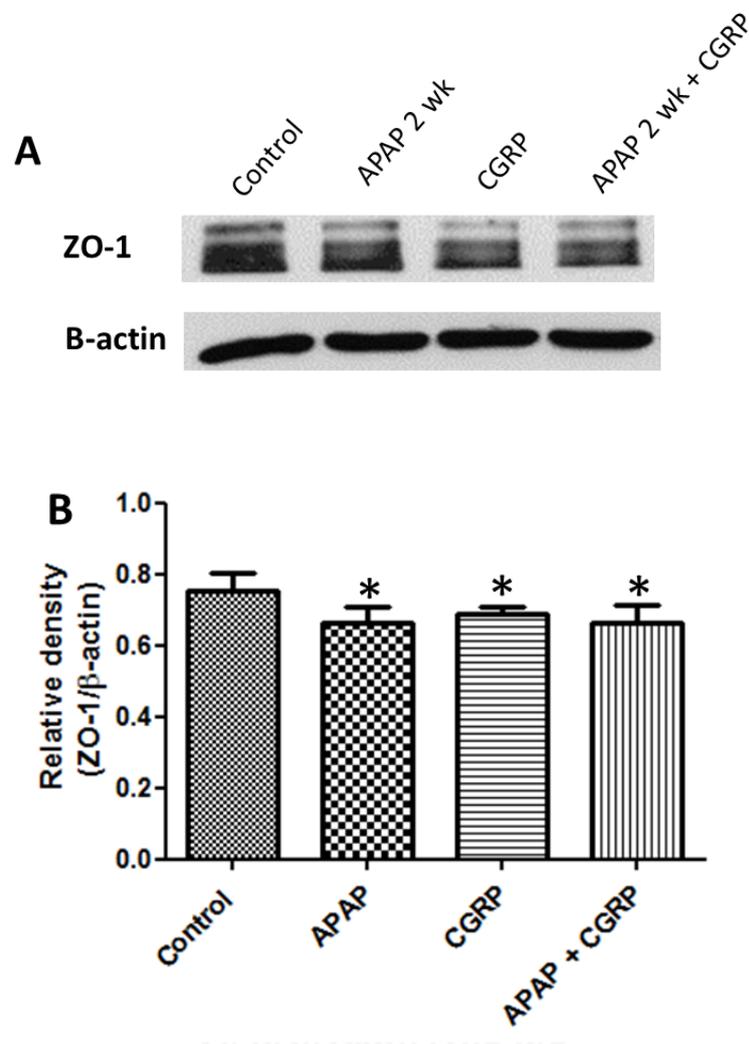
Figure 57 Effects of APAP treatment for 24 h on CGRP-induced the expression of claudin-5 in the bEnd.3 cell.

(A) 10 ug total protein extracts were separated on 12.5% SDS-PAGE before transferred onto nitrocellulose membrane. Anti-claudin-5 and goat anti-rabbit-HRP were used for detection.

(B) Quantitative data are expressed as relative densities compared to β-actin.

The experiment was under taken in 3 dependent times with duplicated assay. Data represented as mean ± SEM. [#]$P<0.05$ compared to the CGRP-treated cells.

Figure 58 Effects of APAP treatment for 2 weeks on CGRP-induced the expression of claudin-5 in the bEnd.3 cell.

(A) 10 ug total protein extracts were separated on 12.5% SDS-PAGE before transferred onto nitrocellulose membrane. Anti-claudin-5 and goat anti-rabbit-HRP were used for detection.

(B) Quantitative data are expressed as relative densities compared to β-actin.

The experiment was under taken in 3 dependent times with duplicated assay. Data represented as mean ± SEM. $^*P<0.05$ compared to the control-treated cells.
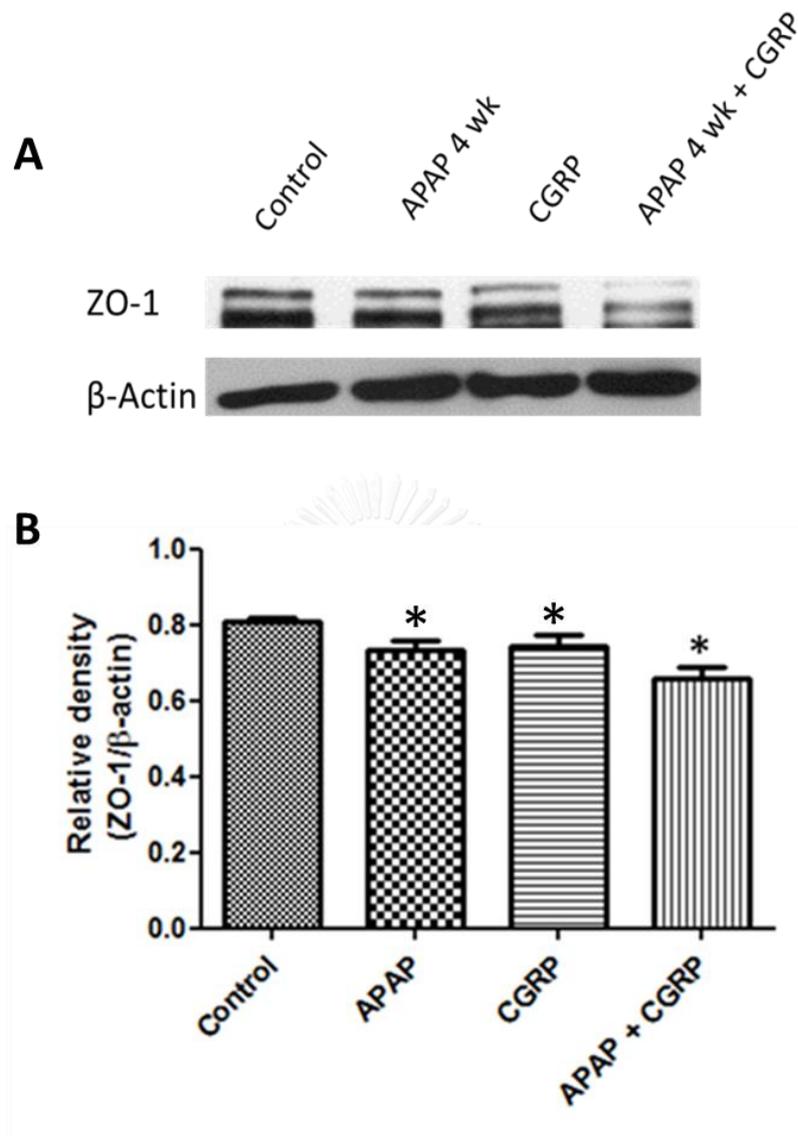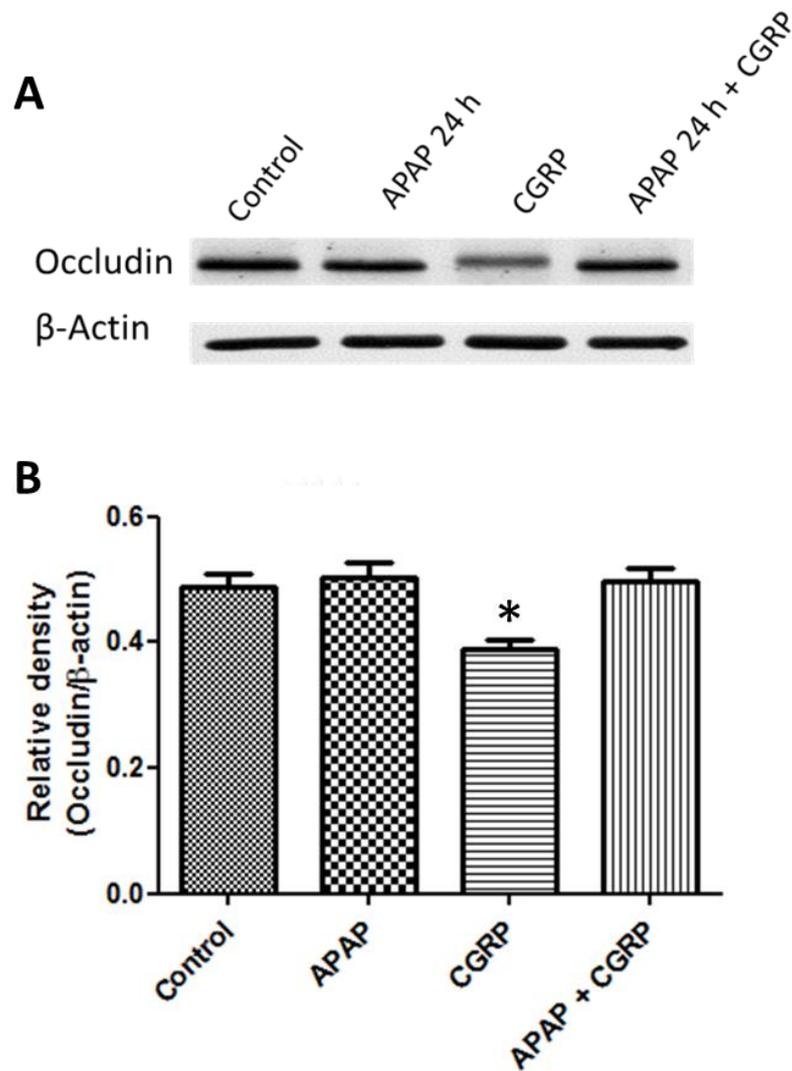
Figure 59 Effects of APAP treatment for 4 weeks on CGRP-induced the expression of claudin-5 in the bEnd.3 cell.

(A) 10 ug total protein extracts were separated on 12.5% SDS-PAGE before transferred onto nitrocellulose membrane. Anti-claudin-5 and goat anti-rabbit-HRP were used for detection.

(B) Quantitative data are expressed as relative densities compared to β-actin.

The experiment was under taken in 3 dependent times with duplicated assay. Data represented as mean ± SEM. $^{*}P<0.05$ compared to the control-treated cells.
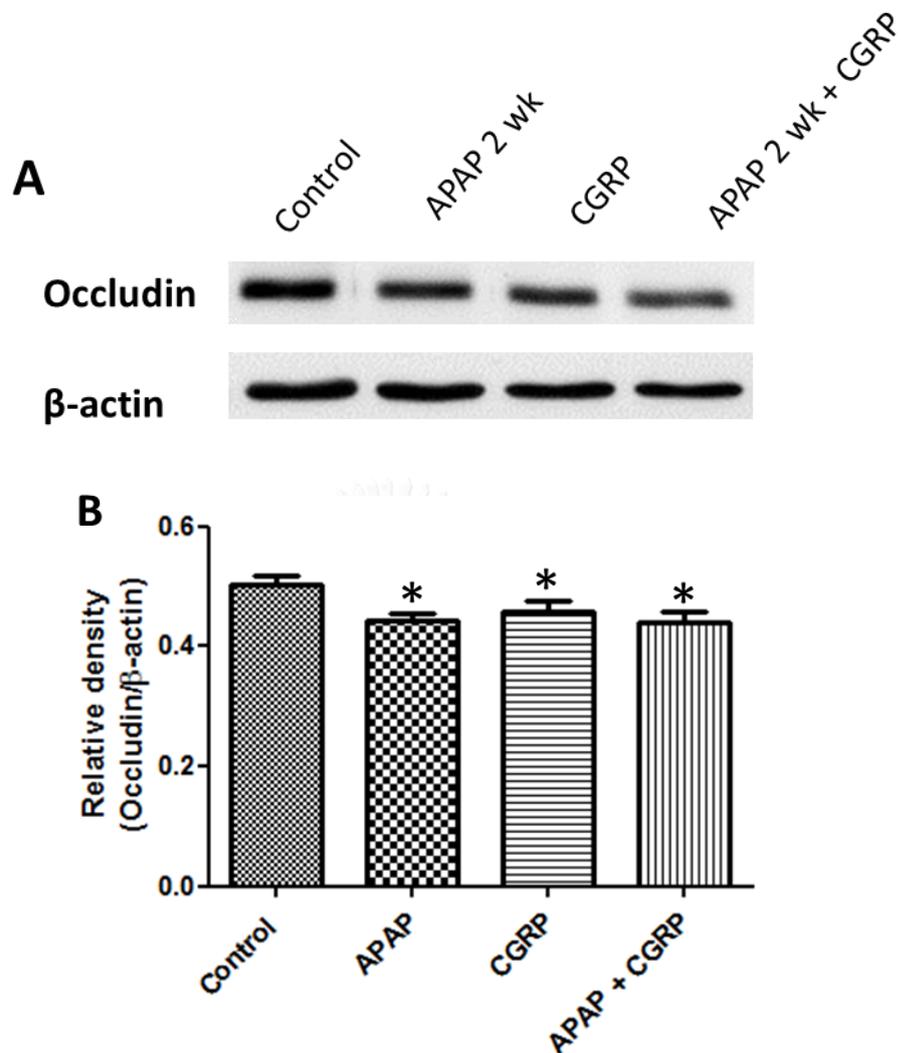
Effect of APAP treatment on the CGRP-induced expression of cell adhesion molecules in cultured mouse brain endothelial (bEnd.3) cells

Three different durations of APAP treatment on the CGRP-induced expression of ICAM-1 and VCAM-1 were investigated in the bEnd.3 cell. The results demonstrated that the CGRP treatment could significantly increase ICAM-1 and VCAM-1 expression at all 3 experiments with different duration of the treatment as compared with control groups($P<0.05$; Figure 60-Figure 65).

While acute APAP treatment for 24 h did not show any effect to the expression of cell adhesion molecules in bEnd.3 cell (Figure 60, Figure 63), chronic APAP treatment (2 and 4 weeks) either alone or in combination with CGRP activation could significantly enhance the expression of both ICAM-1 and VCAM-1 as compared with the control groups ($P<0.05$; Figure 61, Figure 62, Figure 64, Figure 65).

Figure 60 Effects of APAP treatment for 24 h on CGRP-induced the expression of ICAM-1 in the bEnd.3 cell.

(A) 10 ug total protein extracts were separated on 7.5% SDS-PAGE before transferred onto nitrocellulose membrane. Anti-ICAM-1 and rabbit anti-mouse-HRP were used for detection.

(B) Quantitative data are expressed as relative densities compared to β-actin.

The experiment was under taken in 3 dependent times with duplicated assay. Data represented as mean ± SEM. *$P<0.05$ compared to the control-treated cells.
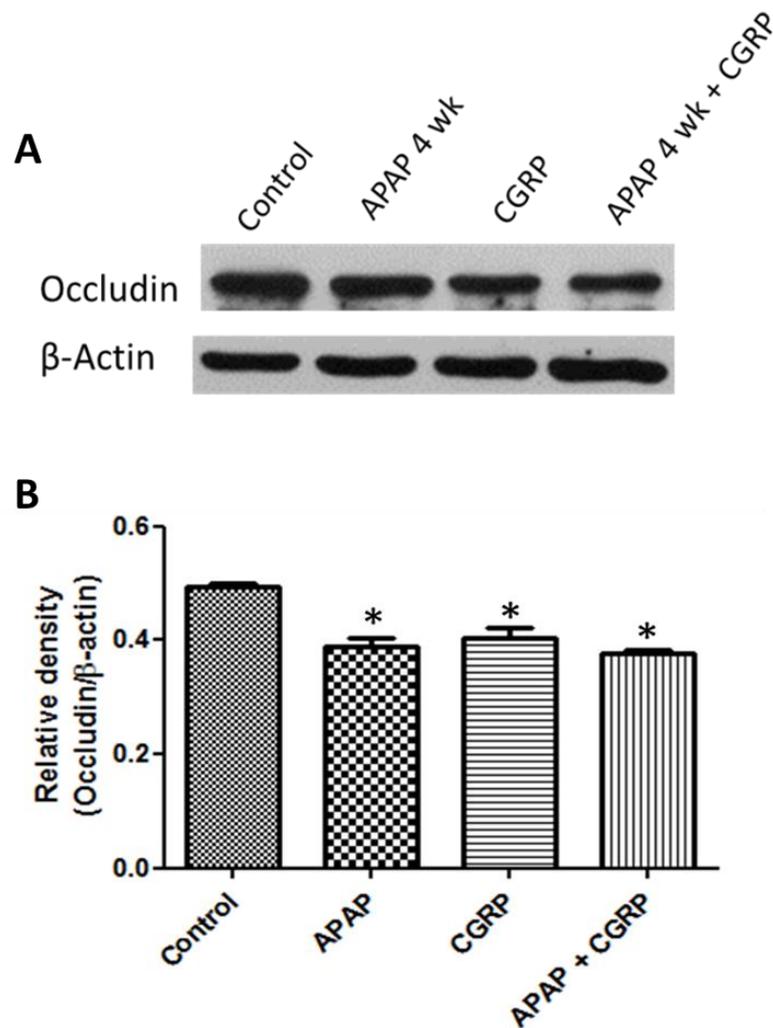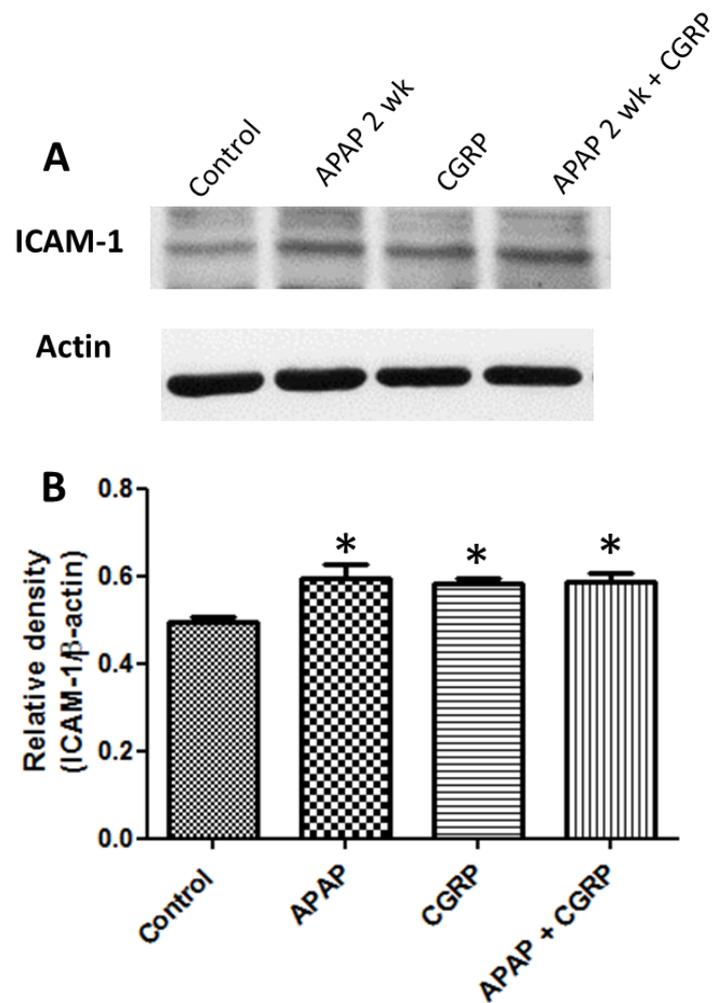
Figure 61 Effects of APAP treatment for 2 weeks on CGRP-induced the expression of ICAM-1 in the bEnd.3 cell.

(A) 10 ug total protein extracts were separated on 7.5% SDS-PAGE before transferred onto nitrocellulose membrane. Anti-ICAM-1 and rabbit anti-mouse-HRP were used for detection.

(B) Quantitative data are expressed as relative densities compared to β-actin.

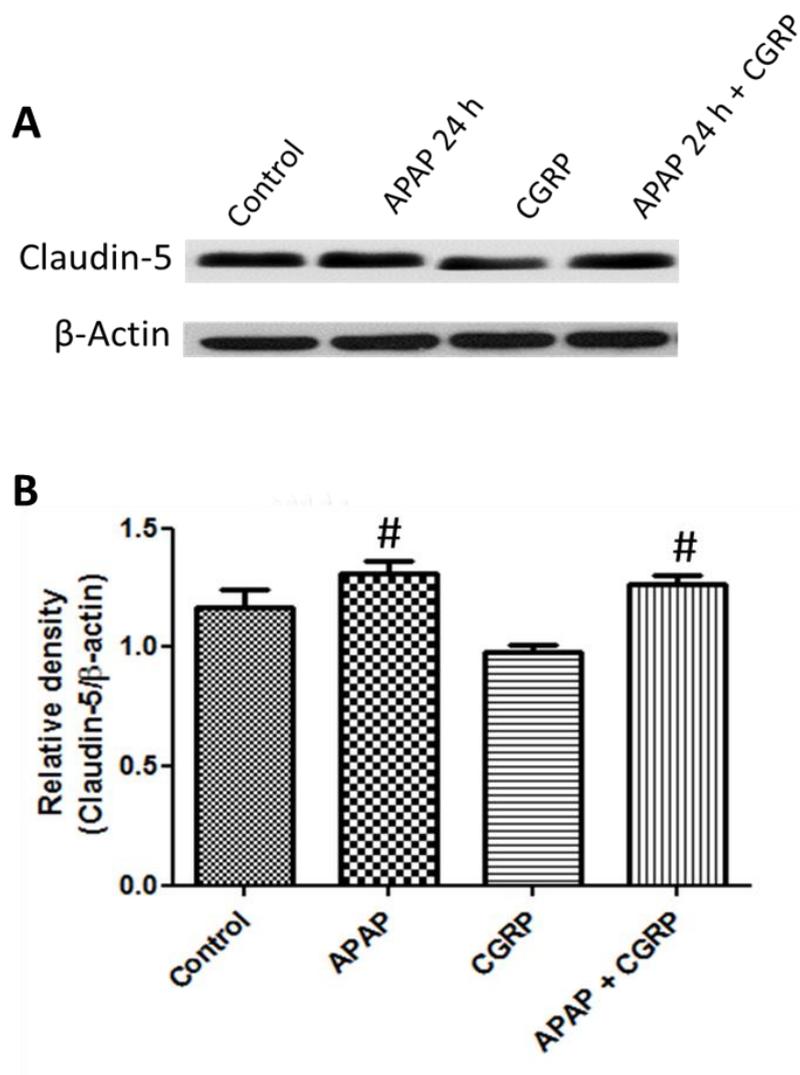The experiment was under taken in 3 dependent times with duplicated assay. Data represented as mean ± SEM. $^*P<0.05$ compared to the control-treated cells. $^*P<0.05$ compared to the control-treated cells.
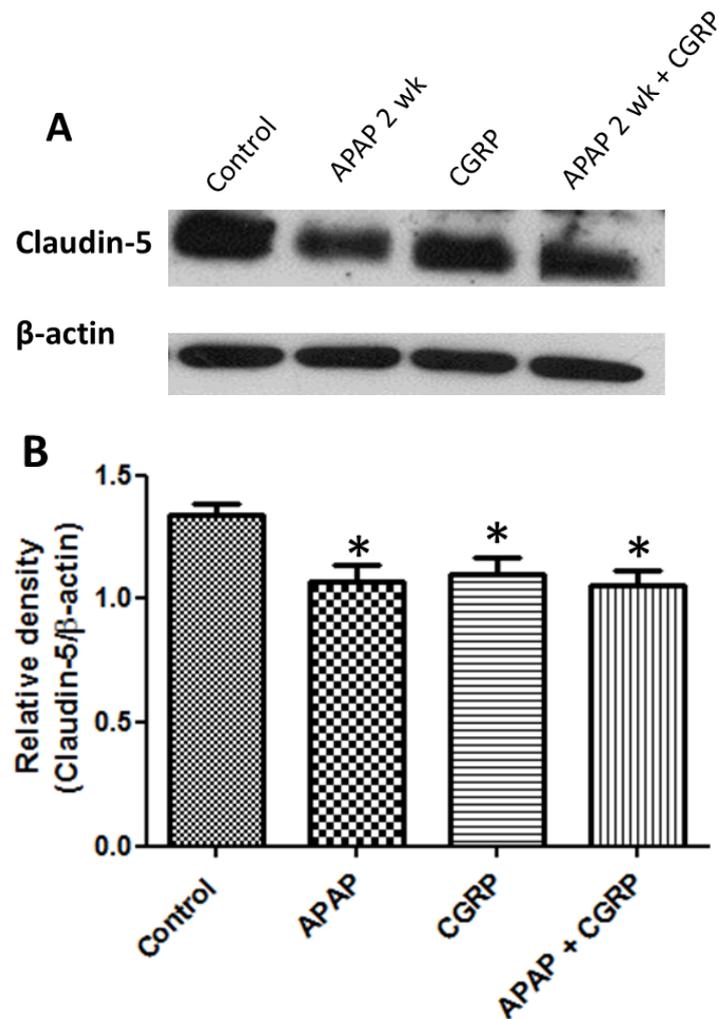
Figure 62 Effects of APAP treatment for 4 weeks on CGRP-induced the expression of
ICAM-1 in the bEnd.3 cell.

(A) 10 ug total protein extracts were separated on 7.5% SDS-PAGE before transferred

onto nitrocellulose membrane. Anti-ICAM-1 and rabbit anti-mouse-HRP were used for

detection.

(B) Quantitative data are expressed as relative densities compared to β-actin.

The experiment was under taken in 3 dependent times with duplicated assay. Data

represented as mean ± SEM. [*]$P<0.05$ compared to the control-treated cells. [*]$P<0.05$

compared to the control-treated cells.

Figure 63 Effects of APAP treatment for 24 h on CGRP-induced the expression of

VCAM-1 in the bEnd.3 cell.

(A) 10 ug total protein extracts were separated on 10% SDS-PAGE before transferred

onto nitrocellulose membrane. Anti-VCAM-1 and goat anti-rabbit-HRP were used for

detection.

(B) Quantitative data are expressed as relative densities compared to β-actin.

The experiment was under taken in 3 dependent times with duplicated assay. Data

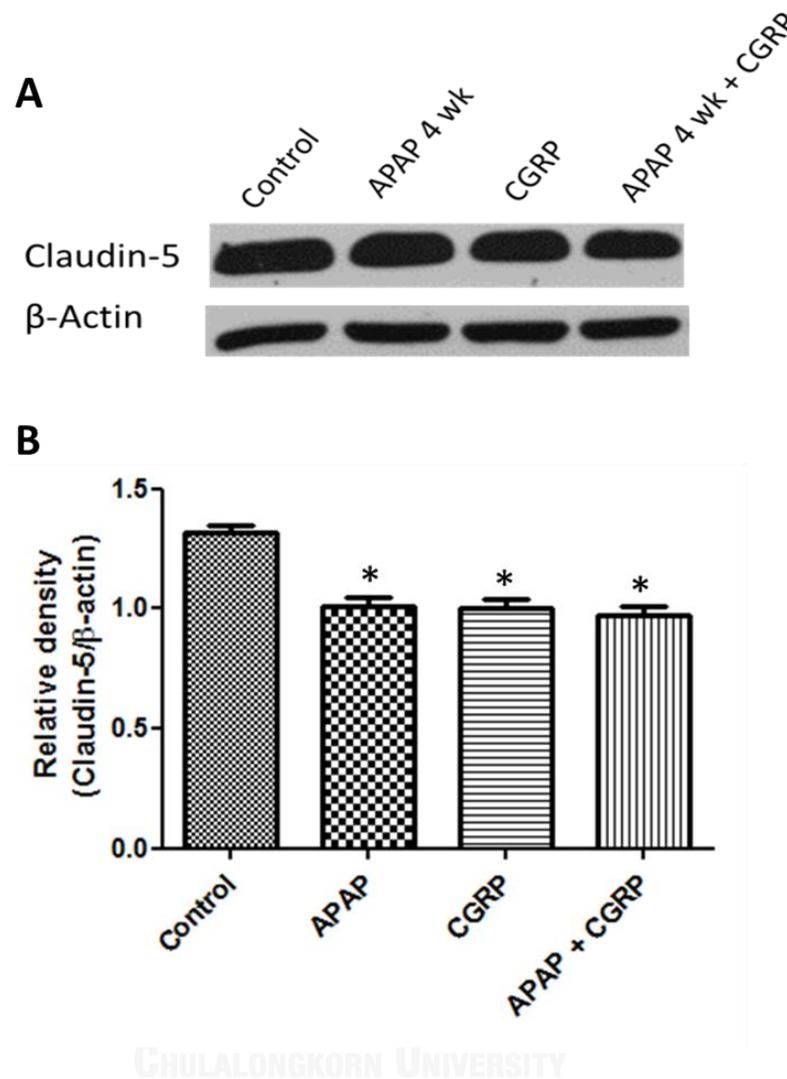represented as mean ± SEM. *P<0.05 compared to the control-treated cells. *P<0.05

compared to the control-treated cells.

Figure 64 Effects of APAP treatment for 2 weeks on CGRP-induced the expression of VCAM-1 in the bEnd.3 cell.

(A) 10 ug total protein extracts were separated on 10% SDS-PAGE before transferred onto nitrocellulose membrane. Anti-VCAM-1 and goat anti-rabbit-HRP were used for detection.

(B) Quantitative data are expressed as relative densities compared to β-actin.

The experiment was under taken in 3 dependent times with duplicated assay. Data represented as mean ± SEM. [*] $P<0.05$ compared to the control-treated cells. [*] $P<0.05$ compared to the control-treated cells.
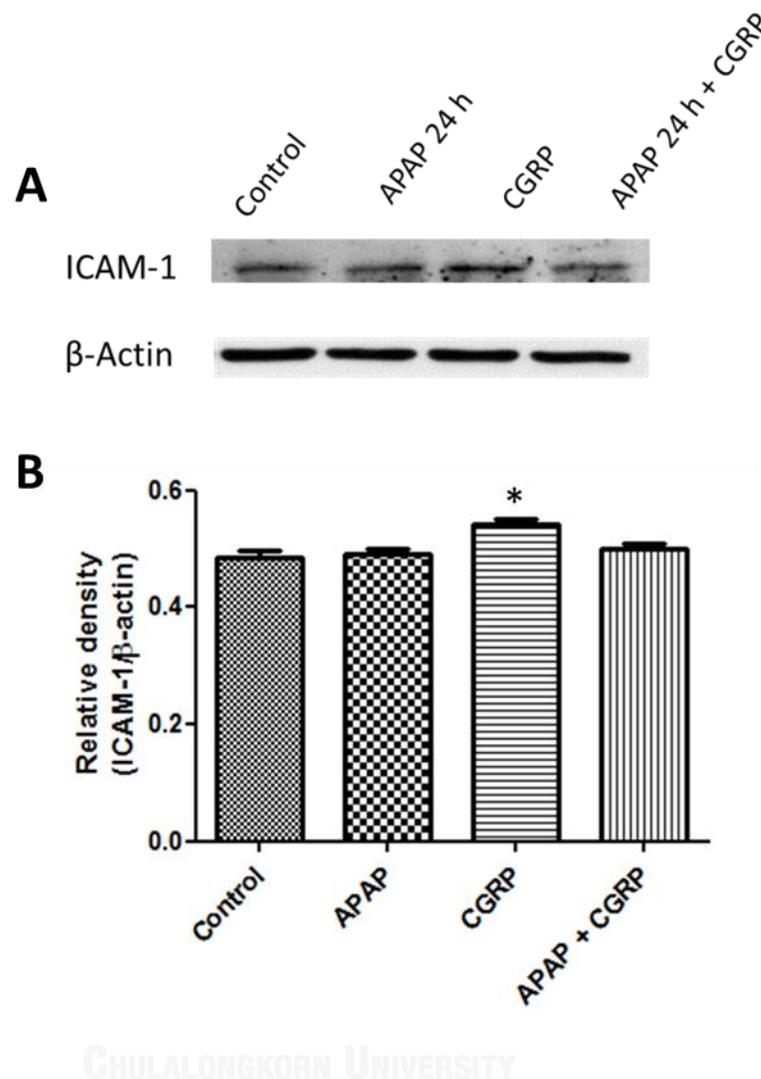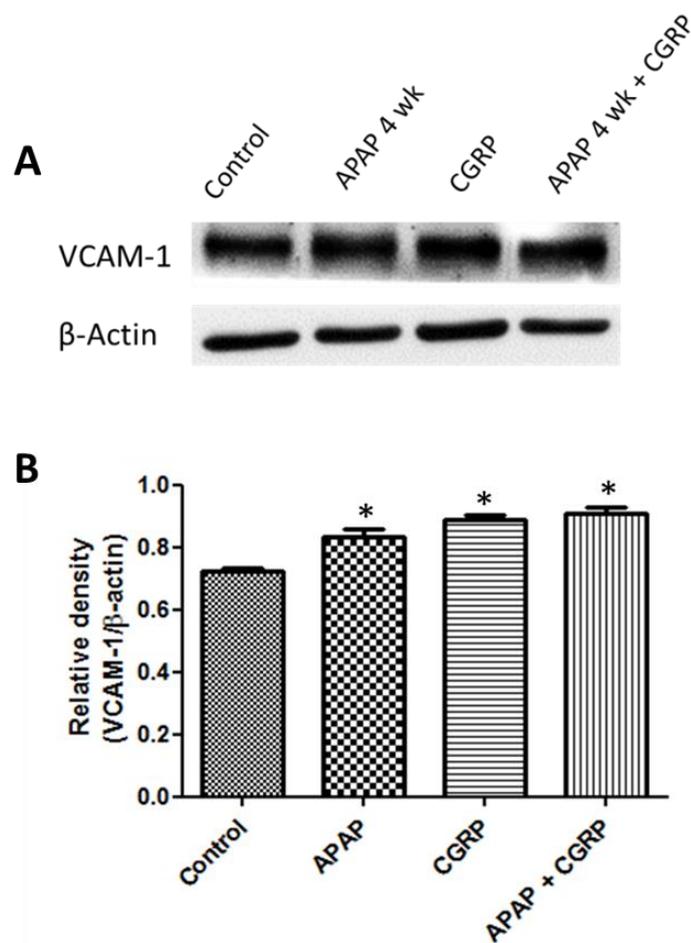
Figure 65 Effects of APAP treatment for 4 weeks on CGRP-induced the expression of VCAM-1 in the bEnd.3 cell.

(A) 10 ug total protein extracts were separated on 10% SDS-PAGE before transferred onto nitrocellulose membrane. Anti-VCAM-1 and goat anti-rabbit-HRP were used for detection.

(B) Quantitative data are expressed as relative densities compared to β-actin.

The experiment was under taken in 3 dependent times with duplicated assay. Data represented as mean ± SEM. *$P<0.05$ compared to the control-treated cells.

*$P<0.05$ compared to the control-treated cells.

Effect of APAP treatment on the CGRP-induced expression of cell adhesion molecules in cultured mouse brain endothelial (bEnd.3) cells

In order to investigate the expression of CYP2E1, 3 different time points of APAP treatment were performed in bEnd.3 cell.3 in the condition with and without CGRP activation.

The results revealed that CGRP activation alone had no effect on the expression of enzyme CYP2E1 activity as compared with the controls. APAP treatment (both acute and chronic treatment) could increase the expression of CYP2E1 comparing with the control group ($P<0.05$; Figure 66, Figure 68). Interestingly, the level of this enzyme was gradually increased since 2 weeks of treatment ($P<0.05$; Figure 67, Figure 68). The highest level of CYP2E1 expression was observed at the fourth weeks of treatment ($P<0.05$; Figure 68).
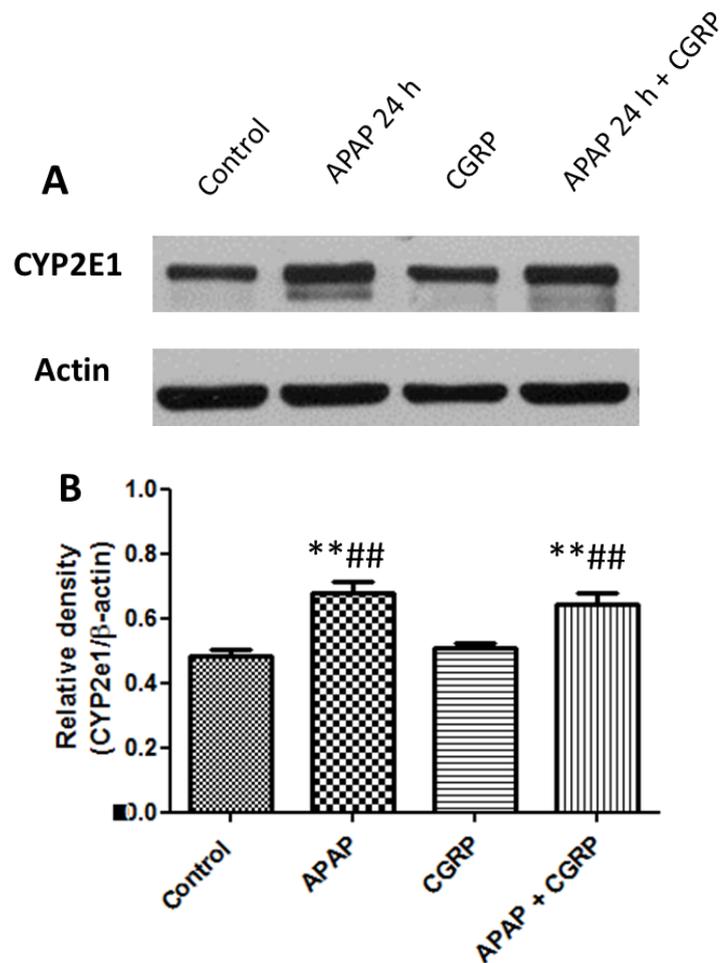
Figure 66 Effects of APAP treatment for 6 h on CGRP-induced the expression of CYP2E1 in the bEnd.3 cell.

(A) 20 ug total protein extracts were separated on 10% SDS-PAGE before transferred onto nitrocellulose membrane. Anti-CYP2E1 and goat anti-rabbit-HRP were used for detection.

(B) Quantitative data are expressed as relative densities compared to β-actin.

The experiment was under taken in 3 dependent times with duplicated assay. Data represented as mean ± SEM. $^*P<0.05$ compared to the control-treated cells. ** $P<0.01$ compared to the control group, $^{##}P<0.01$ compared to the CSD-treated cells.
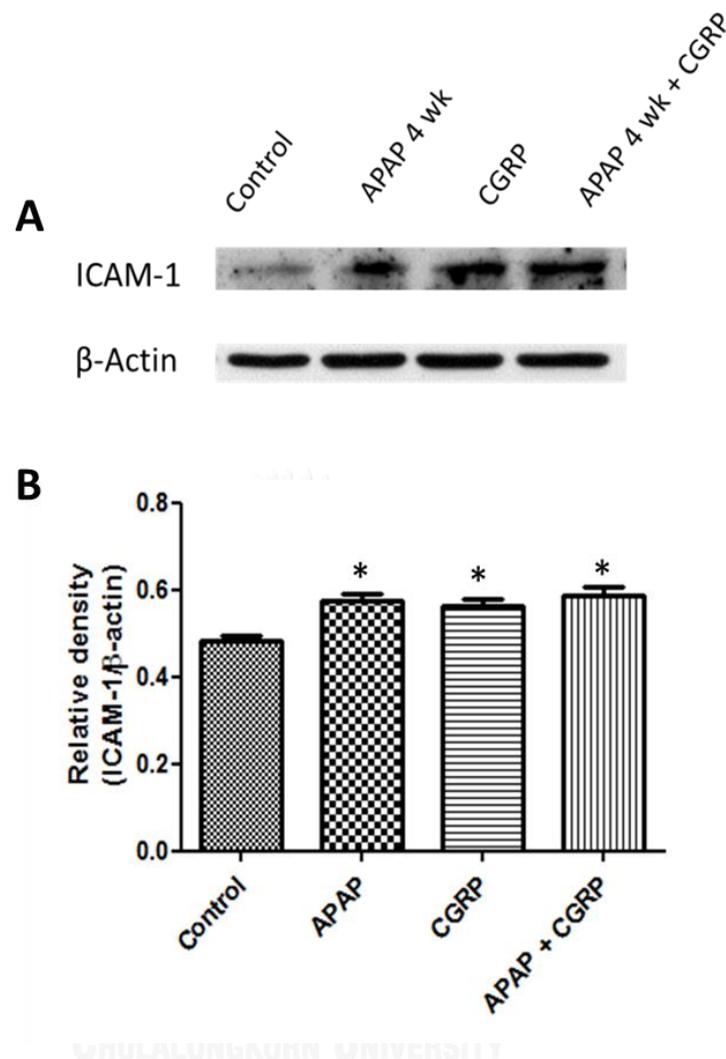
Figure 67 Effects of APAP treatment for 2 weeks on CGRP-induced the expression of CYP2E1 in the bEnd.3 cell.

(A) 20 ug total protein extracts were separated on 10% SDS-PAGE before transferred onto nitrocellulose membrane. Anti-CYP2E1 and goat anti-rabbit-HRP were used for detection.

(B) Quantitative data are expressed as relative densities compared to β-actin.

The experiment was under taken in 3 dependent times with duplicated assay. Data represented as mean ± SEM. *** $P<0.001$ compared to the control-treated cells, ### $P<0.001$ compared to the CSD-treated cells.
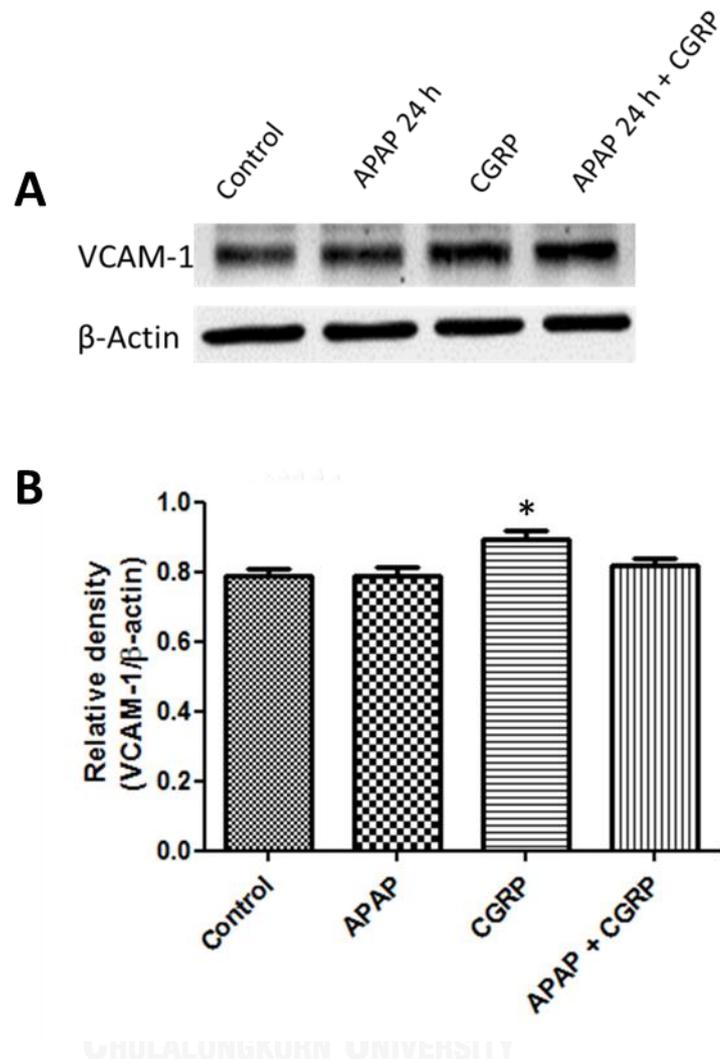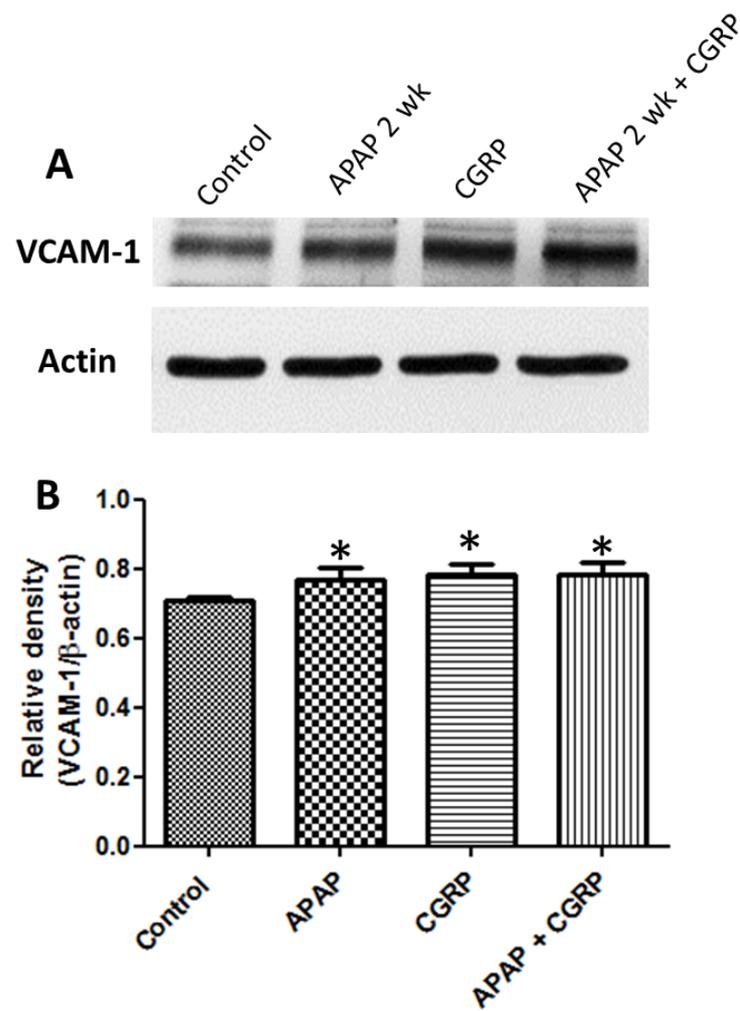
Figure 68 Effects of APAP treatment for 4 weeks on CGRP-induced the expression of CYP2E1 in the bEnd.3 cell.

(A) 20 ug total protein extracts were separated on 10% SDS-PAGE before transferred onto nitrocellulose membrane. Anti-CYP2E1 and goat anti-rabbit-HRP were used for detection.

(B) Quantitative data are expressed as relative densities compared to β-actin.

The experiment was under taken in 3 dependent times with duplicated assay. Data represented as mean ± SEM. *** $P<0.001$ compared to the control-treated cells, ### $P<0.001$ compared to the CSD-treated cells.

Effect of APAP treatment on the activation of the NF-κB signaling pathway in cultured mouse brain endothelial (bEnd.3) cells

In order to confirm whether the effect of APAP treatment involve in the activation of NF-κB signaling pathway, bEnd.3 cell was incubated with APAP treatment at 3 different time points in the condition with and without CGRP activation by western blotting.

With acute APAP treatment, the results demonstrated that there was no difference in the expression of phospho-NF-κB-p65 observed in any groups when compared with the control (Figure 4-59). However, the results demonstrated that the level of phospho-NF-κB-p65 was significantly increased in the chronic APAP-treated cells (2 and 4 weeks) in both with and without CGRP activation (Figure 70; Figure 71). Interestingly, with 4 weeks of APAP treatment, the significant higher of phospho-NF-κB-p65 expression was clearly demonstrated in cells with CGRP activation as compared with the control, CGRP-activated alone, and APAP-treated cells (Figure 71).

Figure 69 Effects of APAP treatment for 24 h on CGRP-induced the expression of

phospho-NF-kB p65 in the bEnd.3 cell.

(A) 20 ug total protein extracts were separated on 10% SDS-PAGE before transferred

onto nitrocellulose membrane. Anti- phospho-NF-kB p65 and goat anti-rabbit-HRP

were used for detection.

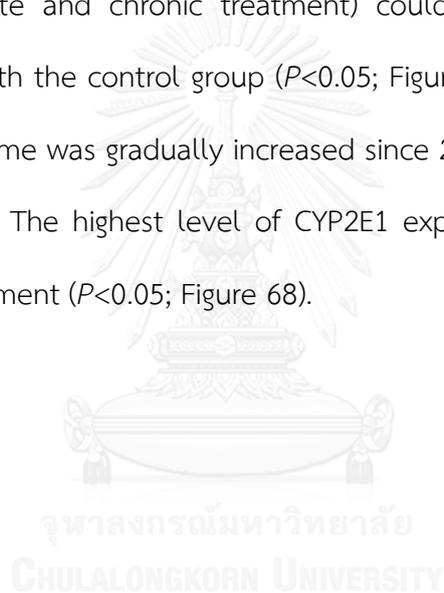(B) Quantitative data are expressed as relative densities compared to total NF-kB.

The experiment was under taken in 3 dependent times with duplicated assay. Data

represented as mean ± SEM.

Figure 70 Effects of APAP treatment for 24 h on CGRP-induced the expression of phospho-NF-kB p65 in the bEnd.3 cell.

(A) 20 ug total protein extracts were separated on 10% SDS-PAGE before transferred onto nitrocellulose membrane. Anti- phospho-NF-kB p65 and goat anti-rabbit-HRP were used for detection.

(B) Quantitative data are expressed as relative densities compared to total NF-kB.

The experiment was under taken in 3 dependent times with duplicated assay. Data represented as mean ± SEM. ** $P<0.01$ compared to the control-treated cells, [#] $P<0.05$ compared to the CSD-treated cells.
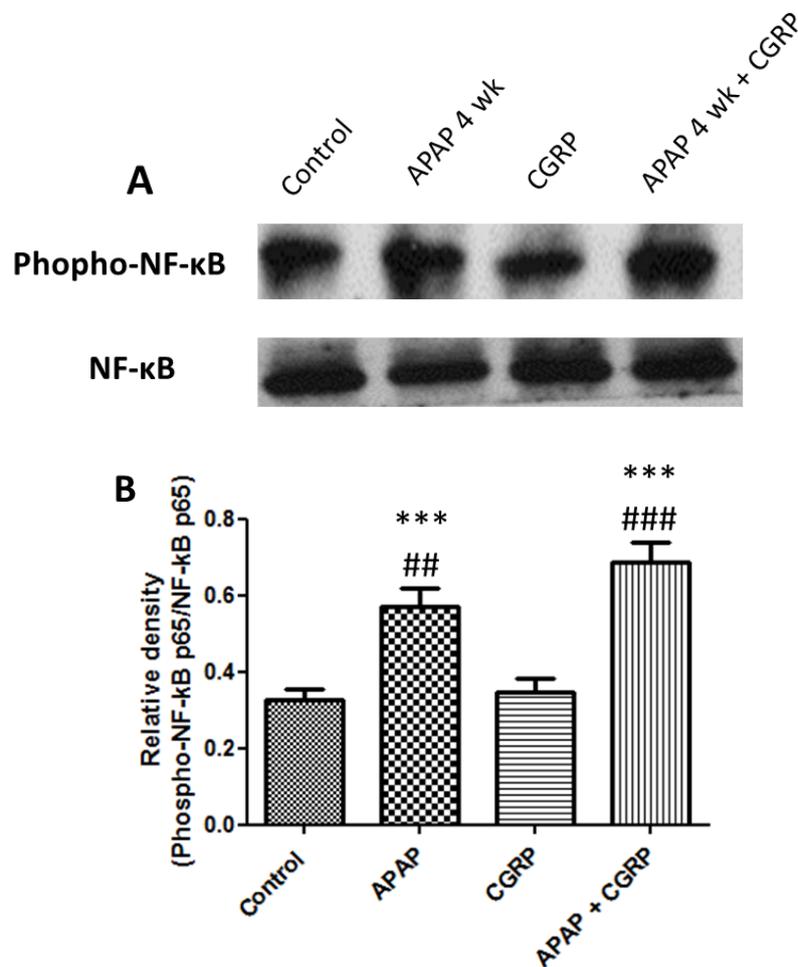
Figure 71 Effects of APAP treatment for 4 weeks on CGRP-induced the expression of phospho-NF-kB p65 in the bEnd.3 cell.

(A) 20 ug total protein extracts were separated on 10% SDS-PAGE before transferred onto nitrocellulose membrane. Anti- phospho-NF-kB p65 and goat anti-rabbit-HRP were used for detection.

(B) Quantitative data are expressed as relative densities compared to total NF-kB.

The experiment was under taken in 3 dependent times with duplicated assay. Data represented as mean ± SEM. *** $P<0.001$ compared to the control-treated cells, [##] $P<0.01$ compared to the CSD-treated cells, [###] $P<0.001$ compared to the CSD-treated cells.

Effect of APAP treatment on the activation of Protein Kinase A in mouse brain endothelial (bEnd.3) cells

At a molecular level, the binding of CGRP to its receptor, expressed on endothelial cells, leads to the activation of adenylate cyclase resulting in an accumulation of cAMP. High levels of cAMP will activate protein kinase A (PKA) signaling pathway. To investigate the effect of APAP treatment on the activation of PKA, levels of phosphorylated PKA were detected at three different time points with or without CGRP activation by Western Blotting. For APAP-treated cells, either acute or chronic treatment, the levels of phosphorylated PKA were not different from that of control cultured cells (Figure 72, Figure 74). Results demonstrated that CGRP activation alone or in combination with chronic APAP treatment (2 and 4 weeks) significantly increased the expression of phosphorylated PKA, when comparing with the control cultured cells (Figure 73, Figure 74). Interestingly, at the fourth weeks of APAP treatment, the increase of phosphorylated PKA expression was observed when the treatment was combined with CGRP activation (Figure 74).
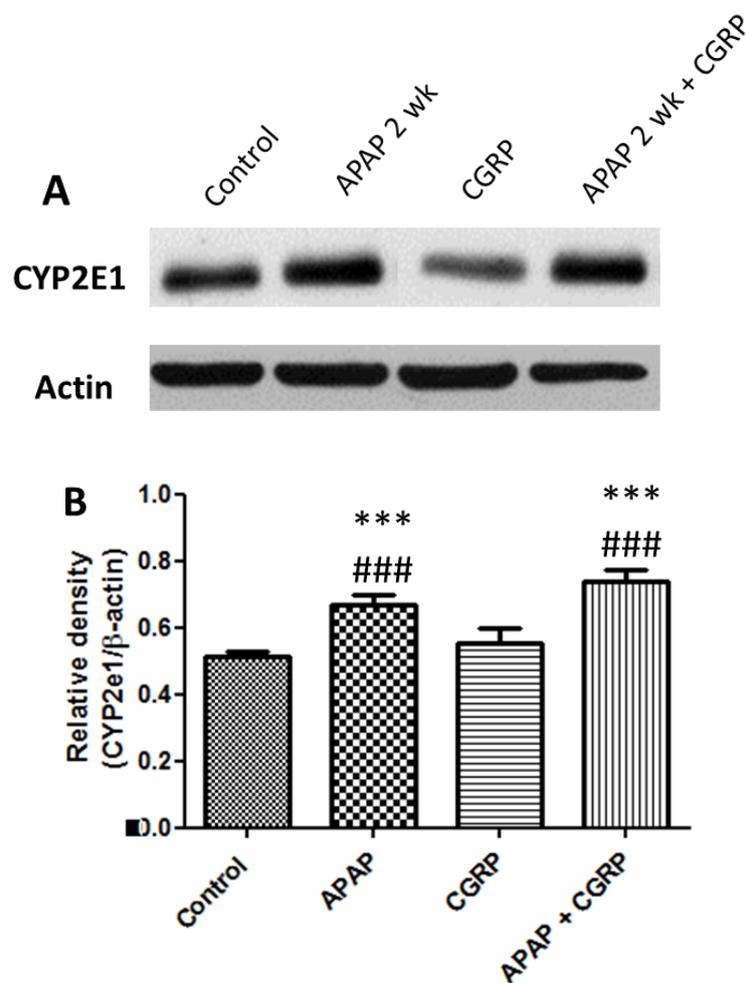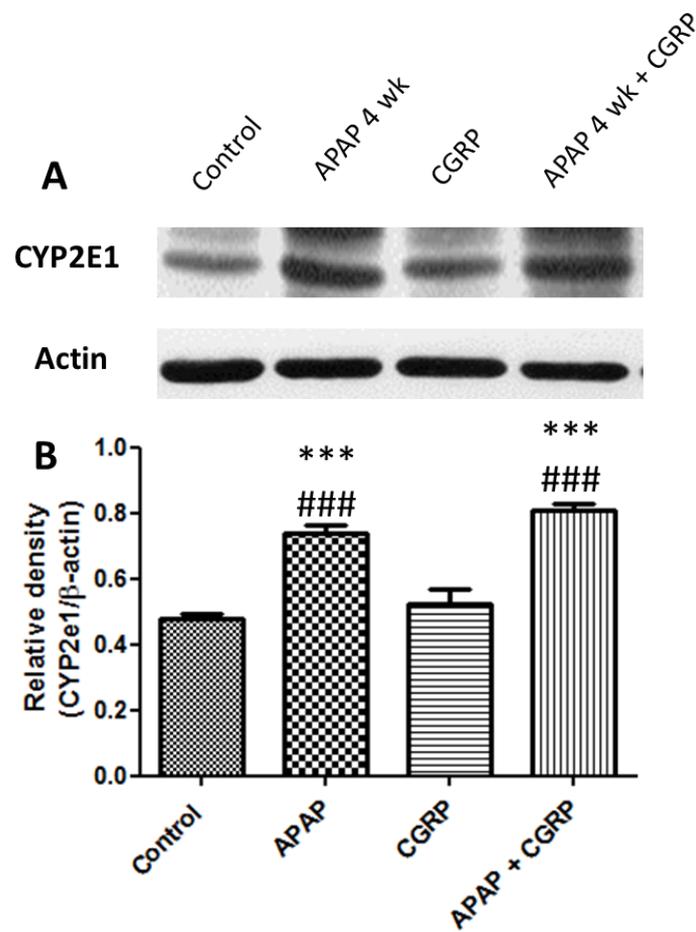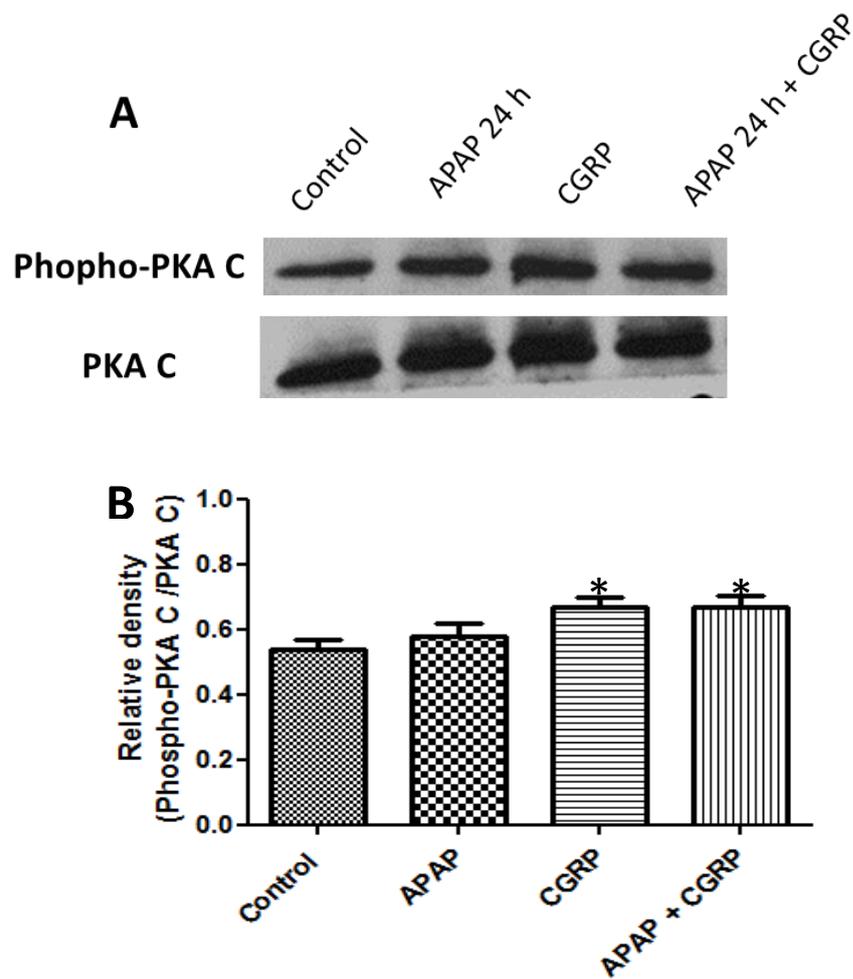
Figure 72 Effects of APAP treatment for 24 h on CGRP-induced the expression of phospho-PKA in the bEnd.3 cell.

(A) 10 ug total protein extracts were separated on 10% SDS-PAGE before transferred onto nitrocellulose membrane. Anti- PKA and goat anti-rabbit-HRP were used for detection.

(B) Quantitative data are expressed as relative densities compared to total PKA.

The experiment was under taken in 3 dependent times with duplicated assay. Data represented as mean ± SEM. $^*P<0.05$ compared to the control-treated cells.
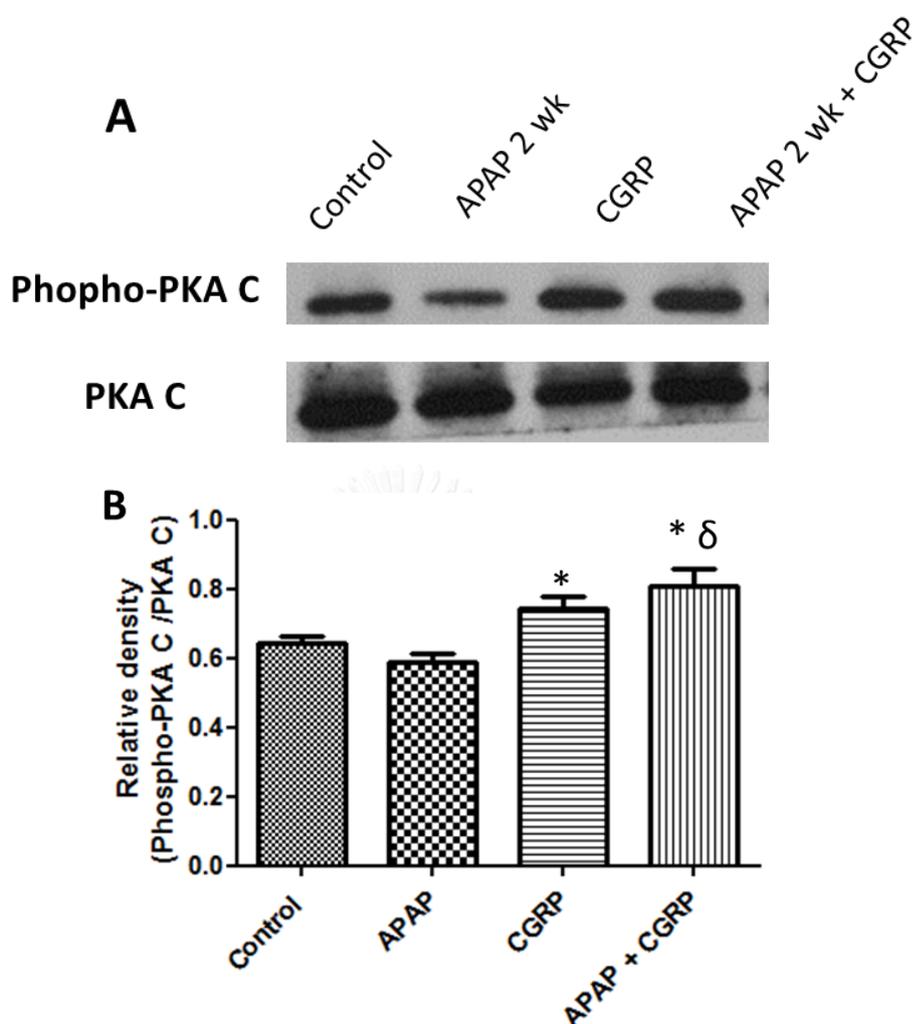
Figure 73 Effects of APAP treatment for 2 weeks on CGRP-induced the expression of phospho-PKA in the bEnd.3 cell.

(A) 10 ug total protein extracts were separated on 10% SDS-PAGE before transferred onto nitrocellulose membrane. Anti- PKA and goat anti-rabbit-HRP were used for detection.

(B) Quantitative data are expressed as relative densities compared to total PKA.

The experiment was under taken in 3 dependent times with duplicated assay. Data represented as mean ± SEM. $^*P<0.05$ compared to the control group, $^\delta P<0.05$ compared to the APAP-treated-treated cells.
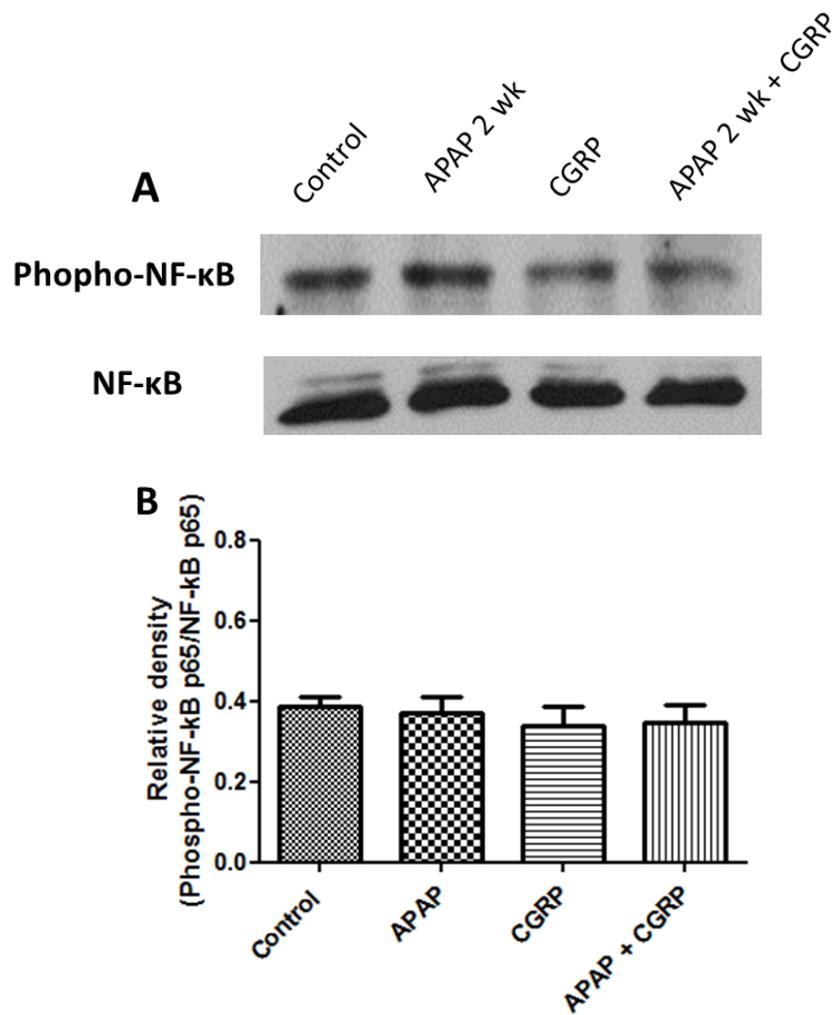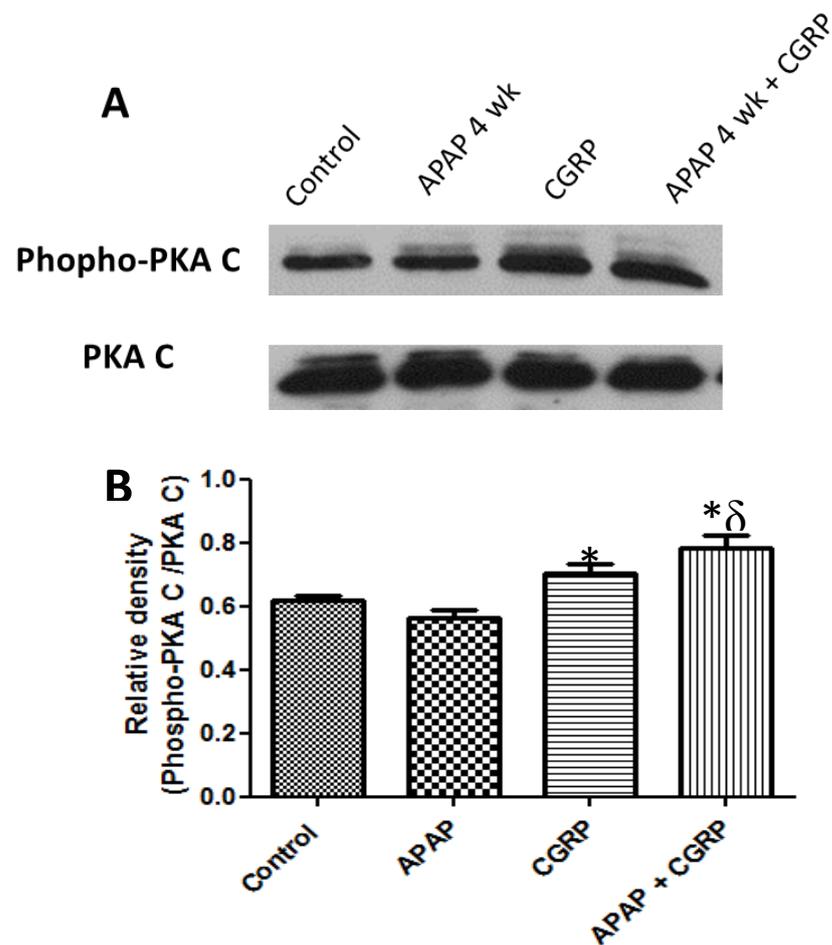
Figure 74 Effects of APAP treatment for 4 weeks on CGRP-induced the expression of phospho-PKA in the bEnd.3 cell.

(A) 10 ug total protein extracts were separated on 10% SDS-PAGE before transferred onto nitrocellulose membrane. Anti- PKA and goat anti-rabbit-HRP were used for detection.

(B) Quantitative data are expressed as relative densities compared to total PKA.

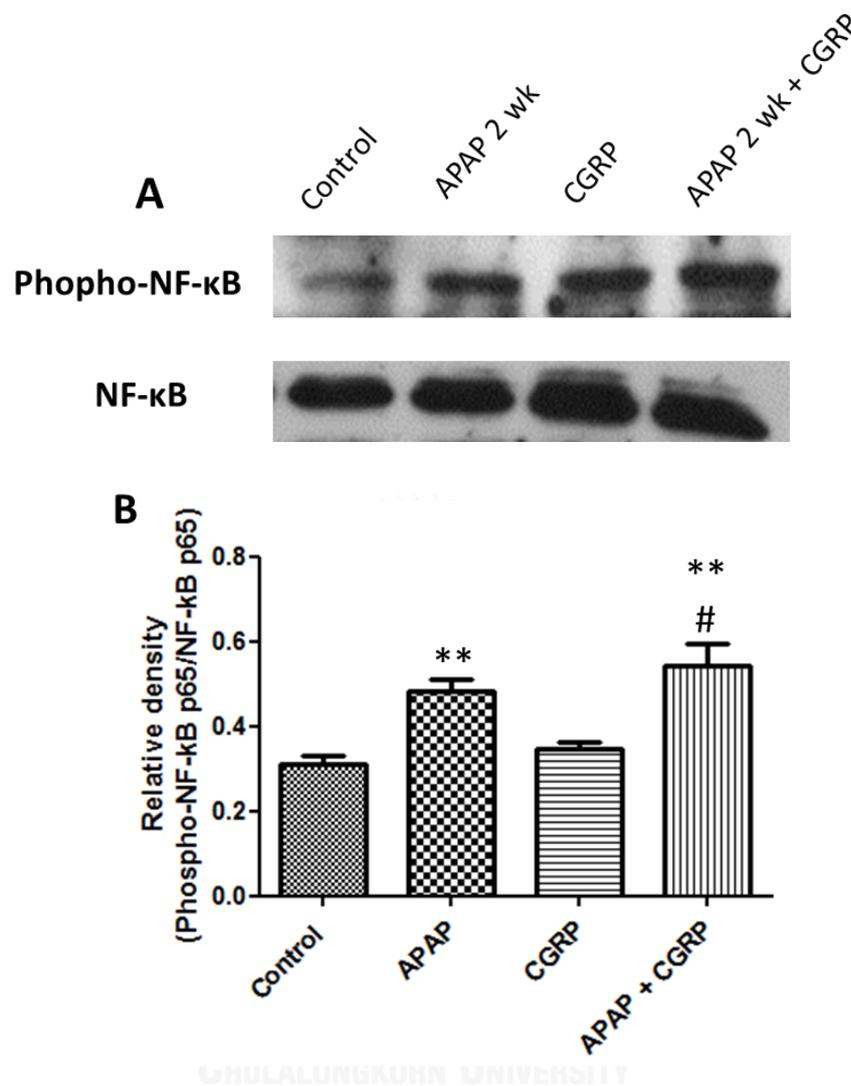The experiment was under taken in 3 dependent times with duplicated assay. Data represented as mean ± SEM.

* $P<0.05$ compared to the control-treated cells, $^{\delta}$ $P<0.05$ compared to the APAP-treated-treated cells.

CHAPTER V
DISCUSSION

The results obtained from the present study, either *in vivo* or *in vitro* study demonstrate that acute and chronic treatments with APAP demonstrate the different effect on the cerebral microvessels. While short-term APAP treatment can protect cerebral microvessels against the CSD or CGRP activation, long-term APAP treatment (≥2 weeks) reveals an opposite effect. Exposure with APAP for long period can result in the alteration of BBB integrity in both cerebral microvessels and cultured endothelial cells. Furthermore, in combination with CSD or CGRP activation, the damage of BBB integrity is more prominent.

The results obtained from *in vivo* study clearly demonstrate that the cerebral microvessels with acute and chronic APAP treatment response differently to the CSD activation.   While acute APAP treatment decreases the alterations of cerebral microvessels induced by CSD, chronic APAP treatment reveals the opposite response.

Cumulative data demonstrated that during CSD activation the alterations in both neural and vascular compartments were observed [64, 99]. Regarding to the alteration in vascular compartment, the changing in cerebral circulation was observed in studies from either migraine patients or animal models. Increases in the expression of vascular adhesion molecules have been detected during migraine attacks [33]. Those alterations of the cerebral microvessels induced by CSD have been further confirmed by the observation of leakage of plasma protein extravasation from rat cerebral vessels after CSD activation [31, 32]. Increase of oxidative stress and neurogenic inflammation due to the release of vasoactive neurotransmitters (i.e., CGRP, SP, and NO) from perivascular nerve terminals are

accepted to be mechanisms involved in these hemodynamic changes [73, 74]. The present results are in line with these observations. The higher alterations of cerebral microvessels including the ultrastructural changes and the expressions of cell adhesion molecules (ICAM-1 and VCAM-1) were observed in animals with CSD activation as compared to the control group.

In this study, pretreatment with APAP 1 hour before CSD activation can attenuate the CSD-induced alterations in cerebral microvessels. This result is in agreement with the result obtained from previous study which demonstrated that acute APAP treatment could attenuate the neuronal excitability induced by CSD [16]. The decrease in the neuronal excitation due to the acute APAP treatment can result in the decreases in the amounts of vasoactive neurotransmitters (CGRP and SP) released from perivascular neurons which leads to the attenuation of the cerebral microvessels changes in this group.

Interestingly, in this study, chronic APAP treatment (15 and 30 days) demonstrated the different effect from acute treatment. The results revealed that treatment with APAP for long term can change the effects of this drug from protective to threatening as demonstrated by the increment of the cerebral microvessels alterations. The opposite effect of APAP when using as a long-term treatment has previously reported in the same animal model [16, 17]. The results demonstrated that, while acute APAP treatment attenuates CSD-induced cortical neuron excitation, chronic APAP treatment enhances the sensitization of these cortical neurons as indicated by the increment of depolarizing shifts frequency after CSD activation [16, 17]. The present study have confirmed the results obtained from the previous studies which demonstrated that chronic APAP treatment alone could

induce alterations of cerebral microvessel , when combined with CSD activation, those alterations were more prominent .

APAP is one of the drugs which can easily cross the BBB. In this case the APAP, after reaching the brain circulation, can be metabolized by the enzyme CYP2E1leading to the formation of NAPQI in the brain [19, 23, 24]. NAPQI is a toxic substance which can be quickly captured by brain GSH. Since GSH plays a major role as a cellular anti-oxidant that neutralizes several types of toxins and free radicals in the brain, thus in case of chronic APAP treatment, low levels of GSH in the brain may be occurred due to the increase production of NAPQI. In this study, the increment of enzyme CYP2E1 activity observed in the cerebral cortex obtained from the rats with long-term APAP treatment can indicate the higher level of NAPQI produced in the brain. Increases in NAPQI levels together with depletions of GSH can result in increases in oxidative stress, which can lead to a series of alterations in the brain including damage of endothelial cells. Furthermore, the recent studies in rats with chronic APAP treatment have demonstrated the increments of pro-inflammatory cytokines in several brain regions including the cerebral cortex and hippocampus [100]; [101]. Based on these accumulative data, the increase in the pro-inflammatory cytokines and oxidative stress in the brain can possibly be mechanism underlying the deterioration of BBB integrity following the chronic treatment of APAP.

The present results are in line with recent studies which demonstrated that chronic APAP treatment changes the properties of its therapeutic effects. At therapeutic doses, cumulative evidence demonstrated that chronic APAP treatment can affect the circulatory system [12-15]. Their results revealed that women and men who frequently took APAP at a dosage of 500 mg/day exhibited a nearly 2-fold

increase in the relative risk of incident hypertension when compared to nonusers [12-14]. Moreover, Sudano et al. (2010) also confirmed non-beneficial effect of chronic APAP treatment on the circulatory system. They demonstrated that collateral treatment with APAP at a therapeutic dose (1 gram/day) and standard cardiovascular therapy for two weeks induced increases in both systolic and diastolic blood pressure in patients with coronary heart disease [15]. Additionally, a study of mouse airways conducted by Nassini et al. (2010) found that single and repeated treatment with APAP at therapeutic doses results in increases in the formation of NAPQI and increases in pro-inflammatory cytokine levels (i.e., monocyte chemotactic protein-1 (MCP-1), IL-1β, and TNF-α) [20]. Furthermore, they also demonstrated that NAPQI plays an important role in the series of alterations that are observed after APAP treatment. This molecule resulted in increments in the amounts of neuropeptides (SP and CGRP) released from the sensory nerve terminal, increases in pro-inflammatory cytokine production and neurogenic inflammation and plasma protein extravasation in the mice airway [20].

Regarding to the role of CGRP on the alteration of the trigeminovascular system, the alteration of the CGRP expression in TG was also monitored in this study. The result demonstrated that induction of CSD significantly increased the average percentage of total CGRP-IR neurons compared with the control groups. With different durations, the treatment with APAP has different effects on CGRP expression in the TG. While acute treatment (day 0) with APAP attenuates CSD-induced CGRP expression in the TG, long term treatment (≥ 2 weeks) with APAP increases CSD-induced CGRP expression in the TG. Interestingly, treatment with APAP alone for more than 2 weeks also up-regulates CGRP expression when compared with controls.

Regarding to the impact of treatment duration on the CGRP expression in TG, studies in other analgesic drugs have previously reported the association between the alteration of CGRP expression and duration of the treatment. In 2010, De Felice et al. revealed that sustained administration of triptan, a standard anti-migraine drug, could induce cutaneous allodynia [102] instead of having the normal anti-migraine effect when used for a short time. The development of allodynia occurred in parallel with increased CGRP expression in trigeminal dural efferents. The authors suggested that these alterations might be the mechanism underlying the transformation of migraines to the medication overuse headache (MOH) [102]. In addition, studies of prolonged morphine treatment have demonstrated remarkable changes in the nociceptive pathway. Rats with prolonged exposure to morphine demonstrated an incremental change in spinal dynorphin as well as a tolerance to the anti-nociceptive effects of this drug [95, 103]. The accumulating evidence strongly suggests that treatment with an analgesic drug for long periods can result in increased release and expression of CGRP, which eventually induces abnormal nociceptive responses. However, the mechanism underlying this shift remains unknown.

Several lines of evidence indicate that in the TG, CGRP itself acts as an autocrine factor, with the ability to modulate its own synthesis and release via CGRP receptor activation [104, 105]. At peripheral nerve terminals, CGRP can modulate synaptic transmission, mast cell degranulation, and cause the release of inflammatory cytokines. These pathophysiological events can induce neurogenic inflammation and activate perivascular neurons, resulting in the activation of the trigeminovascular nociceptive system [104-106]. Together, these data suggest that stimulation of CGRP release from TG can eventually form a positive-feedback loop

with the trigeminal neurons to induce further synthesis and release of CGRP from the nerve terminals.

The present results obtained from *in vivo* study suggest that the short-term use of APAP can protect the cerebral microvessels against CSD activation; however, long-term treatment with this drug causes damage to these vessels. The alterations of BBB are observed in parallel with an increment of the CGRP expression in TG. When combined with CSD activation, the damage of cerebral microvessels induced by long-term APAP treatment is more severe. These data suggest that the accumulation of NAPQI and the increase of CGRP expression are both involved in the alterations of cerebral microvessels observed in the rats with chronic APAP treatment.

The effect of chronic APAP treatment and the involvement of CGRP on the alterations of BBB integrity have been confirmed by the results obtained from the study in cultured mouse endothelial cell.

The results obtained from the study in this part are correlated with those of the study in migraine animal model. The results revealed that while the acute treatment with APAP could attenuate the CGRP-induced the alteration of the tight junction protein in bEnd.3 cell, the chronic treatment demonstrate the opposite effect. Exposure brain endothelial cell to APAP for more than 2 weeks either alone or with CGRP can enhance the CYP2E1 activity as well as expression of cell adhesion molecules (ICAM-1 and VCAM-1). The level of tight junction proteins (ZO-1, occludin, and claudin-5) are also lower in these groups as compared with the control. These results can strongly confirm the involvement of CGRP in the alteration of BBB

integrity after chronic APAP treatment which was observed in the study of the *in vivo* part.

An increase activity of CYP2E1 observed in the cultured brain endothelial cells with chronic treatment of APAP indicating the accumulation of NAPQI in those cells which can leads to the increment of oxidative stress and finally causes the damage of brain endothelial cell and affects tight junction proteins.

Taken the results from the study in CSD animal model together with the results from the study in endothelial cell culture, there is at least two factors involved in the alteration of BBB integrity following the chronic treatment with APAP: oxidative stress and CGRP. In order to confirm whether pathways are involved in these alterations, two different signaling pathways (PKA for CGRP activation, and NF-**K**B for APAP treatment) were also monitored in this study.

In endothelial cell, CGRP, via activation of its receptors ($G_s\alpha$-protein coupled receptor), can result in the elevation of intracellular cAMP level and then stimulates the phosphorylation of PKA signaling molecule which can finally result in the increase of NO production [107]. It is known that an increment of NO can induce endothelial cell damage by interaction with other oxidant molecules [108, 109]. In this experiment, bEnd.3 cell that was activated with CGRP alone demonstrated the higher levels of phosphorylated PKA. Moreover, in combination with chronic APAP treatment, the increment of this signaling molecule seems to be increased than those observed in the CGRP treatment alone.

In addition, the activation of the NF-**K**B signaling pathway was clearly demonstrated after chronic APAP treatment alone (≥2 weeks). In the combination

with CGRP, the activation of this signaling pathway is significant higher than those observed in chronic APAP treatment alone. These data suggest that chronic APAP treatment alone may induce the increase either oxidative stress or inflammatory cytokine production from brain endothelial cell which can consequently result in the alterations of BBB integrity. The expression of these molecules after APAP treatment was previously demonstrated by several studies [19, 93, 100, 110]. The present results also reveal that in combination with CGRP activation, the increment of the activation of the NF-**K**B signaling pathway is more prominent.

In summary, the results obtained from both *in vivo* and *in vitro* studies demonstrate that the short-term treatment of APAP still protect the cerebral microvessels against CSD activation; however, long-term treatment with this drug at the same dose can induce the damage to these vessels. When combined with CSD activation, the damage to cerebral microvessels induced by long-term APAP treatment is more severe. The increment of oxidative stress and CGRP expression in TG due to the chronic APAP treatment are all involved in those alterations. Thus, long-term treatment with APAP for patients with CSD-related disorders, particularly migraine headaches, might need to be carefully monitored.

CHAPTER VI
CONCLUSION

Based on the results observed from both in vivo and in vitro studies, it can be concluded that:

1. Acute and chronic treatments with APAP demonstrate the different effect on the cerebral microvessels.

2. Acute APAP treatment can protect cerebral microvessels against the CSD or CGRP activation.

3. Chronic APAP treatment can induce damage to BBB integrity; decrease of tight junction proteins, increase of ultrastructural alterations of endothelial cells, IgG extravasation and cell adhesion molecules.

4. In combination with CSD or CGRP activation, the damage of BBB integrity is more severe.

5. Chronic APAP treatment can up-regulates CGRP expression in TG.

6. Up-regulation of CGRP is enhanced in chronic APAP treatment in combination with CSD activation.

7. The activation of both PKA and NF-κB signaling pathways are involved in the alterations of BBB integrity observed in chronic APAP treatment.
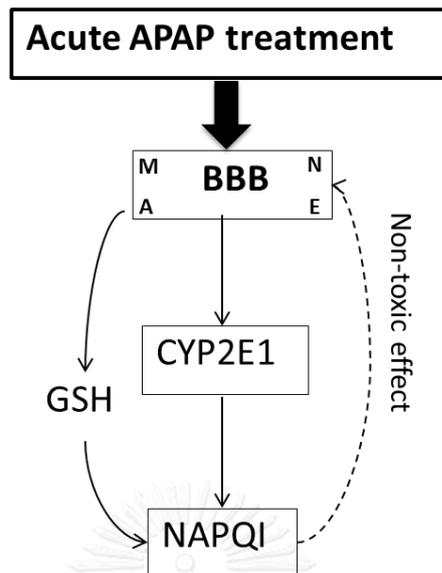
Figure 75 Schematic diagram of effect of acute APAP treatment on BBB integrity.
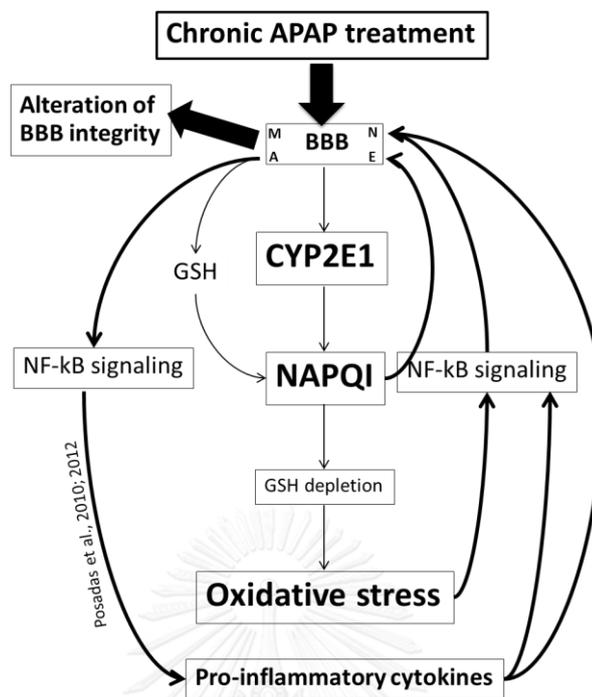
Figure 76 Schematic diagram of effect of chronic APAP treatment on BBB integrity.
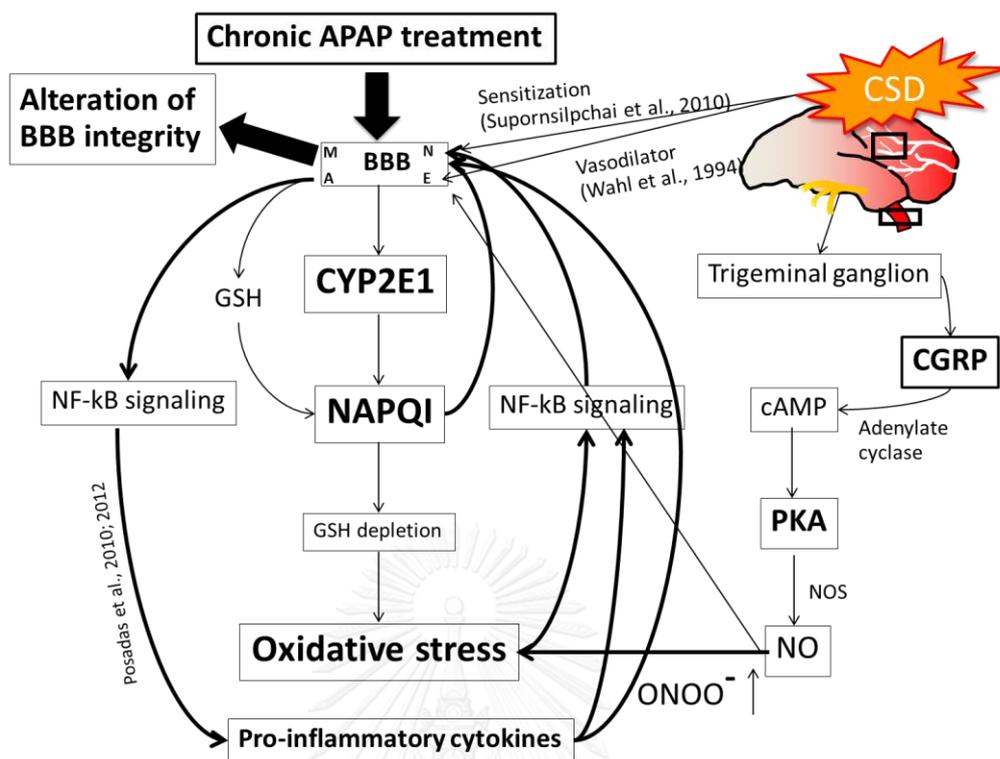
Figure 77 Schematic diagram of effect of chronic APAP treatment in the condition with CSD activation on BBB integrity.

REFERENCES

1. Laurie F Prescott. Paracetamol, alcohol and the liver. Br J Clin Pharmacol. 2000; 49(4): 291-301.

2. Pickering G, Loriot MA, Libert F, Eschalier A, Beaune P, Dubray C. Analgesic effect of acetaminophen in humans: first evidence of a central serotonergic mechanism. Clin Pharmacol Ther. 2006; 79(4): 371-8.

3. Sandrini M, Vitale G, Ruggieri V, Pini LA. Effect of acute and repeated administration of paracetamol on opioidergic and serotonergic systems in rats. Inflamm Res. 2007; 56(4): 139-42.

4. Smith HS. Potential analgesic mechanisms of acetaminophen. Pain Physician. 2009; 12(1): 269-80.

5. Bromm B, Forth W, Richter E, Scharein E. Effects of acetaminophen and antipyrine on non-inflammatory pain and EEG activity. Pain. 1992; 50(2): 213-21.

6. Woodbury DM. The pharmacological basis of therapeutics 3rd edition. The Macmillan Company. New York. 1965: 312–344.

7. Merrill GF, Goldberg E. Antioxidant properties of acetaminophen and cardioprotection. Basic Res Cardiol. 2001; 96(5): 423-30.

8. Jaques-Robinson KM, Golfetti R, Baliga SS, Hadzimichalis NM, Merrill GF. Acetaminophen is cardioprotective against H2O2-induced injury in vivo. Exp Biol Med (Maywood). 2008; 233(10): 1315-22.

9. Tripathy D, Grammas P. Acetaminophen inhibits neuronal inflammation and protects neurons from oxidative stress. J Neuroinflammation. 2009; 6: 10.

10. Tripathy D, Grammas P. Acetaminophen protects brain endothelial cells against oxidative stress. Microvasc Res. 2009; 77(3): 289-96.

11. Slosky LM, Thompson BJ, Sanchez-Covarrubias L, Zhang Y, Laracuente ML, Vanderah TW, Ronaldson PT, Davis TP. Acetaminophen modulates P-glycoprotein functional expression at the blood-brain barrier by a constitutive androstane receptor-dependent mechanism. Mol Pharmacol. 2013; 84(5): 774-86.

12. Curhan GC, Bullock AJ, Hankinson SE, Willett WC, Speizer FE, Stampfer MJ. Frequency of use of acetaminophen, nonsteroidal anti-inflammatory drugs, and aspirin in US women. Pharmacoepidemiol Drug Saf. 2002; 11(8): 687-93.

13. Dedier J, Stampfer MJ, Hankinson SE, Willett WC, Speizer FE, Curhan GC. Nonnarcotic analgesic use and the risk of hypertension in US women. Hypertension. 2002; 40(5): 604-8.

14. Forman JP, Rimm EB, Curhan GC. Frequency of analgesic use and risk of hypertension among men. Arch Intern Med. 2007; 167(4): 394-9.

15. Sudano I, Flammer AJ, Périat D, Enseleit F, Hermann M, Wolfrum M, Hirt A, Kaiser P, Hurlimann D, Neidhart M, Gay S, Holzmeister J, Nussberger J, Mocharla P, Landmesser U, Haile SR, Corti R, Vanhoutte PM, Lüscher TF, Noll G, Ruschitzka F. Acetaminophen increases blood pressure in patients with coronary artery disease. Circulation. 2010; 122(18): 1789-96.

16. Supornsilpchai W, le Grand SM, Srikiatkhachorn A. Cortical hyperexcitability and mechanism of medication-overuse headache. Cephalalgia. 2010; 30(9): 1101-9.

17.   Supornsilpchai W, le Grand SM, Srikiatkhachorn A. Involvement of pro-nociceptive 5-HT2A receptor in the pathogenesis of medication-overuse headache. Headache. 2010; 50(2): 185-97.

18.   Gonzalez-Barcala FJ, Pertega S, Perez Castro T, Sampedro M, Sanchez Lastres J, San Jose Gonzalez MA, Bamonde L, Garnelo L, Valdes L, Carreira JM, Moure J, Lopez Silvarrey A. Exposure to paracetamol and asthma symptoms. Eur J Public Health. 2013; 23(4): 706-10.

19.   Posadas I, Santos P, Blanco A, Muñoz-Fernández M, Ceña V. Acetaminophen induces apoptosis in rat cortical neurons. PLoS One. 2010; 5(12): e15360.

20.   Nassini R, Materazzi S, Andrè E, Sartiani L, Aldini G, Trevisani M, et al. Acetaminophen, via its reactive metabolite N-acetyl-p-benzo-quinoneimine and transient receptor potential ankyrin-1 stimulation, causes neurogenic inflammation in the airways and other tissues in rodents. FASEB J. 2010; 24(12): 4904-16.

21.   Dahlin DC, Miwa GT, Lu AY, Nelson SD. N-acetyl-p-benzoquinone imine: a cytochrome P-450-mediated oxidation product of acetaminophen. Proc Natl Acad Sci U S A. 1984; 81(5): 1327-31.

22.   Huq F. Molecular modelling analysis of the metabolism of paracetamol. ournal of Pharmacology and Toxicology. 2007; 2: 142-50.

23.   Hansson T, Tindberg N, Ingelman-Sundberg M, Köhler C. Regional distribution of ethanol-inducible cytochrome P450 IIE1 in the rat central nervous system. Neuroscience. 1990; 34(2): 451-63.

24. Haorah J, Knipe B, Leibhart J, Ghorpade A, Persidsky Y. Alcohol-induced oxidative stress in brain endothelial cells causes blood-brain barrier dysfunction. J Leukoc Biol. 2005; 78(6): 1223-32.

25. Manyike PT, Kharasch ED, Kalhorn TF, Slattery JT. Contribution of CYP2E1 and CYP3A to acetaminophen reactive metabolite formation. Clin Pharmacol Ther. 2000; 67(3): 275-82.

26. Jaeschke H, Knight TR, Bajt ML. The role of oxidant stress and reactive nitrogen species in acetaminophen hepatotoxicity. Toxicol Lett. 2003; 144(3): 279-88.

27. James LP, Mayeux PR, Hinson JA. Acetaminophen-induced hepatotoxicity. Drug Metab Dispos. 2003; 31(12): 1499-506.

28. Kumpulainen E, Kokki H, Halonen T, Heikkinen M, Savolainen J, Laisalmi M. Paracetamol (acetaminophen) penetrates readily into the cerebrospinal fluid of children after intravenous administration. Pediatrics. 2007; 119(4): 766-71.

29. Just S, Arndt K, Weiser T, Doods H. Pathophysiology of migraine: A role for neuropeptides. Drug Discovery Today: Disease Mechanisms. 2006. 3(3): 327-33.

30. Edvinsson L, Villalón CM, MaassenVanDenBrink A. Basic mechanisms of migraine and its acute treatment. Pharmacol Ther. 2012; 136(3): 319-33.

31. Gursoy-Ozdemir Y, Qiu J, Matsuoka N, Bolay H, Bermpohl D, Jin H, et al, Cortical spreading depression activates and upregulates MMP-9. J Clin Invest. 2004; 113(10): 1447-55.

32. Moskowitz MA. Genes, proteases, cortical spreading depression and migraine: impact on pathophysiology and treatment. Funct Neurol. 2007; 22(3): 133-6.

33. Sarchielli P, Alberti A, Baldi A, Coppola F, Rossi C, Pierguidi L, et al. Proinflammatory cytokines, adhesion molecules, and lymphocyte integrin expression in the internal jugular blood of migraine patients without aura assessed ictally. Headache. 2006; 46(2): 200-7.

34. Tietjen GE, Khubchandani J. Platelet dysfunction and stroke in the female migraineur. Curr Pain Headache Rep. 2009; 13(5): 386-91.

35. Tietjen GE1, Khubchandani J, Herial NA, Shah K. Adverse childhood experiences are associated with migraine and vascular biomarkers. Headache. 2012; 52(6): 920-9.

36. Arulmani U, Maassenvandenbrink A, Villalón CM, Saxena PR. Calcitonin gene-related peptide and its role in migraine pathophysiology. Eur J Pharmacol. 2004; 500(1-3): 315-30.

37. Durham PL. Inhibition of calcitonin gene-related peptide function: a promising strategy for treating migraine. Headache. 2008; 48(8): 1269-75.

38. Durham PL, Vause CV.Calcitonin gene-related peptide (CGRP) receptor antagonists in the treatment of migraine. CNS Drugs. 2010; 24(7): 539-48.

39. Goadsby PJ, Lipton RB, Ferrari MD. Migraine-current understanding and treatment. N Engl J Med. 2002; 346(4): 257-70.

40. Persidsky Y, Ramirez SH, Haorah J, Kanmogne GD. Blood-brain barrier: structural components and function under physiologic and pathologic conditions. J Neuroimmune Pharmacol. 2006; 1(3): 223-36.

41. Cardoso FL, Brites D, Brito MA. Looking at the blood-brain barrier: molecular anatomy and possible investigation approaches. Brain Res Rev. 2010; 64(2): 328-63.

42.   Abbott NJ. Astrocyte-endothelial interactions and blood–brain barrier permeability. J Anat. 2002; 200(6): 629-38.

43.   Ballabh P, Braun A, Nedergaard M. The blood-brain barrier: an overview: structure, regulation, and clinical implications. Neurobiol Dis. 2004; 16(1): 1-13.

44.   Ge S, Song L, Pachter JS. Where is the blood-brain barrier ... really? J Neurosci Res. 2005; 79(4): 421-7.

45.   Choi YK, Kim KW. Blood-neural barrier--its diversity and coordinated cell-to-cell communication. BMB Rep. 2008; 41(5): 345-52.

46.   Hawkins BT, Davis TP. The blood-brain barrier/neurovascular unit in health and disease. Pharmacol Rev. 2005; 57(2): 173-85.

47.   Rash JE, Yasumura T, Hudson CS, Agre P, Nielsen S. Direct immunogold labeling of aquaporin-4 in square arrays of astrocyte and ependymocyte plasma membranes in rat brain and spinal cord. Proc Natl Acad Sci U S A. 1998; 95(20): 11981-6.

48.   Abbott NJ, Rönnbäck L, Hansson E. Astrocyte-endothelial interactions at the blood-brain barrier. Nat Rev Neurosci. 2006; 7(1): 41-53.

49.   Yamagata K, Tagami M, Nara Y, Mitani M, Kubota A, Fujino H. Astrocyte-conditioned medium induces blood-brain barrier properties in endothelial cells. Clin Exp Pharmacol Physiol. 1997; 24(9-10): 710-3.

50.   Zlokovic BV. The blood-brain barrier in health and chronic neurodegenerative disorders. Neuron. 2008; 57(2): 178-201.

51.   Wolburg H, Lippoldt A. Tight junctions of the blood-brain barrier: development, composition and regulation. Vascul Pharmacol. 2002; 38(6): 323-37.

52. Abbott NJ, Rönnbäck L, Hansson E. Astrocyte–endothelial interactions at the blood–brain barrier. Nat Rev Neurosci. 2006; 7(1): 41-53.

53. Furuse M, Hirase T, Itoh M, Nagafuchi A, Yonemura S, Tsukita S, et al. Occludin: a novel integral membrane protein localizing at tight junctions. J J Cell Biol. 1993; 123(6 Pt 2): 1777-88.

54. McCarthy KM, Skare IB, Stankewich MC, Furuse M, Tsukita S, Rogers RA, et al. Occludin is a functional component of the tight junction. J Cell Sci. 1996; 109 (Pt 9): 2287-98.

55. Vorbrodt AW, Dobrogowska DH. Molecular anatomy of intercellular junctions in brain endothelial and epithelial barriers: electron microscopist's view. Brain Res Brain Res Rev. 2003; 42(3): 221-42.

56. Nitta T, Hata M, Gotoh S, Seo Y, Sasaki H, Hashimoto N, et al, Size-selective loosening of the blood–brain barrier in claudin-5-deficient mice. J J Cell Biol. 2003 12; 161(3): 653-60.

57. Fanning AS, Jameson BJ, Jesaitis LA, Anderson JM The tight junction protein ZO-1 establishes a link between the transmem- brane protein occludin and the actin cytoskeleton. J Biol Chem. 1998; 273(45): 29745-53.

58. Itoh M, Morita K, Tsukita S. Characterization of ZO-2 as a MAGUK family member associated with tight as well as adherens junctions with a binding affinity to occludin and α catenin. J Biol Chem. 1999; 274(9): 5981-6.

59. Hawkins BT, Davis TP. The blood-brain barrier/neurovascular unit in health and disease. Pharmacol Rev. 2005; 57(2): 173-85.

60. Headache classification subcommitee of the HIS. Classification and WHO ICD-10NA Codes. Cephalalgia, 2004. 24: 16-22.

61. Phanthumchinda K, Sithi-Amorn C. Prevalence and clinical features of migraine: a community survey in Bangkok, Thailand. Headache. 1989; 29(9): 594-7.

62. Gerth WC, Carides GW, Dasbach EJ, Visser WH, Santanello NC. The multinational impact of migraine symptoms on healthcare utilisation and work loss. Pharmacoeconomics. 2001; 19(2): 197-206.

63. Lipton RB, Stewart WF, Diamond S, Diamond ML, Reed M. Prevalence and Burden of Migraine in the United States: Data From the American Migraine Study II. Headache. 2001; 41(7): 646-57.

64. Leão AAP Spreading depression of activity in the cerebral cortex. J Neurophysiol. 1944. **7(6)**: 359-90.

65. Sánchez-del-Rio M, Reuter U. Migraine aura: new information on underlying mechanisms. Curr Opin Neurol. 2004; 17(3): 289-93.

66. Wahl M, Schilling L, Parsons AA, Kaumann A. Involvement of calcitonin gene-related peptide (CGRP) and nitric oxide (NO) in the pial artery dilatation elicited by cortical spreading depression. Brain Res. 1994; 637(1-2): 204-10.

67. Edvinsson L. Blockade of CGRP receptors in the intracranial vasculature: a new target in the treatment of headache. Cephalalgia. 2004; 24(8): 611-22.

68. Rosenfeld MG, Mermod JJ, Amara SG, Swanson LW, Sawchenko PE, Rivier J, et al. Production of a novel neuropeptide encoded by the calcitonin gene via tissue-specific RNA processing. Nature. 1983; 304(5922): 129-35.

69. Wimalawansa SJ. Blood pressure and cardiovascular tone: role of CGRP family of peptides. The Scientific World. 2001; **1**: 32.

70. Lassen LH, Haderslev PA, Jacobsen VB, Iversen HK, Sperling B, Olesen J. CGRP may play a causative role in migraine. Cephalalgia. 2002; 22(1): 54-61.

71. Juhasz G, Zsombok T, Modos EA, Olajos S, Jakab B, Nemeth J, Szolcsanyi J, Vitrai J, Bagdy G. NO-induced migraine attack: strong increase in plasma calcitonin gene-related peptide (CGRP) concentration and negative correlation with platelet serotonin release. Pain. 2003; 106(3): 461-70.

72. Holzer P. Neurogenic vasodilatation and plasma leakage in the skin. Gen Pharmacol. 1998; 30(1): 5-11.

73. Brain SD, Grant AD. Vascular actions of calcitonin gene-related peptide and adrenomedullin. Physiol Rev. 2004; 84(3): 903-34.

74. Busija DW, Bari F, Domoki F, Horiguchi T, Shimizu K. Mechanisms involved in the cerebrovascular dilator effects of cortical spreading depression. Prog Neurobiol. 2008; 86(4): 379-95.

75. Tsiotou AG, Sakorafas GH, Anagnostopoulos G, Bramis J.Anagnostopoulos G. and Bramis J, Septic shock; current pathogenetic concepts from a clinical perspective. Med Sci Monit. 2005; 11(3): 76-85.

76. Sultan S, Gosling M, Nagase H, Powell JT. Shear stress-induced shedding of soluble intercellular adhesion molecule-1 from saphenous vein endothelium. FEBS Lett. 2004; 564(1-2): 161-5.

77. Caminero AB, Sánchez Del Río González M. Migraine as a cerebrovascular risk factor. Neurologia. 2012; 27(2): 103-11.

78. Schürks M, Rist PM, Bigal ME, Buring JE, Lipton RB, Kurth T. Migraine and cardiovascular disease: systematic review and meta-analysis. BMJ. 2009; 339: b3914.

79.	Kruit MC, Launer LJ, van Buchem MA, Terwindt GM, Ferrari MD. MRI findings in migraine. Rev Neurol (Paris). 2005; 161(6-7): 661-5.

80.	Scher AI, Gudmundsson LS, Sigurdsson S, Ghambaryan A, Aspelund T, Eiriksdottir G, et al. Migraine headache in middle age and late-life brain infarcts. JAMA. 2009; 301(24): 2563-70.

81.	Ross R. Atherosclerosis--an inflammatory disease. N Engl J Med. 1999; 340(2): 115-26.

82.	Tietjen EG. Migraine and ischaemic heart disease and stroke: potential mechanisms and treatment implications. Cephalalgia. 2007; 27(8): 981-7.

83.	Ciancarelli I, Tozzi-Ciancarelli MG, Di Massimo C, Marini C, Carolei A. Urinary nitric oxide metabolites and lipid peroxidation by-products in migraine. Cephalalgia. 2003; 23(1): 39-42.

84.	Waeber C, Moskowitz MA. Moskowitz, Migraine as an inflammatory disorder. Neurology. 2005; 64(10 Suppl 2): S9-15.

85.	Tjølsen A, Lund A, Hole K. Antinociceptive effect of paracetamol in rats is partly dependent on spinal serotonergic systems. Eur J Pharmacol. 1991; 193(2): 193-201.

86.	Alloui A, Chassaing C, Schmidt J, Ardid D, Dubray C, Cloarec A, et al. Paracetamol exerts a spinal, tropisetron-reversible, antinociceptive effect in an inflammatory pain model in rats. Eur J Pharmacol. 2002; 443(1-3): 71-7.

87.	Pickering G, Estève V, Loriot MA, Eschalier A, Dubray C. Acetaminophen reinforces descending inhibitory pain pathways. Clin Pharmacol Ther. 2008; 84(1): 47-51.

88. Chandrasekharan NV, Dai H, Roos KL, Evanson NK, Tomsik J, Elton TS, et al. COX-3, a cyclooxygenase-1 variant inhibited by acetaminophen and other analgesic/antipyretic drugs: cloning, structure, and expression. Proc Natl Acad Sci U S A. 2002; 99(21): 13926-31.

89. Flower RJ, Vane JR. Inhibition of prostaglandin synthetase in brain explains the anti-pyretic activity of paracetamol (4-acetamidophenol). Nature. 1972; 240(5381): 410-1.

90. Björkman R. Central antinociceptive effects of non-steroidal anti-inflammatory drugs and paracetamol. Experimental studies in the rat. Acta Anaesthesiol Scand Suppl. 1995; 103: 1-44.

91. Heard KJ. Acetylcysteine for Acetaminophen Poisoning. N Engl J Med. 2008; 359(3): 285-92.

92. Dimova S, Hoet PH, Nemery B. Paracetamol (acetaminophen) cytotoxicity in rat type II pneumocytes and alveolar macrophages in vitro. Biochem Pharmacol. 2000; 59(11): 1467-75.

93. Posadas I, Santos P, Ceña V. Acetaminophen induces human neuroblastoma cell death through NFKB activation. PLoS One. 2012; 7(11): e50160.

94. Tak PP, Firestein GS. NF-kappaB: a key role in inflammatory diseases. J Clin Invest. 2001; 107(1): 7-11.

95. Wang Z, Ma W, Chabot JG, Quirion R. Cell-type specific activation of p38 and ERK mediates calcitonin gene-related peptide involvement in tolerance to morphine-induced analgesia. FASEB J. 2009; 23(8): 2576-86.

96. http://doctorstevesbanjo.com/, 2009.

97. Dimova S, Hoet PH, Dinsdale D, Nemery B. Acetaminophen decreases intracellular glutathione levels and modulates cytokine production in human alveolar macrophages and type II pneumocytes in vitro. Int J Biochem Cell Biol. 2005; 37(8): 1727-37.

98. Hasler JA. Human cytochromes P450. Mol Aspects Med. 1999; 20(1-2): 12-24, 25-137.

99. Lauritzen M, Fabricius M. Real time laser-Doppler perfusion imaging of cortical spreading depression in rat neocortex. Neuroreport. 1995; 6(9): 1271-3.

100. Chantong C , Y., Thongtan T , Maneesri-le Grand S. Increases of pro-inflammatory cytokine expression in hippocampus following chronic paracetamol treatment in rats. Asian Archives of Pathology. 2013; **9**(4): 137-46.

101. Maneesri-le Grand S, Chantong C, Yisarakun W, Srikiatkhachorn A. Chronic paracetamol usage induces proinflammatory cytokines and vascular cell adhesion molecules expression via NF-kB signaling. J Neurochem. 2011; **118**(Supplement s1): 4–83.

102. De Felice M, Ossipov MH, Wang R, Lai J, Chichorro J, Meng I, et al. Triptan-induced latent sensitization: a possible basis for medication overuse headache. Ann Neurol. 2010; 67(3): 325-37.

103. Gardell LR, Wang R, Burgess SE, Ossipov MH, Vanderah TW, Malan TP Jr, et al. Sustained morphine exposure induces a spinal dynorphin-dependent enhancement of excitatory transmitter release from primary afferent fibers. J Neurosci. 2002; 22(15): 6747-55.

104. Thalakoti S, Patil VV, Damodaram S, Vause CV, Langford LE, Freeman SE,   et al. Neuron-glia signaling in trigeminal ganglion: implications for migraine pathology. Headache. 2007; 47(7): 1008-23; discussion 24-5.

105. Zhang Z, Winborn CS, Marquez de Prado B, Russo AF. Sensitization of calcitonin gene-related peptide receptors by receptor activity-modifying protein-1 in the trigeminal ganglion. J Neurosci. 2007; 27(10): 2693-703.

106. Li J, Vause CV, Durham PL. Calcitonin gene-related peptide stimulation of nitric oxide synthesis and release from trigeminal ganglion glial cells. Brain Res. 2008; 1196: 22-32.

107. Brain SD, Grant AD. Vascular actions of calcitonin gene-related peptide and adrenomedullin. Physiol Rev. 2004; 84(3): 903-34.

108. Brown GC, Borutaite V. Nitric Oxide, Mitochondria, and Cell Death. IUBMB Life. 2001; 52(3-5): 189-95.

109. Calcerrada P, Peluffo G, Radi R. Nitric oxide-derived oxidants with a focus on peroxynitrite: molecular targets, cellular responses and therapeutic implications. Curr Pharm Des. 2011; 17(35): 3905-32.

110. Maneesri-le Grand S, Chantong C, Yisarakun W, Srikiatkhachorn A. Chronic paracetamol usage induces proinflammatory cytokines and vascular cell adhesion molecules expression via NF-kB signaling. J Neurochem. 2011; **118**(Supplement s1): 4–83.

APPENDIX

Reagent preparation

10X SDS-PAGE running buffer, final volume = 1 litre: [250 mM Tris-HCl, 1.92 M Glycine, 1% SDS pH 8.3]

   - Tris-base (MW 121.14)   30.28 g

   - Glycine (MW 75.07)   144.13 g

   - Sodium dodecylsulfate (SDS) 10 g

   Add SDS after Tris and Glycine totally dissolved

   Add 18.2 MΩ H$_2$O up to 1000 ml

10X Transfer buffer final volume = 800 ml: [250 mM Tris-HCl, 1.92 M Glycine, pH 8.3]

   - Tris-base (MW 121.14)   30.28 g

   - Glycine (MW 75.07)   144.13 g

   Add 18.2 MΩ H$_2$O up to 800 ml

   Store at room temperature

10X Tris-buffer saline (TBS) volume 1 litre: [200 mM Tris, 1.5 M NaCl, pH 7.6]

(For prepare antibody and washing)

   - Tris-base (MW 121.14)   24.23 g

   - NaCl (MW 58.4)   80.06 g

   Add dH$_2$O almost ~ 800 ml - -> adjust pH to 7.6 by HCl

   Add dH$_2$O up to 1000 ml

   Store at room temperature

10X TBS buffer volume 1 litre: [50 mM Tris, 150 mM NaCl, pH 7.6]

(For cleaning membrane after transfer)

   -Tris-base (MW 121.14)   60.57 g

   - NaCl (MW 58.4)   87.6 g

   Add dH$_2$O almost ~800 ml - -> adjust pH to 7.6 by HCl

   Add dH$_2$O up to 1000 ml

   Store at room temperature

10% SDS (w/v) volume = 100 ml:

    - Weighed out sodium dodecylsulfate (SDS)   10   g

    Add dH_2O up to 100 ml

Store at room temperature

4X Running Gel buffer, final volume = 200 ml: **[1.5 M Tris-HCl, pH 8.8]**

    - Tris-base (MW 121.14)   36.3   g

    Add dH_2O almost ~ 150 ml   - ->   adjust pH to 8.8 by HCl

    Add dH_2O up to 200 ml

    Store at 4°C

4X Stacking Gel buffer, final volume = 50 ml: [0.5 M Tris-HCl, pH 6.8]

    - Tris-base (MW 121.14)   3.05   g

    Add dH_2O almost ~ 40 ml   - ->   adjust pH to 6.8 by HCl

    Add dH_2O up to 50 ml

    Store at 4°C

4X SDS Protein Sample Buffer (4X Loading dye), final volume 10 ml: [240 mM Tris-HCl (pH 6.8), 40% Glycerol, 8% SDS, 0.04% Bromophenol blue, 5% **β**-mercaptoethanol]

    -1 M Tris-base (pH 6.8)   2.4   ml

    -100 % Glycerol   4   ml

    -SDS   0.8   g

    -1% Bromophenol blue   0.4   ml

    - **β**-mercaptoethanol   0.5   ml

    Add dH_2O 2.7   ml

Coomassie blue staining, final volume 1 litre: [0.1%(w/v) Coomassie Brilliant Blue R250, 40% methanol, 10% glacial acetic acid]

    - Coomassie Brilliant Blue R250   1   g

    - Methanol   400   ml

    Stir ~3 hours until dissolved. Then add:

    - Glacial acetic acid   100   ml

    Add dH_2O up to 1000 ml *filter before store*

    Store at room temperature

Destaining solution I volume 1 litre: [40 % methanol, 10 % acetic acid]

- Methanol   400   ml
- Acetic acid   100   ml

Add dH$_2$O up to 1000 ml

Store at room temperature

Destaining solution II volume 1 litre: [10 % Methanol, 5 % Acetic acid]

- Methanol   100   ml
- Acetic acid   50   ml

Add dH$_2$O up to 1000 ml

Store at room temperature

Ice-cold Tris buffer (5mM Tris-HCl, pH 7.4 autoclave), final volume 500 ml:

(For washing specimen before extracting)

- Tris-base (MW 121.14)   0.3   g

Add dH$_2$O almost ~ 400 ml   - ->   adjust pH to 7.4 by HCl

Add dH$_2$O up to 500 ml

Store at 4°C

SDS-PAGE

Stacking gel (for 2 gels)				
30% Acrylamide	0.44 ml			
4X Stacking gel buffer	0.83 ml			
10% SDS	33 µl			
dH$_2$O	2.03 ml			
10% Ammonium persulfate	25 µl			
TEMED	3 µl			
Separating gel (for 2 gels)				
	7.5%	10%	12.5%	15%
30% Acrylamide	2.5 ml	3.3 ml	4.2 ml	5 ml
4X Stacking gel buffer	2.5 ml	2.5 ml	2.5 ml	2.5 ml
10% SDS	100 µl	100 µl	100 µl	100 µl
dH$_2$O	4.9 ml	4.0 ml	3.2 ml	2.4 ml
10% Ammonium persulfate	65 µl	65 µl	65 µl	65 µl
TEMED	5 µl	5 µl	5 µl	5 µl

VITA

Name   Miss Waranurin Yisarakun

Date of birth   5 September 1979

Place of birth   Trat, Thailand

Address   Faculty of Allied Health Sciences, Burapha University 169 Long-Hard Bangsaen Road, Saen Sook Sub-district, Mueang District, Chonburi 20131

Instruction attended   Bachelor of Science (Biology)

Department of Biology, Faculty of Science, Burapha University (1998-2001)

Master of Science (Pathobiology)

Department of Pathobiology, Faculty of Science, Mahidol University (2002-2005)